DISCOVERY OF A NOVEL LIPOXYGENASE PATHWAY IN SKIN

By

Zheyong Yu

Dissertation

Submitted to the Faculty of the

Graduate School of Vanderbilt University

in partial fulfillment of the requirements

for the degree of

DOCTOR OF PHILOSOPHY

in

Pharmacology

December, 2005

Nashville, Tennessee

Approved:

Jason D. Morrow, M.D.

Alan R. Brash, Ph.D.

Richard M. Breyer, Ph.D.

H. Alex Brown, Ph.D.

Diane S. Keeney, Ph.D.

ACKNOWLEDGEMENTS

This work would not have been possible without the help and encouragement of a large number of people. First, I would like to offer a special thank to my mentor Dr. Alan Brash. He has been unfailingly enthusiastic about this project. Without his encouragement and trust, I surely would not have completed my degree. Most of all, his door is always open, so that I can get guidance and help from him at any time. I would also like to thank the other members of my committee: Dr. Jason Morrow, Dr. Rich Breyer, Dr. Alex Brown, and Dr. Diane Keeney. I really appreciate the time and effort they put into thinking critically about my experiments and hypotheses. Dr. Diane Keeney also kindly provided important guidance and suggestions on skin and keratinocyte related experiments, which are critical to this project.

I also have to thank William Boeglin and Dr. Claus Schneider in our lab. They are always ready to share expertise or constructive criticism, as well as provide valuable help in my experiments. Dr. Claus Schneider also has read manuscripts and this dissertation. Without them this project would not have been possible.

The Mass Spectrometry Research Center, NMR core and Skin Disease Research Center in Vanderbilt University has been critical to the completion of this work. Betty Fox, Dr. David Hachey and Dr. Huiyong Yin provided the technical help of mass spectrometry. Dr. Dingzhi Wang and Dr. Raymond DuBois help me to set up the PPAR activation assay. I must thank all of them.

Finally I have to thank my family for their love and emotional support. Without them I will never have any success.

TABLE OF CONTENTS

LIST OF TABLES

LIST OF FIGURES

LIST OF ABBREVIATIONS

AA	arachidonic acid
ALA	α-linolenic acid
ALX	lipoxin A_4 receptor
ATP	adenosine triphosphate
AU	absorbance unit
BLT	leukotriene B_4 receptor
CD	circular dichroism
cDNA	complementary deoxyribonucleic acid
cm	centimeters
COSY	correlation spectroscopy
COX	cyclooxygenase
CysLT	cysteinyl-leukotriene
DGAT	diacylglycerol acyltransferase
DGLA	dihomo-γ-linolenic acid
DHA	docosahexaenoic acid
EET	epoxyeicosatrienoic acid
EFA	essential fatty acid
eLOX3	epidermis-type lipoxygenase-3
EPA	eicosapentaenoic acid
ESI	electrospray ionization
eV	electron volt

FLAP	5-lipoxygenase activating protein
GC	gas chromatography
GLA	γ-linolenic acid
GPCR	G-protein coupled receptor
GSH	glutathione
H(P)ETE	hydro(pero)xyeicosatetraenoic acid
H(P)ODE	hydro(pero)xyoctadecadienoic acid
HCl	hydrochloric acid
His	histamine
HPLC	high performance liquid chromatography
kDa	kilodalton
KETE	ketoeicosatetraenoic acid
LA	linoleic acid
LC	liquid chromatography
LDL	low density lipoprotein
LOX	lipoxygenase
LT	leukotriene
LX	lipoxin
M	molar
m/z	mass to charge ratio
μg	microgram
min	minutes
μl	microliter

ml	milliliter
μM	micromolar
mm	millimeter
mM	millimolar
MS	mass spectrometry
NaCl	sodium chloride
NCIE	non-bullous congenital ichthyosiform erythroderma
NDGA	nordihydroguaiaretic acid
ng	nanogram
NMR	nuclear magnetic resonance
NSAID	non-steroidal anti-inflammatory drugs
PAGE	polyacrylamide gel electrophoresis
PBS	phosphate buffered saline
PCR	polymerase chain reaction
PFB	pentafluorobenzyl
PG	prostaglandin
PKC	protein kinase C
PLA2	phospholipase A2
PPAR	peroxisome proliferator-activated receptor
PUFA	polyunsaturated fatty acid
RP	reversed phase
RXR	retinoid X receptor
SDS	sodium dodecyl sulphate

sEH	soluble epoxide hydrolase
SP	straight phase
SRS-A	slow reacting substance of anaphylaxis
TMS	trimethylsilyl
TPP	triphenylphosphine
UV	ultraviolet

CHAPTER I

INTRODUCTION

For more than 70 years, essential fatty acid deficiency has been known to cause skin disease. In a pioneering paper published in 1929, Burr and Burr described that when rats were fed with a fat-free diet, "an abnormal, scaly condition of the skin is observed between the 70^{th} and 90^{th} day of life" (Burr and Burr, 1929). The typical lesions also include dryness, redness, weeping, and other manifestation of inflammation. One year later, both investigators showed that linoleic acid (LA, 18:2ω6) alone could reverse the symptoms resulting from the fat-free diet (Burr and Burr, 1930). They named LA as an essential fatty acid (EFA). Although the underlying molecular and cellular mechanism in EFA deficiency skin is not well understood, evidence is accumulating to show that the rate of epidermal cell proliferation, transepidermal water loss in skin barrier, and some intracellular metabolic activities are dramatically increased (Basnayake and Sinclair, 1954; Lowe and DeQuoy, 1978; Robillard and Christon, 1993; Smit *et al.*, 2004).

The effects of EFA deficiency on skin abnormalities that were observed in rats were also reported in humans. Babies fed with artificial milk formula deficient in EFAs developed skin lesions similar to those seen in rats (Hansen, A. E. *et al.*, 1958). Some human skin disorders, such as psoriasis, ichthyosis and eczema, also show a somewhat similar phenotype. These diseases have a specific genetic or inflammatory origin. Whether EFA could influence their pathogenesis is still unclear. If the EFA abnormality

is causal, as that in EFA deficient rat skin, measures to correct it should lead to clinical improvement in the skin condition.

Skin EFAs might play roles in the maintenance of the epidermal water barrier and the regulation of epidermal proliferation and differentiation. Some evidence suggests that LA is an important component of the epidermal water barrier (Wertz and Downing, 1983; Hansen, H. S. and Jensen, 1985; Melton *et al.*, 1987). Except for this structural role, most functions of EFAs might be fulfilled by their pharmacologically active metabolites. The metabolism of EFAs in the epidermis is highly active. They are good substrates for epidermal enzymes such as cyclooxygenase (COX), lipoxygenase (LOX) and P450 enzymes. Conversion by these enzymes generates specific molecules in cell signaling which are important for normal skin function.

Essential fatty acids and their metabolites in skin

While warm-blooded animals can synthesize saturated and monounsaturated fatty acids from acetyl co-enzyme A (and thus from non-lipid endogenous sources), they are unable to synthesize *de novo* either ω6 or ω3 polyunsaturated fatty acids (PUFAs). These fatty acids must be supplied in the diet and are termed essential fatty acids (EFAs).

LA is the first identified EFA (Burr and Burr, 1930). It undergoes further chain elongation and desaturation to form arachidonic acid (AA, 20:4ω6) and other ω6 series of PUFAs. Another fundamental EFA is α-linolenic acid (ALA, 18:3ω3) which is the precursor of other ω3 series of fatty acids such as eicosapentaenoic acid (EPA, 20:5ω3) and docosahexaenoic acid (DHA, 22:6ω3) (Figure 1). Although AA, EPA and DHA can

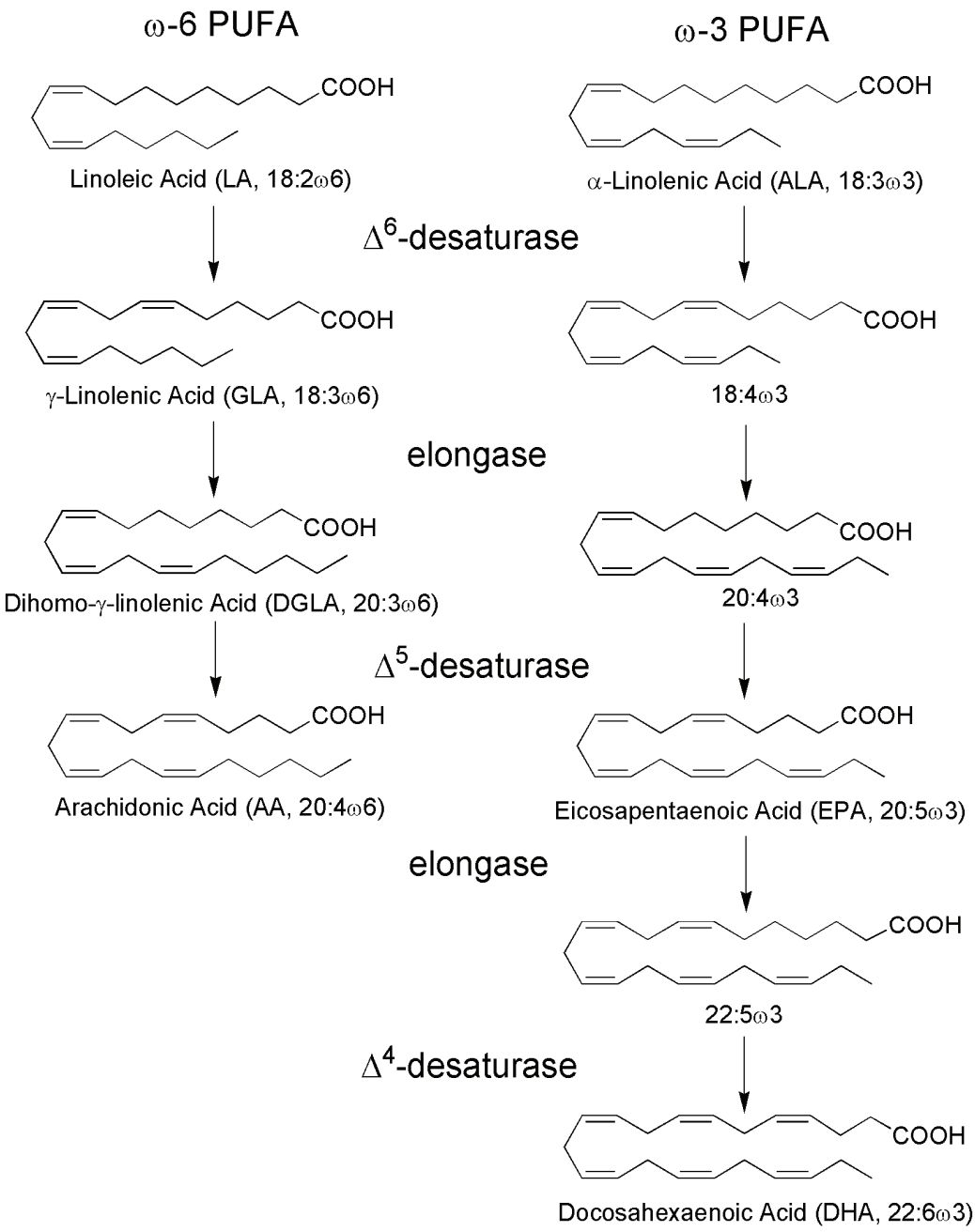

Figure 1. ω-6 and ω-3 series essential fatty acids.

be endogenously synthesized from LA and ALA, nutritional studies suggest they are also somewhat "essential" and their inclusion in the diet is also required (McCowen and Bistrian, 2005).

Since the original studies by Burr and Burr, it has been well established that ω6 series of fatty acids are important for normal skin function and their deficiency will cause skin disease. For the ω3 fatty acids, there is no evidence to suggest they are related to skin abnormalities (Ziboh and Chapkin, 1987). Here I will only discuss the ω6 series of EFAs and their metabolites in skin.

As the most abundant PUFA in skin, LA is not only identified in the phospholipid of the cellular membrane, it is also a major component of the epidermal water barrier. This barrier is constituted by lipid bilayers or lamellae and resides in the lower part of the stratum corneum (the uppermost layer of the epidermis). The lipids in the epidermal water barrier contain large amounts of sphingolipids, including acylglucosylceramide and acylceramide, and up to 70% of which contains esterified LA (Wertz and Downing, 1983; Bowser *et al.*, 1985). The principal pathway of LA metabolism in normal epidermis appears to be transfer from phospholipids to acylglucosylceramide and acylceramide (Wertz and Downing, 1990).

The significance of LA-containing sphingolipids in skin permeability was also suggested in a recent Acyl-CoA:diacylglycerol acyltransferase 2 (DGAT2) knockout study (Stone *et al.*, 2004). DGAT2 is the major enzyme in triglyceride synthesis. DGAT2 knockout mice show impaired permeability barrier function in the skin and die soon after birth. Analysis of the skin lipid revealed that not only the triglyceride content, but also the LA-containing acylceramide was reduced (Stone *et al.*, 2004).

Whether the reversal of the major cutaneous symptoms of EFA deficiency by LA is through the structural function of LA itself in the epidermal water barrier is still questionable. At least the metabolism of the linoleyl moiety of the barrier sphingolipids by a LOX-like reaction is required before the barrier function is exhibited (Nugteren *et al.*, 1985). Although the lipoxygenation is not a major route in the metabolism of normal epidermal LA (Wertz and Downing, 1990), the biological function of such a reaction cannot be neglected. As mentioned later, a LOX reaction forms hydroperoxy fatty acids, which are reduced to hydroxy fatty acids. Human epidermis mainly metabolizes LA to form 13-hydroxyoctadecadienoic acid (13-HODE). Reversal of the EFA-deficiency by dietary LA resulted in tissue elevation of 13-HODE and 13-HODE-substituted diacylglycerol (Cho Y, 1995). The latter has a selective inhibitory effect on epidermal membrane protein kinase C (PKC) (Cho Y, 1996). This signaling was thought to be associated with attenuation of the EFA-deficient-induced hyperproliferation.

Except for LA, feeding studies with different fatty acids suggest AA supplementation can also decrease the trans-epidermal water loss in EFA-deficient rats (Hansen, H. S. and Jensen, 1985). AA is the second most abundant PUFA in skin. The AA biosynthesis in most tissues includes the conversion of LA to γ-linolenic acid (GLA, 18:3ω6) by Δ^6-desaturase, chain elongation of GLA to dihomo-γ-linolenic acid (DGLA, 20:3ω6) by elongase, and formation of AA from DGLA by Δ^5-desaturase (Figure 1). The elongase activity is present in the epidermis while both desaturases are absent (Chapkin and Ziboh, 1984). Thus skin cannot convert LA to AA. AA in the epidermis is “essential” and must come from either dietary sources or other tissues such as the liver.

Although both LA and AA can reverse the phenotype caused by EFA-deficiency, their mechanism might be different since the abnormal epidermal permeability barrier function in EFA deficient rats can be corrected by topical administration of LA without prior systemic reversal of the deficiency state (i.e., without skin AA formation) (Elias *et al.*, 1980). The functional role of AA depends largely on its transformation to biologically potent oxidative metabolites by COX, LOX and P450 enzymes. These hormone-like metabolites (eicosanoids) include leukotrienes, lipoxins, prostaglandins, thromboxanes, hydroxy fatty acids and other oxygenated 20-carbon fatty acid derivatives. They are potent short-lived modulators in inflammatory responses, vasodilation/constriction and chemotactic processes in the immune system. Their function in skin physiology has also been widely studied (Ziboh *et al.*, 2002).

AA is well known to be metabolized in epithelial cells via the COX pathway to produce prostaglandins (PGs), which have been shown to have proinflammatory properties (Vane *et al.*, 1998). Several studies also suggest prostaglandin function in skin. For example, intradermal injections of prostaglandin D_2 (PGD_2) and E_2 (PGE_2) into human skin cause erythema (Flower *et al.*, 1976). In the EFA deficient mice both PGE_2 and $PGF_{2\alpha}$ levels in skin were much reduced (Lowe and DeQuoy, 1978). However, the COX pathway might not play a direct role in the epidermal permeability barrier since the rapid recovery of barrier function by LA occurs even with the inhibition of prostaglandin biosynthesis (Elias *et al.*, 1980).

In addition to the COX pathway, in skin it is particularly the LOX pathway that is of interest, and LOX products have been well investigated for their epidermal pathophysiological roles. Among them, leukotrienes (LTs) and 12-hydroxyeicosatetra-

enoic acid (12-HETE) are mainly proinflammatory in the skin whereas 15-HETE has anti-inflammatory capacities. These effects will be discussed later. 12*R*-HETE should receive most attention because it is predominantly a product of skin/epidermal tissue and its concentration is unusually elevated in psoriatic lesions (Woollard, 1986).

Mammalian lipoxygenases: nomenclature and classification

As mentioned earlier, the LOX pathway is more important than the COX pathway in epidermal barrier function. LOX enzymes are a family of non-heme iron containing dioxygenases that catalyze the addition of molecular oxygen to polyunsaturated fatty acids with a *cis,cis*-1,4-pentadiene system to form specific unsaturated fatty acid hydroperoxide derivatives (Brash, 1999; Kuhn and Thiele, 1999) (Figure 2). They are found widely in plants, fungi, animals (Brash, 1999), and, very rarely, in bacteria (Porta and Rocha-Sosa, 2001).

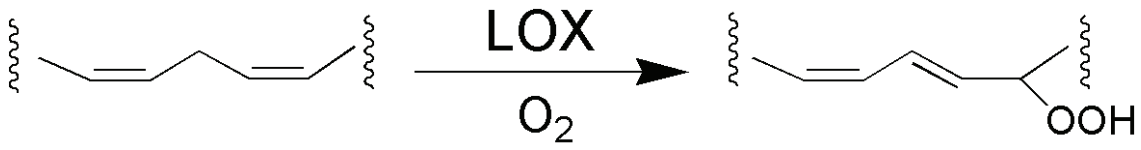

Figure 2. Reaction catalyzed by lipoxygenases.

Identification of LOX activity in mammalian cells was first described in 1974 (Hamberg and Samuelsson, 1974). Since the full sequence of human 5-LOX was published in 1988 (Dixon *et al.*, 1988; Matsumoto *et al.*, 1988), more than twenty mammalian LOX cDNAs have been cloned from various species (Figure 3). Their main reaction products are 5-, 8-, 12-, or 15-hydroperoxyeicosatetraenoic acids (HPETEs).

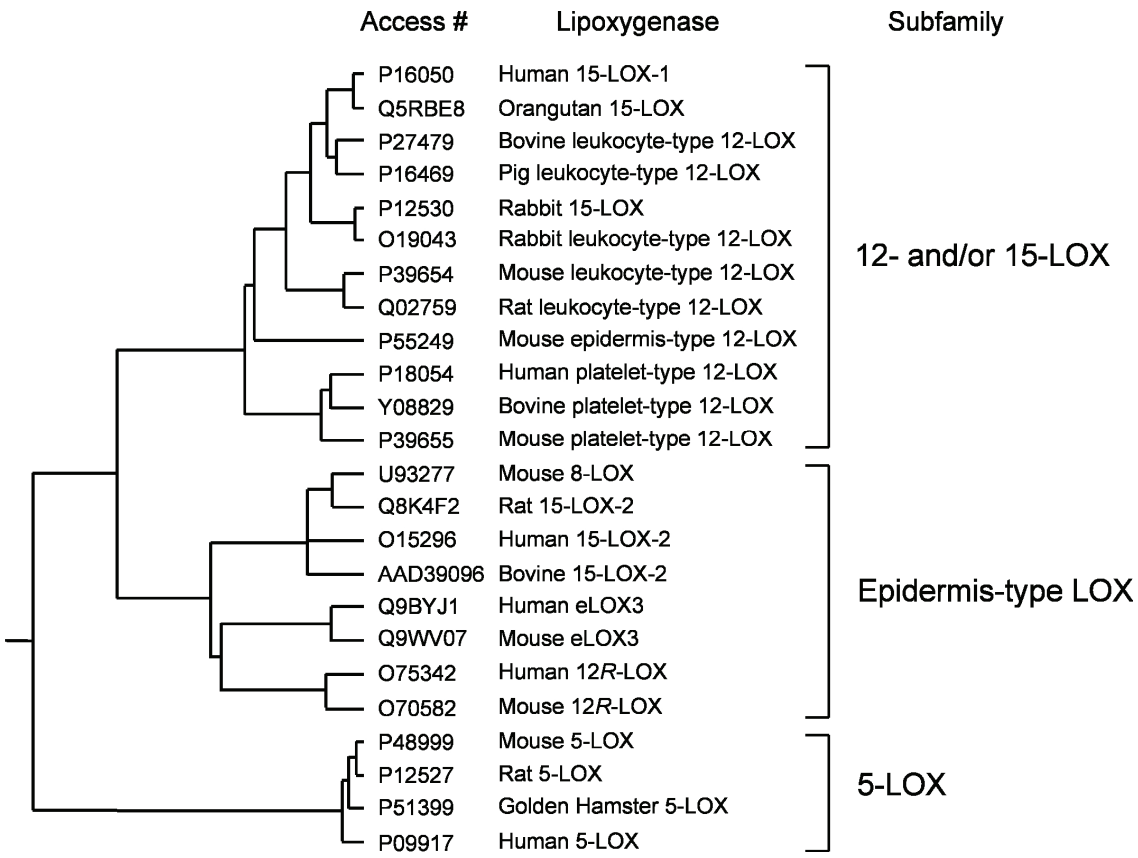

Figure 3. Mammalian lipoxygenase phylogenetic tree. Representative mammalian lipoxygenases were compiled into the phylogenetic tree using MegAlign (DNASTAR, Inc). Three branches of subfamilies were shown.

Usually these mammalian LOX enzymes are named by the position of oxygen insertion into their most common substrate, arachidonic acid. Using this nomenclature, mammalian LOX enzymes are classified as 5-, 8-, 12-, and 15-LOX, respectively (Yamamoto, 1992; Funk, C. D., 1996). Some LOX enzymes within a species form the same product and they are currently distinguished by the nomenclature related to their original source of isolation, for example, platelet-type 12-LOX versus leukocyte-type 12-LOX. When necessary, the stereoconfiguration (*R* or *S*) of the HPETE products are also specified.

Except for the recently identified 12*R*-LOX (Boeglin *et al.*, 1998), all mammalian LOX enzymes generate primary reaction products with *S*-chirality.

Classifying the mammalian LOX enzymes into 5-, 8-, 12-, and 15-LOX based on the positional specificity of oxygenation is straightforward. But the situation is complicated by the fact that enzymes forming the same products are not necessarily similar proteins. For example there are three different mouse 12-LOX isoforms, epidermal-type 12-LOX, platelet-type 12-LOX, and leukocyte-type 12-LOX. The disparity among these 12-LOX isoforms (about 59% amino acid identity) is even greater than that between certain 12- and 15-LOX isoforms (e.g., leukocyte-type 12-LOX and reticulocyte 15-LOX, about 73% identity) (Kuhn and Thiele, 1999). On the other hand, a different product formation is not necessarily associated with a substantial difference in the LOX amino acid sequence. For example, human 15-LOX-1 has high amino acid sequence identity with its mouse ortholog, mouse leukocyte-type 12*S*-LOX (about 73%). Human 15-LOX-2 also has high amino acid sequence identity with its mouse ortholog, mouse 8*S*-LOX (about 78%). However, these two human 15-LOX proteins which by name have the same products, only share about 35% amino acid sequence identity. In these cases, the classification based on the selectivity of oxygenation is somewhat misleading. With the growing list of cloned mammalian LOX enzymes, they are currently classified based on the sequence identity. In the phylogenetic tree of mammalian LOX enzymes (Figure 3), three branches of LOX genes can be recognized: the 12- and/or 15-LOX enzymes, the epidermis-type LOX enzymes, and the 5-LOX. Most enzymes in each subfamily can be detected in skin and are related to the skin physiology.

1. 5-LOX

5-LOX is mainly expressed in leukocytes, macrophages, mast cells and lymphocytes, and plays an essential role in the biosynthesis of leukotrienes (LTs). It possesses dual enzymatic activities: the oxygenase activity which converts arachidonic acid to 5*S*-HPETE and the leukotriene A_4 (LTA_4) synthase activity which dehydrates 5*S*-HPETE to form the epoxide LTA_4 (Samuelsson *et al.*, 1987b). 5-LOX enzymatic activity *in vitro* can be modulated by calcium, ATP, phosphatidylcholine and lipid hydroperoxides. Nevertheless *in vivo* activation of cellular 5-LOX in response to external stimuli is rather incompletely understood. After cell activation and in response to a Ca^{2+} flux, 5-LOX translocates to the nuclear envelope, where arachidonic acid, released by phospholipase A2 (PLA2), is presented to 5-LOX by 5-LOX activating protein (FLAP). LTA_4 is subsequently transformed into either LTB_4 by cytosolic LTA_4 hydrolase or to LTC_4 by LTC_4 synthase, which is an integral perinuclear membrane protein that conjugates glutathione (GSH) to LTA_4. LTC_4 and its metabolites LTD_4 and LTE_4 are collectively termed cysteinyl-leukotrienes (CysLTs).

2. 12- and/or 15-LOX enzymes

This subfamily can be classified into three groups. Three mouse 12*S*-LOX enzymes (platelet-type, leukocyte-type, and epidermis-type) are representative. The sequence identities between the groups are about 50-60%. The LOX enzymes within each group exhibit about 70-90% sequence identity. All of these LOX enzymes display less than 40% identity to 5-LOX.

Mouse platelet-type 12*S*-LOX and its human ortholog, human 12*S*-LOX, are expressed in platelets and epidermis. They primarily use free arachidonic acid as a substrate and produce predominantly 12*S*-HPETE, which is further reduced by peroxidases to 12*S*-HETE. Immunohistochemical analysis suggests mouse platelet-type 12*S*-LOX expression in skin is localized to the stratum granulosum (Johnson, E. N. *et al.*, 1999), while the human enzyme is limited to the basal layer (Hussain *et al.*, 1994). The biological function of mouse platelet-type 12*S*-LOX in maintaining the epidermal water barrier is indicated by the platelet-type 12*S*-LOX deficient mice which exhibited an increase in basal transepidermal water loss while little alteration in basal mitotic activity (Johnson, E.N. *et al.*, 1998).

Mouse epidermis-type 12*S*-LOX is the only member in this group so far. Its human ortholog is a pseudogene. The mRNA transcribed from this pseudogene contains a premature stop codon. So there is no active epidermis-type 12*S*-LOX protein in human. Unlike platelet-type 12*S*-LOX, mouse epidermis-type 12*S*-LOX exhibits very low reactivity towards free arachidonic or linoleic acid, but metabolizes the corresponding fatty acid methyl esters (Siebert *et al.*, 2001). In situ hybridization revealed highly specific expression of this enzyme in differentiated keratinocytes of the epidermis (Funk, C. D. *et al.*, 1996). Epidermis-type 12*S*-LOX expression also can be detected during early embryogenesis using RT-PCR, indicating a potential role for this LOX in early development (McDonnell *et al.*, 2001).

Mouse, rat, pig, and bovine leukocyte-type 12*S*-LOX show very high sequence identity (70-85%) with human and rabbit reticulocyte 15*S*-LOX (now called 15-LOX-1). Although their primary products have different positional specificity, they are still

grouped together and called 12/15-LOX enzymes. LOX enzymes in this group show broader but substantially different tissue distribution from species to species. Mouse leukocyte-type 12*S*-LOX is mainly expressed in macrophages, pineal gland, pituitary and kidney. In the rat the leukocyte-type 12*S*-LOX is most abundant in pineal gland, followed by lung, spleen, aorta, adrenal gland, spinal cord, and pancreas. Human 15-LOX-1 can be detected in reticulocyte, eosinophil and tracheal epithelium. The reactions catalyzed by the LOX enzymes in this group also show the lowest specificity in all mammalian LOX enzymes. They oxygenate not only all major naturally occurring polyenoic free fatty acids, such as arachidonic acid, linoleic acid, linolenic acid, or eicosapentaenoic acid (EPA), but also complex substrates such as phospholipids and cholesterol esters of biomembranes and low density lipoproteins (LDL) (Kuhn *et al.*, 1994a). Both the leukocyte-type 12*S*-LOX and the reticulocyte 15*S*-LOX from various species exhibit a dual positional specificity with arachidonic acid. The ratio of 12*S*-H(P)ETE to 15*S*-H(P)ETE products varies depending on the specific LOX enzyme.

3. Epidermis-type LOX enzymes

This subfamily includes human 15-LOX-2, mouse 8*S*-LOX, human and mouse 12*R*-LOX, and human and mouse epidermis-type LOX-3 (eLOX3). Although the reactions catalyzed show various positional and stereo specificities, they are grouped together because of their high sequence identity (at least 50% identity) and similar tissue distribution (skin). The mouse epidermis-type LOX genes are clustered at the central region of chromosome 11, suggesting possible formation by gene duplication. The same

genomic organization of epidermis-type LOX enzymes is also observed at human chromosome 17p13.1.

Human 15-LOX-2 is mainly expressed in skin, prostate, lung, and cornea. It converts arachidonic acid exclusively to 15*S*-HPETE, and linoleic acid is also a good substrate (Brash *et al.*, 1997; Kilty *et al.*, 1999). This catalytic activity is different from human 15-LOX-1, which oxygenates arachidonic acid to form mainly 15*S*-HPETE, but also partly 12*S*-HPETE, and for which linoleic acid is an excellent substrate. The expression of human 15-LOX-2 in epidermis was restricted to the basal cell layer (Shappell, S.B. *et al.*, 2001b). This is consistent with the finding that skin 15*S*-HETE is formed predominantly by the proliferating keratinocytes (Henneicke-von Zepelin *et al.*, 1991). The detection of high 15*S*-HETE compared to low 12*S*-HETE in the same layer of epidermis also suggests that 15-LOX-2, not 15-LOX-1, is the main enzyme forming 15*S*-HETE in skin.

Mouse 8*S*-LOX shares 78% amino acid identity with human 15-LOX-2. It is thought to be the mouse ortholog of the human 15-LOX-2 although encoding a LOX with different positional specificity. However, the expression of mouse 8*S*-LOX in skin is mainly in the differentiated epidermal layer, the stratum granulosum (Jisaka *et al.*, 1997), indicating different biological functions between human 15-LOX-2 and its mouse ortholog 8*S*-LOX.

12-HETE has been shown as one of the main eicosanoids formed by the epidermis and with the discovery of large quantities of 12-HETE in human psoriatic lesions (Hammarstrom *et al.*, 1979). In normal skin and psoriasis lesions, 12-HETE is predominantly of the "*R*" stereoconfiguration, 12*R*-HETE (Woollard, 1986). For many

years, 12*R*-HETE was considered to be the product of a cytochrome P450 (Holtzman *et al.*, 1989). The discovery of 12*R*-LOX in human skin suggests this enzyme accounts for the selective formation of 12*R*-HETE (Boeglin *et al.*, 1998). The mechanism of H-abstraction supports this conclusion (Boeglin *et al.*, 1998). The location of 12*R*-HETE formation in skin, which is mainly in the upper epidermal layers (Henneicke-von Zepelin *et al.*, 1991), indicating the location of 12*R*-LOX expression in skin.

Human and mouse 12*R*-LOX have different substrate selectivity. Human 12*R*-LOX forms 12*R*-HPETE from arachidonic acid and exhibits a slightly acidic pH-optimum (Schneider *et al.*, 2001a). The mouse ortholog does not use free acid as substrate. In vitro experiments showed that arachidonic acid methyl ester is the only substrate. Also in mouse, no 12*R*-HETE has been described as an endogenous product. Mouse 12*R*-LOX may use a yet unknown natural substrate and has different functions compared to human 12*R*-LOX.

Epidermis-type LOX-3 (eLOX3, gene symbol *ALOXE3*) was described first in the mouse (Kinzig *et al.*, 1999), and in humans in 2001 (Krieg *et al.*, 2001). eLOX3 has a limited scope of tissue expression, being mainly confined to keratinized epithelia such as skin. From PCR evidence it seems to be co-expressed in tissues that express the 12*R*-LOX (Heidt *et al.*, 2000; Krieg *et al.*, 2001). The amino acid sequence of human and mouse eLOX3 also shows the closest similarity to 12*R*-LOX (54% identity) and 15-LOX-2 (51%). The sequence of eLOX3 contains the characteristic well conserved amino acid residues found in all LOX enzymes including the putative iron-binding ligands and additional structure-determining residues (Krieg *et al.*, 2001). These features clearly indicate that eLOX3 belongs to the LOX gene family. The question of the oxygenase

activity of eLOX3, nonetheless, has remained elusive. No enzymatic activity has been detected by using linoleic or arachidonic acids, the prototypical C18 and C20 LOX substrates, or with the esters methyl arachidonate or cholesteryl arachidonate (Krieg *et al.*, 2001).

Mechanism of mammalian LOX catalysis

LOX enzymes contain a non-heme iron in the catalytic center which cycles between ferrous form (Fe^{2+}) and ferric form (Fe^{3+}) during the reaction (Figure 4). The isolated enzyme contains predominantly, if not exclusively, Fe^{2+}, but the catalytically active form of the enzyme has Fe^{3+}. The activating oxidation of the iron takes place in a reaction with lipid-hydroperoxide. The dioxygenase cycle is initiated by a stereospecific elimination of hydrogen from the methylene group between two double bonds on the substrate to form a pentadienyl radical and a proton. This step is considered to be rate limiting in LOX catalysis. The remaining electron reduces the iron to the Fe^{2+} state. Insertion of molecular oxygen in the carbon 1 or 5 position of the pentadienyl radical generates a peroxyl radical, which is reduced to the hydroperoxide by accepting a proton and the simultaneous oxidation of iron to the ferric state. The hydroperoxide product contains a *Z,E* conjugated diene which has a characteristic maximum UV absorbance at 235 nm. Oxidation of arachidonic acid by the ferric enzyme is shown in Figure 4. The hydroperoxide products are unstable and easily reduced to the corresponding hydroxy derivatives by cytosolic glutathione peroxidases or converted into various other types of eicosanoids including leukotrienes, lipoxins and hepoxilins.

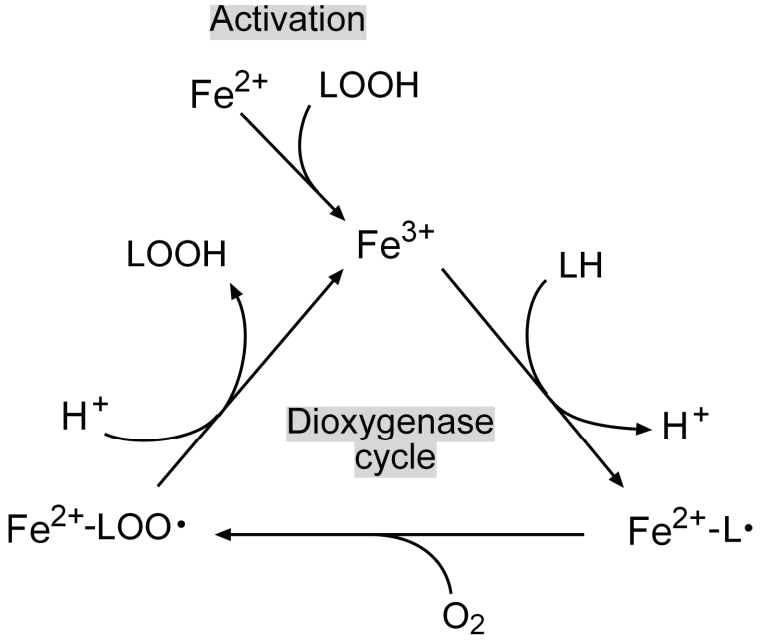

Figure 4. Mechanism of LOX activation and catalysis. Fe^{3+}: LOX with oxidized iron, Fe^{2+}: LOX with reduced iron, LH: arachidonate, L•: lipid alkyl radical, LOO•: lipid peroxyl radical, LOOH: lipid hydroperoxide. Activation of the enzyme requires trace hydroperoxide.

LOX has a reducing agent-dependent pseudoperoxidase activity which was first identified in soybean LOX and then confirmed in mammalian LOX (Riendeau *et al.*, 1991). In the activation step of LOX, the ferrous form LOX reacts with a fatty acid hydroperoxide to form the ferric LOX. Reducing agents such as N-hydroxyureas, hydroxybenzofurans, hydroxamic acids, hydroxylamines, and catechols, are capable of reducing the ferric form LOX to ferrous and thus inhibit the dioxygenase cycle. As a result, the fatty acid hydroperoxide only undergoes a one-electron reduction, rather than the two-electron reduction typical of peroxidase reactions. The primary one-electron

reduction product (an alkoxyl radical) decomposes to a mixture of end products (Kemal *et al.*, 1987; Riendeau *et al.*, 1991).

Although the LOX reaction requires hydroperoxides for the activation, under certain circumstances, LOX enzymes are sensitive to inactivation by fatty acid hydroperoxides. But the mechanism of this suicidal inactivation reaction remains poorly defined (Hartel *et al.*, 1982; De Carolis *et al.*, 1996).

The structure of mammalian LOX

Mammalian LOX proteins have a single polypeptide chain with a molecular mass of 75-81 kDa (about 662-711 amino acids) which is a little smaller than plant LOX enzymes (94-104 kDa). The primary structures of mammalian LOX enzymes are closely related, exhibiting 40-90% amino acid identity and containing well-conserved amino acid residues that are critical for the catalytic activity. Most of the mammalian LOX genes are split into 14 exons and 13 introns that are organized in the same exon/intron format with boundaries in the highly conserved positions (Funk, C. D., 1996). 12*R*-LOX and eLOX3 genes make exceptions in that they have an additional intronic sequence that divides exon 4. As a result, they have 15 exons.

The first and so far still the only crystal structure of a mammalian LOX (rabbit reticulocyte-type 15-LOX) was published in 1997 (Gillmor *et al.*, 1997). The enzyme is a two-domain protein which is similar to the published plant LOX enzymes (Boyington *et al.*, 1993; Skrzypczak-Jankun *et al.*, 1997). The N-terminal domain contains eight-stranded anti-parallel β-barrel, which is similar to the β-barrel domain in mammalian lipases. The C-terminal domain mainly consists of 18 helices and contains the catalytic

non-heme iron, which is ligated by four histidines (H361, H366, H541, H545) and the C-terminal isoleucine. Sequence alignment of the mammalian LOX enzymes suggests that except for one histidine (H545 in rabbit reticulocyte-type 15-LOX) which appears as Asn or Ser in some LOX enzymes, the other iron ligands are completely conserved. These ligands coordinate the iron atom with an excellent octahedral geometry.

X-ray crystallographic studies show a U-shaped active site cavity lined with side chains from F353, M419, I418, and I593 of the reticulocyte 15*S*-LOX (Gillmor *et al.*, 1997; Borngraber *et al.*, 1999). The positional specificity of LOX is determined by the overall size and shape of this arachidonic acid binding pocket. This pocket is predicted to be a little bigger (6%) in leukocyte-type 12*S*-LOX than that of the reticulocyte 15*S*-LOX (Gillmor *et al.*, 1997; Borngraber *et al.*, 1999). Mutation of the pocket amino acids in human 15-LOX-1 to residues with smaller side chains increases the pocket volume, and converts the enzyme to an efficient 12-LOX (Sloane *et al.*, 1995). The opposite type of mutation can convert porcine leukocyte 12*S*-LOX to a 15-LOX (Suzuki *et al.*, 1994).

Receptors for mammalian LOX-derived products

The best recognized function of mammalian LOX is to produce ligands for cellular receptors. Currently, several receptors for 5-LOX-derived eicosanoids have been cloned.

LTB4 is a potent chemotactic compound and granulocyte activating factor. Two cell surface receptors for LTB4 (BLT1 and BLT2) have been isolated (Yokomizo *et al.*, 1997; Kamohara *et al.*, 2000; Yokomizo *et al.*, 2000). They are G-protein-coupled receptors (GPCR) and share about 45% amino acid identity. BLT1 is mainly expressed in

leukocytes and shows high affinity for LTB4, whereas BLT2 is expressed ubiquitously with the high expression in spleen, ovary, liver and leukocytes and shows low affinity for LTB4. The differences in tissue distribution and pharmacological characteristics of two LTB4 receptors suggest that they have different functions.

The CysLTs (LTC_4, D_4 and E_4) are inflammatory mediators. They were previously referred to as Slow Reacting Substance of Anaphylaxis (SRS-A). The action of CysLTs is through cell surface receptors. Pharmacological and binding studies in different tissues suggest there are two CysLT receptors, CysLT1 which is sensitive to the classical CysLT1 antagonists and CysLT2 which is resistant to these antagonists. The recent molecular cloning, expression and characterization of two CysLT receptors (CysLT1 and CysLT2) confirmed much of the earlier pharmacological characterization of the two receptors (Lynch *et al.*, 1999; Heise *et al.*, 2000). However, a third CysLT receptor subtype may exist based on some inconsistent pharmacological effects (Back *et al.*, 2000).

Lipoxins (LX) are eicosanoids containing trihydroxy and conjugated tetraene system. There are two forms of LXs that are positional isomers, LXA4 and LXB4. They are generated during the transcellular metabolism of arachidonic acid via the sequential actions of the 15- and 5- or 5- and 12-LOX enzymatic pathways (Serhan *et al.*, 1984; Samuelsson *et al.*, 1987a). Of the non-prostanoid eicosanoid receptors, the LXA_4 receptor (ALX) was the first recognized at the molecular level. It is also a GPCR (Fiore *et al.*, 1994). The putative receptor activated by LXB_4 has not been cloned.

For the other LOX products, the existence of cellular receptors has not been confirmed. Several reports suggested the presence of specific 12*S*-HETE and/or 15*S*-

HETE binding sites in some cell types (Gross *et al.*, 1988; Vonakis and Vanderhoek, 1992; Herbertsson and Hammarstrom, 1997). The function of these binding sites was indicated by the observation that psoriatic epidermal cells showed a fourfold decrease in the number of 12-HETE binding sites as compared with normal healthy individuals (Arenberger *et al.*, 1992). A reported 12-HETE binding site is cytosolic (Herbertsson and Hammarstrom, 1997). Nonetheless, there is evidence that cell surface HETE receptors might exist: The neuroprotective effect of 12*S*-HETE in rat exhibits a pertussis toxin-sensitive mechanism, implying the existence of a G-protein-coupled 12*S*-HETE receptor (Hampson and Grimaldi, 2002).

Some LOX products were studied for their activation of nuclear receptors. Peroxisome proliferator-activated receptors (PPARs) are members of the nuclear receptor superfamily and are expressed in a variety of tissues including skin and cells of the immune system. There are three types of PPARs: PPARα, PPARγ, and PPARβ/δ. They act as ligand-dependent transcription factors which heterodimerize with retinoid X receptors (RXR) to allow binding to and activation of PPAR responsive genes. Through this mechanism, PPAR ligands can control a wide range of physiological processes. A variety of LOX products were shown to bind and activate PPARs. For example, the mouse 8-LOX product, 8*S*-HETE, is a high affinity ligand for the PPARα whereas 8*R*-HETE was much less potent (Yu, K. *et al.*, 1995; Forman *et al.*, 1997; Kliewer *et al.*, 1997). The 5-LOX product, LTB4, was also shown to be an activating ligand for the same receptor (Devchand *et al.*, 1996). The 15-LOX-2 product, 15*S*-HETE, was reported as a ligand for PPARγ (Shappell, S.B. *et al.*, 2001a). However, the concentrations of these ligands needed for PPAR activation are in the micromolar range. Considering that

nanomolar concentrations of LTs and prostaglandins are sufficient for the activation of eicosanoid GPCRs, the physiological significance of these PPAR effects is questionable.

Biological functions of mammalian LOX enzymes

Inflammation

Among all the mammalian LOX enzymes, the biological function of 5-LOX is the best understood. The 5-LOX pathway leading to leukotriene formation has long been recognized as a proinflammatory cascade. LTB4 is a potent chemoattractant for neutrophils, eosinophils, and monocytes and has other potent proinflammatory properties (Ford-Hutchinson *et al.*, 1980). The cysteinyl LTs, LTC4, LTD4, and LTE4, are potent bronchoconstrictors that enhance vascular permeability and stimulate mucus secretion from the airways. They are active at nanomolar concentrations, being approximately 1000-fold more potent than histamine in eliciting airway constriction in vitro (Dahlen *et al.*, 1980; Lee *et al.*, 1984). The LT mediated effects cause increased activation, recruitment, migration and adhesion of immune cells. The use of mice deficient in 5-LOX, FLAP, LTA_4 hydrolase, LTC_4 synthase or LT receptors has enabled a detailed examination of the LTs in murine models, firmly establishing their roles in inflammation (Goulet *et al.*, 1994; Byrum *et al.*, 1997; Byrum *et al.*, 1999; Kanaoka *et al.*, 2001; Maekawa *et al.*, 2002; Beller *et al.*, 2004).

Leukotriene synthesis inhibitors (5-LOX inhibitors) such as zileuton (Zyflo) have been shown to possess therapeutic potential for the treatment of asthma, allergic disorders and other inflammatory diseases (Riccioni *et al.*, 2004). CysLT receptor antagonists such

as zafirlukast (Accolate) and montelukast (Singulair) are also widely used in long-term maintenance of asthma control (Riccioni *et al.*, 2004).

In addition to the 5-LOX products, there is the occasional reference linking the 12-LOX product, 12*S*-HETE, to inflammation. For example, this metabolite has direct chemotactic effect showing the most potent stimulatory effect on smooth muscle cell migration among the mono-HETEs (Nakao *et al.*, 1982).

Atherosclerosis

Atherosclerosis is now considered as an inflammatory disease (Lusis, 2000), which is caused by excessive and prolonged inflammatory responses. The ability to form inflammatory lipid mediators by LOX enzymes indicates an important function for these enzymes in the development and progression of atherosclerosis. This was first proposed following the observations of specific LOX products (HETEs and HODEs) in the early phase of atherosclerosis (Nakao *et al.*, 1982), along with protein and mRNA expression (Yla-Herttuala *et al.*, 1990; Hugou *et al.*, 1995).

12/15-LOX (human 15-LOX-1 and mouse leukocyte-type 12-LOX) was suggested to be involved in atherogenesis because of its ability to oxidize LDL (Belkner *et al.*, 1993). The oxidative modification of LDL has been considered to be an important factor in atherogenesis (Holvoet and Collen, 1994), but the mechanisms responsible for oxidation in vivo remain unknown. Previous studies have suggested that 12/15-LOX may be one of the factors involved since 13*S*-HPODE, the product of 12/15-LOX from linoleic acid, was found to be the predominant oxidized fatty acid on human monocyte-oxidized LDL (Folcik *et al.*, 1995).Treatment of human aortic endothelial cells with 12*S*-

HETE, the stereospecific product of the same enzyme from arachidonic acid, directly induced monocyte binding to the endothelial cells, which is a key early step in the development of atherosclerosis. No such effect was observed with the stereoisomer 12*R*-HETE (Patricia *et al.*, 1999; Reilly *et al.*, 2004). Higher levels of 15-LOX-1 enzymatic activity were also shown in the atherosclerotic lesions of rabbit and human aorta than corresponding normal arteries (Simon *et al.*, 1989). Transfer of the human 15-LOX-1 gene into rabbit iliac arteries results in the appearance of oxidation-specific lipid-protein adducts characteristic of oxidized LDL (Yla-Herttuala *et al.*, 1995), implicating 15-LOX-1 in the oxidative modification of LDL. However, the involvement of 15-LOX-1 in atherogenesis was demonstrated to be present only in early stage but not in later lesions, where oxidized lipids lost their stereospecificity and non-enzymatic lipid peroxidation occurred (Kuhn *et al.*, 1994b).

Animal models also implicate a key role of the 12/15-LOX in the pathogenesis of atherosclerosis. Overexpression of human 15-LOX-1 in the vascular endothelium could accelerate early atherosclerosis in LDL receptor-deficient mice (Harats *et al.*, 2000). Furthermore, treatment the rabbit with a specific 15-LOX-1 inhibitor, PD 146176, can significantly reduce the progression of diet-induced atherosclerosis (Sendobry *et al.*, 1997). Convincing evidence of 12/15-LOX in the pathogenesis of atherosclerosis came from the recent knock-out experiments showing that disruption of mouse leukocyte-type 12-LOX gene attenuates atherosclerosis in both apo E deficient mice and LDL receptor deficient mice (Cyrus *et al.*, 1999; George *et al.*, 2001), and this was attributed to reduced LDL oxidation and lipid peroxidation (Zhao and Funk, 2004). Paradoxically, however, a remaining enigma is that overexpression of human 15-LOX-1 in rabbits is resulted in

reduced atherosclerosis (Shen *et al.*, 1996). A possible explanation for this antiatherogenic effect of 15-LOX-1 is that the role of this enzyme may not be restricted to oxidative LDL modification. Its expression may impact both lipid uptake and intracellular lipid turnover (Belkner *et al.*, 2005).

5-LOX and its LT products may also contribute to atherosclerosis. LT production in atherosclerotic lesions was found to be increased when compared with normal tissue (De Caterina *et al.*, 1988). The direct evidence comes from the recent finding in animal model, which shows that 5-LOX is a major gene involved in the development of atherosclerotic lesions in mice (Mehrabian *et al.*, 2002). Specific LTB4 receptor antagonist can significantly inhibited atherosclerotic lesion development in atherosclerosis-susceptible apoE deficient and LDL-receptor knockout mice (Aiello *et al.*, 2002). LTB4 receptor BLT1 deficient mice had a significant reduction in atherosclerosis comparing to the wild-type mice, suggesting LTB4 contributes in a causal manner to mouse lesion formation (Heller *et al.*, 2005). In human beings, no such direct evidence suggests that 5-LOX can influence atherosclerosis. However, higher 5-LOX expression was detected within the arterial wall during atherogenesis (Spanbroek *et al.*, 2003). By studying the relationship between 5-LOX promoter genotypes and carotid-artery intima–media thickness (which is a marker of the atherosclerotic burden), it has been found that variation in the 5-LOX could alter eicosanoid-mediated inflammatory circuits in the artery wall and promote atherogenesis (Dwyer *et al.*, 2004).

Cancer

LOX enzymes and the signaling pathways involved in LOX activation are also important for carcinogenesis and tumor progression. The LOX enzymes with blood cell origin, such as 5-LOX, 12-LOX and 15-LOX-1, appear to have a pro-carcinogenic effect. Although 5-LOX mainly plays roles in inflammation, several precedents indicate its role in various types of cancers. A convincing example is in human pancreatic cancer tissues, where marked expression of 5-LOX or the receptor for its downstream metabolite, LTB4, was observed, but little or no expression can be seen in normal pancreatic tissues or cultured cells (Hennig *et al.*, 2002). The up-regulation of 5-LOX can be detected in all grades of human early pancreatic intraepithelial neoplasias and early lesions of pancreatic cancer in animal models (Hennig *et al.*, 2005), indicating that 5-LOX plays a key role in the development of pancreatic cancer. Similar to 5-LOX, platelet-type 12*S*-LOX expression in prostate cancer was elevated (Gao *et al.*, 1995). Its product, 12*S*-HETE, can block the induction of apoptosis by activating the transcription of bcl-2 (Tang, D.G. *et al.*, 1996). 12*S*-LOX and 12*S*-HETE were also found to stimulate angiogenesis, a process required for tumor growth and progression (Nie and Honn, 2004). Another LOX which has a pro-carcinogenic effect is the leukocyte-type 12*S*-LOX. Its expression was up-regulated in a transgenic mouse model of prostate carcinoma (Shappell, S. B. *et al.*, 2003). Over-expression of leukocyte-type 12*S*-LOX in tumor cells significantly extends cell survival and delays apoptosis (Pidgeon *et al.*, 2003). The human homolog of mouse leukocyte-type 12*S*-LOX, 15-LOX-1, was also up-regulated in prostate tumors and is implicated in tumorigenesis (Kelavkar *et al.*, 2002).

15-LOX-2, which nominally has the same product as 15-LOX-1, elicits different effect in tumor development. Down-regulation of 15-LOX-2 expression has been found in prostate adenocarcinoma (Shappell, S.B. *et al.*, 1999), suggesting a possible anti-tumorigenic effect of this enzyme. In addition to 15-LOX-2, recent evidence suggests that other LOX enzymes with epithelium origin also play an anti-carcinogenic role. For example, mouse epidermis-type 12*S*-LOX was found to be down-regulated during mouse skin carcinogenesis (Muller *et al.*, 2002). Mouse 8*S*-LOX is a homolog of human 15-LOX-2. In normal mouse skin, the level of 8*S*-LOX expression as well as its product, 8*S*-HETE, is nearly undetectable. Skin-targeted 8*S*-LOX transgenic mice significantly reduce the papilloma development in mouse skin carcinogenesis (Kim *et al.*, 2005). Recently, Krieg and colleagues found that inducible expression of human 15-LOX-2 and mouse 8-LOX inhibits the growth of premalignant mouse keratinocytes (Schweiger *et al.*, 2005).

Potential roles of mammalian LOX enzymes in skin

Skin displays a highly active metabolism of essential fatty acids (EFAs). The relationship between EFA deficiency and the scaly skin phenotype has been described above. However, so far no good evidence is available to determine how EFA metabolism affects skin physiology and causes a scaly skin phenotype. Although COX enzymes and their prostaglandin products have been detected in skin and somewhat associated with keratinocyte differentiation (Leong *et al.*, 1996) and development of skin cancer (Buckman *et al.*, 1998), generally NSAID inhibitors do not influence EFA-related symptoms, and the LOX pathways are considered the more important for skin physiology.

High levels of LOX products have been detected in normal skin. Unusual production of these metabolites in skin diseases suggests the importance of LOX enzymes.

Psoriasis is a common and chronic skin disorder. Psoriatic skin is characterized by keratinocyte hyperproliferation, inflammation and impaired differentiation. The lesions are infiltrated, scaly and erythematous. Psoriasis is usually considered as an inflammatory skin disease. LOX enzymes may play an important role in the pathogenesis of psoriasis because of the presence of their products in the lesional skin. For example, release of LTB4 in biologically active concentrations from psoriatic epidermis has been reported (Brain *et al.*, 1984). Single topical applications of LTB4 to normal human skin result in the formation of intraepidermal microabscesses (Camp *et al.*, 1984), which is one of the earliest and characteristic morphologic events in psoriasis. In psoriatic patients a significant increase in cysteinyl leukotrienes has also been found when comparing to the healthy human volunteers (Fauler *et al.*, 1992). However, selective leukotriene biosynthesis inhibitors have no therapeutic utility in psoriasis (Ford-Hutchinson, 1993), indicating that 5-LOX is not important for the treatment of this disease.

In psoriatic skin one of the most prominent eicosanoids is 12-HETE. It is present in much higher concentration in chronic psoriatic plaques compared with normal skin, and consists predominantly of 12*R*-HETE (Woollard, 1986). Thus the enzyme producing this stereospecific eicosanoid, 12*R*-LOX, has gained more interest.

The genetic evidence of an involvement of LOX enzymes in skin pathophysiology was provided by the hallmark study of Fischer and colleagues in 2002: "Lipoxygenase-3 (ALOXE3) and 12(R)-lipoxygenase (ALOX12B) are mutated in non-bullous congenital ichthyosiform erythroderma (NCIE) linked to chromosome 17p13.1"

(Jobard *et al.*, 2002). NCIE is a major subtype of autosomal recessive congenital ichthyosis characterized by a generalized ichthyosiform (scaly skin) phenotype (Webster *et al.*, 1978; Akiyama *et al.*, 2003). The scaling of the skin is caused by a failure of the keratinocytes to correctly differentiate when forming the permeability barrier of human skin in conjunction with an accelerated mitotic rate in the epidermis (Fartasch, 1997; Elias *et al.*, 2002; Kalinin *et al.*, 2002; Madison, 2003). The authors found that one or other of these two LOX genes was mutated in this group of patients, and they speculated that the two enzymes operate in the same metabolic pathway. Many of the studies to be described in this thesis are new developments stemming from these seminal observations.

Specific Aims

Although eLOX3 is clearly a member of the LOX gene family, it does not have the LOX activity predicted from proteomic analysis. Prompted by the genetic findings we examined eLOX3 for the ability to metabolize the products of other LOX enzymes. Our specific aims include:

1. To characterize the catalytic activity of eLOX3 and the further metabolism of its products.

2. To determine the functional relationship between 12*R*-LOX and eLOX3 and the effect of naturally occurring mutations.

3. To investigate differences in human and mouse eLOX3 catalytic activity.

4. To determine the targets and biological activities of the 12*R*-LOX and eLOX3 derived products.

CHAPTER II

IDENTIFICATION OF THE CATALYTIC ACTIVITY OF A NOVEL HUMAN EPIDERMAL LIPOXYGENASE, eLOX3

Introduction

LOX enzymes are found widely in plants, fungi and animals (Brash, 1999). They consist of a family of non-heme iron-containing enzymes which oxygenate polyunsaturated fatty acids such as arachidonic acid and linoleic acid to their specific hydroperoxide derivatives. A typical LOX catalysis includes a Fe^{2+}/Fe^{3+} redox cycle. The Fe^{3+} enzyme is the active form that performs the stereospecific hydrogen abstraction from the *bis*-allylic methylene of the fatty acid substrate. The redox cycle is completed by the oxygenation of the fatty acid radical and then reduction of the formed peroxyl radical to the fatty acid hydroperoxide. In a cellular environment the hydroperoxide products are unstable and readily reduced to the corresponding hydroxy derivatives (eg. HETE) by cytosolic glutathione peroxidases or converted into other bioactive lipid mediators including leukotrienes, lipoxins (Samuelsson *et al.*, 1987a) and hepoxilins (Pace-Asciak, C.R. and Asotra, 1989).

Although LOX enzymes are catalytically active with free fatty acid substrates, some will also oxygenate esterified substrates such as the phospholipid or cholesterol esters. In certain cases the hydroperoxide products can be further metabolized by the same enzyme to form di-hydroperoxides or epoxides. The well-known example for the latter is the mammalian 5-LOX, which contains both oxygenase and LTA4 synthase

activities, and performs two consecutive hydrogen abstractions to form the epoxide, LTA4.

There are five active lipoxygenases found in human beings: 5-LOX, 12*S*-LOX, 12*R*-LOX, 15-LOX-1, and 15-LOX-2. A sixth gene family member, epidermis-type lipoxygenase-3 (eLOX3, gene symbol *ALOXE3*) was described first in the mouse and in 2001, in human (Kinzig *et al.*, 1999; Krieg *et al.*, 2001). The amino acid sequence of human eLOX3 shows the closest similarity to 12*R*-LOX (54% identity) and 15-LOX-2 (51%). It contains the characteristic well-conserved amino acid residues found in all LOX enzymes, including the putative iron-binding ligands and additional structure-determining residues. These features clearly indicate that eLOX3 belongs to the LOX gene family. The question of the catalytic activity of eLOX3 has, nonetheless, remained elusive. No enzymatic activity has been detected using linoleic or arachidonic acids, the prototypical C18 and C20 LOX substrates, nor with methyl arachidonate or cholesteryl arachidonate (Kinzig *et al.*, 1999). However, the hydroperoxide products of other LOX enzymes have never been tested.

Studies in humans and mice indicate that eLOX3 has a limited scope of tissue expression, being mainly confined to keratinized epithelia such as skin (Krieg *et al.*, 2001). Although no catalytic activity has been detected, eLOX3 function in skin pathophysiology was strongly suggested by a recent genetic study reporting that eLOX3 or 12*R*-LOX are mutated in six families affected by non-bullous congenital ichthyosiform erythroderma (NCIE), which is a major subtype of autosomal recessive congenital ichthyosis characterized by a generalized ichthyosiform (scaly skin) phenotype (Jobard *et al.*, 2002). The authors speculated that the two enzymes operate in the same metabolic

pathway. This hypothesis is consistent with the expression pattern of eLOX3. From PCR evidence it appears to be co-expressed only in tissues that express the 12*R*-LOX (Krieg *et al.*, 2001).

Prompted by the genetic findings, in this study we tested the eLOX3 catalytic activity for the ability to metabolize the products of other LOX enzymes.

Experimental Procedures

Expression and purification of human eLOX3

The cDNA for human eLOX3 was cloned by PCR with cDNA prepared from human keratinocytes. To prepare the eLOX3 protein with an N-terminal $(His)_6$ tag, the eLOX3 cDNA was subcloned into the pET3a expression vector (Novagen, Madison, WI) with the 5' sequence encoded as ATG CAT CAC CAT CAC CAT CAC GCA-, with the last codon representing the start of the wild type enzyme. The human eLOX3 was expressed in *E. coli* BL21 (DE3) cells (Novagen, Madison, WI) and the $(His)_6$ tagged protein was purified on Ni-NTA agarose (Qiagen, Valencia, CA) according to the manufacturer's instructions. Fractions of 0.5 ml were collected off the affinity column and assayed by using SDS/PAGE. Fractions containing eLOX3 were pooled and dialyzed against a buffer of 50 mM Tris (pH 7.5) containing 300 mM NaCl to remove the imidazole.

Preparation of hydroperoxides

HPETEs with specific positional and stereo configurations were prepared from arachidonate methyl ester by the following route: (i) autoxidation of 500 mg arachidonate methyl ester (Nu Chek Prep, Elysian, MN) in the presence of 70 mg α-tocopherol (Sigma Chemical Company, St. Louis, MO) at 37 °C for 3 days replenishing oxygen every 24 hours (Peers and Coxon, 1983); (ii) dissolving the autoxidation product in 5 ml 5% ethyl acetate in hexane and incubation at -30 °C overnight to allow the α-tocopherol phase to separate from the hexane phase (upper phase, clear, containing HPETE methyl esters); (iii) isolation and purification of HPETE methyl esters by using an Econosil Silica 10u column (2.25 × 25 cm) and eluted at flow rate of 7 ml/min with the program: 0-5 min, 5% ethyl acetate in hexane; 5-125 min, linear gradient from 5% to 15% ethyl acetate in hexane; the HPETE methyl esters come out between 50 min and 75 min in following sequence: 15-, 12-, 11-, 8-, 9-, and 5-HPETE-Me; (iv) resolution of *R*- and *S*-HPETE methyl esters using a Chiralpak AD-RH column, eluted with a solvent of methanol/water 88:12 by volume, and a flow rate of 1 ml/min; the *R* enantiomer eluted earlier than the *S* enantiomer; (v) preparation of the free acids by treatment with 0.5 M KOH in water/methanol/ dichloromethane (1:1:0.1) at room temperature for 30 min, followed by acidification to pH 6.0 and extraction into dichloromethane; (vi) final purification of the free acids by SP-HPLC (Alltech Econosil Silica column, solvent system of hexane/isopropanol/acetic acid 100:1:0.1 by volume, flow rate of 2 ml/min).

[^{18}O]15*S*-HPETE was prepared from arachidonic acid using soybean lipoxygenase (Sigma type V) under an atmosphere of $^{18}O_2$ (Isotec Inc., Miamisburg, OH).

eLOX3 activity assay

Incubation with the purified enzyme was typically conducted in 500 μl incubation buffer (50 mM Tris, 150 mM NaCl, pH 7.5) using 0.01 – 0.1 μM enzyme concentration in a 1 cm path length microcuvette. 5-10 μg HPETE was added and incubated at room temperature for 10 min. eLOX3 activity was monitored by repetitive scanning in the range 350 - 200 nm, or by monitoring disappearance of the signal at 235 nm in the time-drive mode. To measure the rate of eLOX3 reaction over the substrate concentration range of 5 – 250 μM, reactions were conducted in a 2 mm path length microcuvette (0.5 ml); the decrease of absorbance at 235 nm was followed, and the rate was calculated from the initial linear part of the curve.

HPLC analysis

Products of the eLOX3 reactions with HPETE substrates were analyzed initially by RP-HPLC using a Waters Symmetry C18 5-μm column (0.46 × 25 cm) eluted at a flow rate of 1 ml/min with methanol/water/acetic acid (80:20:0.01 by volume), and UV detection at 205, 220, 235, and 270 nm using an Agilent 1100 series diode array detector. The main products were recovered from the reversed-phase solvent by the addition of water and extraction with dichloromethane. Further purification was carried out by SP-HPLC using an Alltech Econosil Silica column (0.46 × 25 cm), a solvent system of hexane/isopropanol/acetic acid (100:2:0.1 by volume), and a flow rate of 1 ml/min.

Derivatization

Methyl esters of the products were prepared using ethereal diazomethane/methanol (5:1); pentafluorobenzyl esters were prepared using the method of Greeley (Greeley, 1974). Catalytic hydrogenations were performed in 100 µl of ethanol using about 1 mg of palladium on alumina and bubbling with hydrogen for 2 min at room temperature. Reactions were terminated by the addition of water and extraction with ethyl acetate. Trimethylsilyl ester and trimethylsilyl ether derivatives were prepared by treatment overnight with *bis*(trimethylsilyl)trifluoracetamide (10 µl) and pyridine (5 µl) at room temperature. Subsequently, the reagents were evaporated under a stream of nitrogen and the samples were dissolved in hexane for GC-MS.

GC-MS analysis

Analysis of the methyl ester trimethylsilyl ether derivatives of the products was carried out in the positive ion electron impact mode (70 eV) using a Hewlett-Packard 5989A mass spectrometer coupled to a Hewlett-Packard 5890 gas chromatograph equipped with a RTX-1701 fused silica capillary column (17 m × 0.25 mm, internal diameter). Samples were injected at 150°C, and after 1 min the temperature was programmed to 300°C at 12 or 20°C/min. For analysis of ^{18}O content of 15-HETE and its epoxyalcohol product, samples were analyzed as the pentafluorobenzyl (PFB) ester trimethylsilyl ether derivatives in the negative ion-chemical ionization mode. Rapid repetitive scanning was carried out over the mass ranges covering the [M-PFB] ions of the unlabeled and ^{18}O-labeled species (*m/z* 388-399 for the HETE derivative, and *m/z*

405-415 for the epoxyalcohol). Spectra collected during elution of the GC peak (typically about 20 spectra) were averaged for calculation of the isotopic compositions.

NMR

^{1}H NMR and 2D (H,H-COSY) NMR spectra were recorded on a Bruker DRX 400 MHz spectrometer. The ppm values are reported relative to residual non-deuterated solvent (δ = 7.24 ppm for C_6H_6; δ = 1.92 ppm for CD_3CN).

CD spectroscopy

The methyl ester of the product from 12*R*-HPETE (25 μg) was dissolved in 50 μl of dry acetonitrile and reacted with 1 μl of benzoyl chloride in the presence of 1 μl DBU and a few grains of dimethylaminopyridine at room temperature overnight. After evaporation of the solvent, 500 μl of water were added and the product was extracted with 1 ml of dichloromethane. The methyl ester, benzoate was isolated by RP-HPLC using a Waters Symmetry C18 5-μm column (0.46 x 25 cm) eluted with a solvent of methanol/water/acetic acid (95:5:0.01 by volume) at a flow rate of 1 ml/min and UV detection at 235 nm. The product eluting at 6.7 min was collected and extracted from the HPLC solvent using dichloromethane. Its structure was confirmed by ^{1}H-NMR (400 MHz, in CD_3CN).

The methyl ester, benzoate derivative was dissolved in acetonitrile to a final OD of 1 AU at 226 nm. CD spectra were recorded on a JASCO J-700 spectropolarimeter. Hydroxyl chirality of the main product from 12*R*-HPETE was assigned from the Cotton effects on the benzoate ester derivative (Schneider *et al.*, 1997; Schneider *et al.*, 2001b).

The benzoate derivative was selected because its longitudinal transition moment is sufficiently close to that of the adjacent double bond in the fatty acid carbon chain to allow for an efficient coupling of the double bond and benzoate chromophores (Humpf *et al.*, 1995). Due to the relatively low λ_{max} of both chromophores only the first Cotton effect at around 227 nm is observed, which, however, is sufficient to determine the absolute configuration of the molecule (Gonnella *et al.*, 1982; Humpf *et al.*, 1995).

Results

Lack of lipoxygenase activity of eLOX3

To investigate the catalytic activity of eLOX3 toward the oxygenation of fatty acid substrates, the mouse and human eLOX3 were both expressed in HeLa cells and in a bacterial system using *E. coli*. For the incubations, HeLa cell homogenates were used directly while the enzyme from bacterial expression was used after affinity purification. In the incubations labeled and unlabeled fatty acids and derivatives were tested, and the product formation was analyzed using RP-HPLC. The following substrates were tested and found not be oxygenated by the mouse or human eLOX3: linoleic, arachidonic, and eicosapentaenoic acids, the methyl esters of arachidonic acid and linoleic acid, arachidonyl phosphatidylcholine, anandamide, and the cholesteryl ester of arachidonic acid. Because the activity of the related human 12*R*-LOX was found to have a narrow pH optimum at slightly acidic pH (Schneider *et al.*, 2001a), radiolabeled linoleic and arachidonic acids (50 μM) were used at pH values of 6, 7, and 8 of the incubation buffer, but again, no oxygenated products could be detected. These results confirm and extend the findings of Krieg, Fürstenberger and colleagues who previously reported the absence of detectable oxygenation of various polyunsaturated fatty acid substrates using the mouse eLOX3 expressed in HEK 293 cells (Kinzig *et al.*, 1999).

The reaction of eLOX3 with HPETEs

To test whether human eLOX3 can react with the hydroperoxy fatty acid products of other lipoxygenases, individual HPETE or HPODE isomers (50-75 μM) were

incubated in a microcuvette at room temperature with human eLOX3 (1-4 μg/ml protein, ≈12-50 nM) and the UV spectrum was monitored at different reaction times. Figure 5 shows the incubation of 12*R*-HPETE with human eLOX3. The characteristic absorbance of the 12*R*-HPETE substrate decreased during the incubation. This decreased absorbance at 235 nm was accompanied by a lesser rise in the UV absorbance at 285 nm. The reaction rate was dependent on the amount of enzyme used. Controls lacking enzyme showed no effect. Heat-pretreatment (60°C, 10 min) of the enzyme impaired the activity. When the enzyme was placed in boiling water for 10 min before the incubation, almost no change in the absorbance at 235 nm was detected (Figure 6). These experiments demonstrate that eLOX3 can react with the typical LOX-derived HPETEs and that this activity is thermally-inactivated.

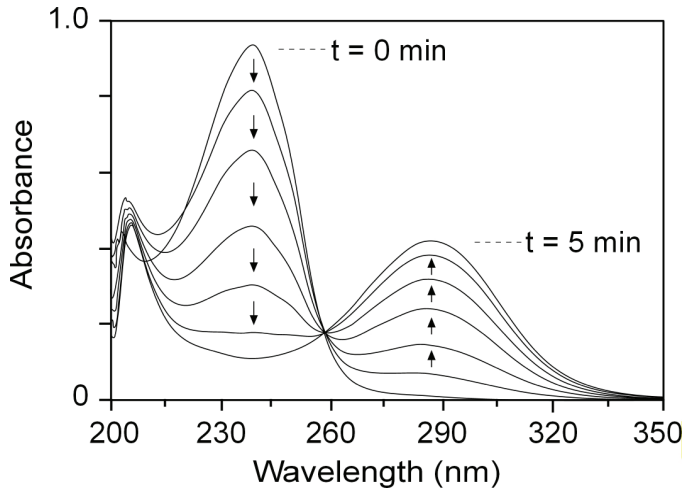

Figure 5. Overlay of UV spectra of eLOX3 reaction with 12*R*-HPETE. Human eLOX3 (0.05 μM) was incubated with 12*R*-HPETE (40 μM) in a 500 μl cuvette at room temperature. The sample was scanned from 350 nm to 200 nm before addition of enzyme (t = 0 min), and then immediately after mixing (about 15 sec), and at reaction times of 1, 2, 3, 4 and 5 min. The arrows indicate the decreasing absorbance at 235 nm and the increase at 285 nm during the reaction.

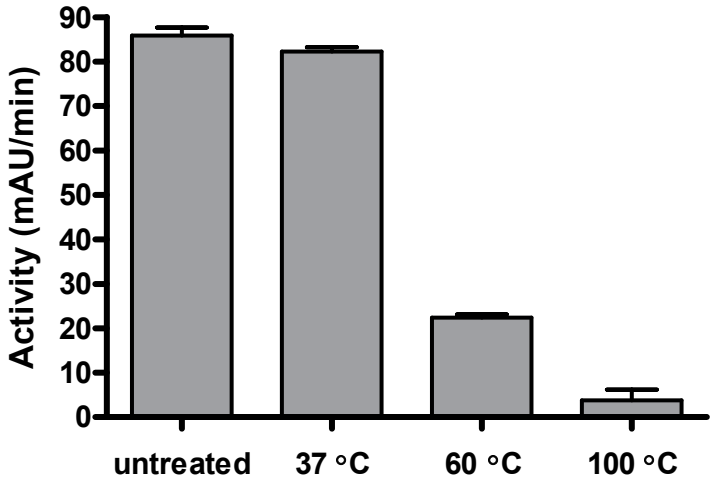

Figure 6. Thermal inactivation of eLOX3 activity. 12*R*-HPETE (30 μm) was used as substrate with 0.025 μM of eLOX3 enzyme in the spectrophotometric assay. The enzyme was either untreated (control), or pretreated at 37°C, 60°C, or 100°C for 10 min. Activity was determined by the initial rate of the UV absorbance decrease at 235 nm.

Since human eLOX3 has tissue expression limited to skin, the natural HPETEs which were formed by skin LOX enzymes (12*R*-HPETE, 12*S*-HPETE and 15*S*-HPETE) were tested in kinetic studies (Figure 7). At the same enzyme and substrate concentration, different HPETEs showed different rates of reaction, with 12*R*-HPETE being the best substrate tested (Figure 7). Initial rates for 12*R*-HPETE metabolism corresponded to approximately five turnovers/sec. 12*S*-HPETE, 15*S*-HPETE were converted at 5- to 7-fold lower rates, with reaction continuing for over an hour. The kinetic parameters for the conversion of HPETE substrates are summarized in Table 1. Other fatty acid hydroperoxides including the other nine hydroperoxides of arachidonic acid (5*R*-, 5*S*-, 8*R*-, 8*S*-, 9*R*-, 9*S*-, 11*R*-, 11*S*, and 15*R*-HPETE) and four hydroperoxides of linoleic acid (9*R*-, 9*S*-, 13*R*-, and 13*S*-HPODE) were also tested as substrates. All of them can react

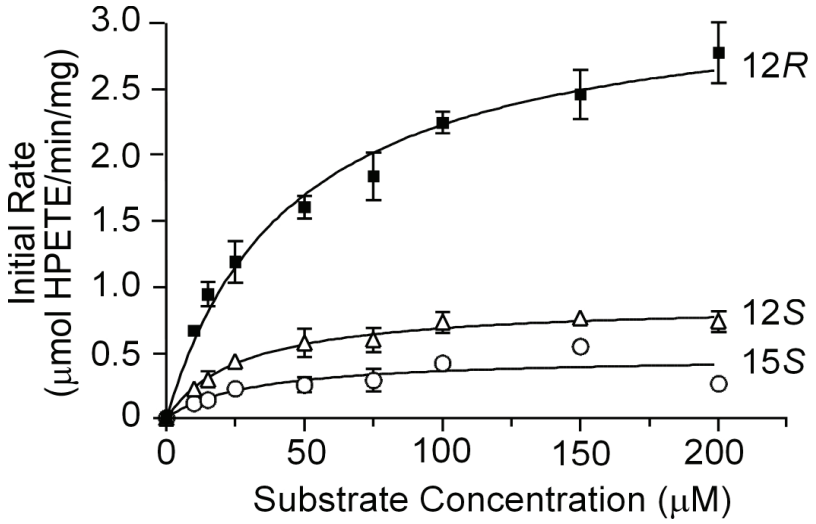

Figure 7. Reaction of human eLOX3 with 12*R*-, 12*S*-, and 15*S*-HPETE. Rates were measured by continuous recording of the decrease in absorbance at 235 nm. Reactions were carried out in a 0.2 cm path length microcuvette to allow measurement of the higher substrate concentrations.

Table 1. Kinetic parameters V_{max} (maximum rate) and K_m (Michaelis constant) for the conversion of HPETE substrates by eLOX3. Values given are the mean of three determinations ± S.D.

substrate	V_{max} (mAU/min)	K_m (μM)
12*R*-HPETE	29.7 ± 1.3	45.9 ± 5.5
12*S*-HPETE	7.9 ± 0.4	27.8 ± 4.4
15*S*-HPETE	4.3 ± 0.5	31.6 ± 13.0

with human eLOX3, with rates similar to or lower than 12*S*- and 15*S*-HPETE (data not shown).

The reaction of 12*R*-HPETE with eLOX3 was monitored at pH 7.5 or pH 6. Reactions proceeded similarly, with slightly more ketodiene chromophore appearing at pH 7.5, and, significantly, with similar rates at the two pH values. The lower pH value was tested because this corresponds to the pH optimum of human 12*R*-LOX in the conversion of arachidonic acid to the 12*R* hydroperoxide (Schneider *et al.*, 2001a). This may have physiological significance, given the evidence for an acidic environment in epidermis where 12*R*-LOX and eLOX3 are expressed (Rippke *et al.*, 2002).

RP-HPLC analysis of eLOX3 reaction products

The products of eLOX3 reactions were extracted and analyzed by RP-HPLC (Figure 8). A typical chromatogram from 12*R*-HPETE incubations (Figure 8, panel A) is dominated by a main product with retention time of ≈10 min that displayed only end absorbance in the UV (205 nm signal). A second product that eluted near 18 min had the UV spectrum of a conjugated dienone with λmax at 285 nm in the reversed-phase column solvent. Treatment of this product with $NaBH_4$ yielded a product that co-chromatographed on RP-HPLC with a 12-HETE standard, which, in accord with the UV spectrum and the mobility on RP-HPLC, points to this product being 12-ketoeicosa-5*Z*, 8*Z*,10*E*,14*Z*-tetraenoic acid (12-KETE). GC-MS analysis (electron impact mode) of the hydrogenated methyl ester derivative (Figure 9) gave a mass spectrum with structurally significant ions at *m*/*z* 341 $[M+1]^+$, 309 $[M\text{-}OCH_3]^+$, 141 (C12 – C20, $[COC_7H_{14}CH_3]^+$), 227 (C1 – C12, $[CH_3CO_2C_{10}H_{20}CO]^+$), 184 (C1 – C10, $[CH_3CO_2C_8H_{16}CH]^{\bullet +}$), 156 (C11

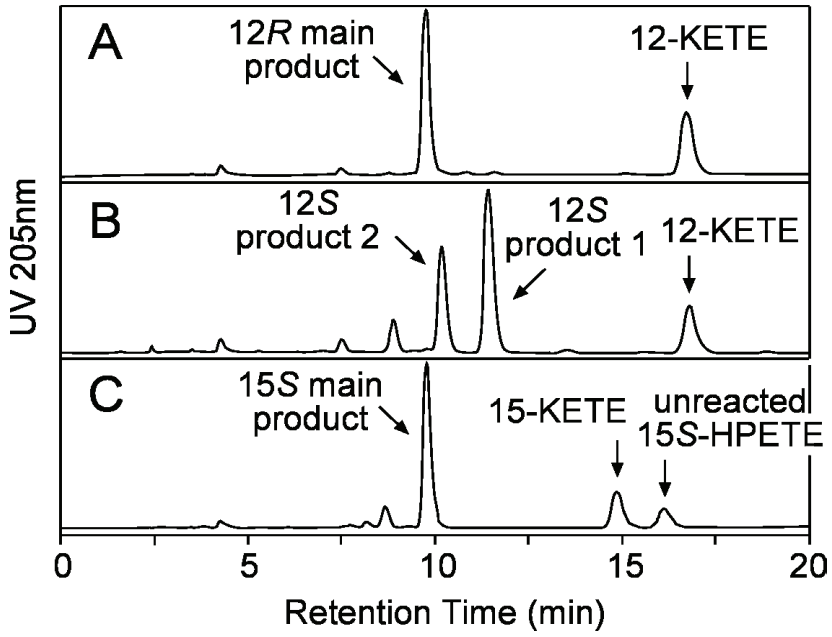

Figure 8. RP-HPLC analysis of the products in eLOX3 reactions. (A) 12*R*-HPETE + eLOX3. (B) 12*S*-HPETE + eLOX3. (C) 15*S*-HPETE + eLOX3. The products were analyzed by RP-HPLC using a Waters Symmetry C18 5μm column (0.46 x 25 cm) eluted at a flow rate of 1 ml/min with methanol/water/acetic acid (80:20:0.01 by volume), and UV detection at 205 nm. In panels A and B, the 12*R*-HPETE or 12*S*-HPETE substrate (retention time 18 min) was completely converted and does not appear on the chromatograms.

– C20, $[CH_3COC_7H_{14}CH_3]^+$), 242 (C1 – C13, $[CH_3CO_2C_{10}H_{20}COCH_3]^+$), and 98 (C14 – C20, $[CHC_5H_{10}CH_3]^{\bullet +}$). The spectrum is completely consistent with a structure of methyl 12-KETE; the ions at *m*/*z* 141 and 227 indicate α-cleavage of the 12-keto group and the last four fragments are derived from β-cleavage. The mass spectrum showed the predicted shifts in major ion fragments compared to the reported spectrum of methyl 15-KETE (Hamberg and Samuelsson, 1967).

The RP-HPLC chromatogram from incubation of 12*S*-HPETE with eLOX3 (Figure 8, panel B) was more complex, with a series of peaks at retention times of 7 – 9 min, the major product at 12 min, the second major product at 10.5 min, and a peak of

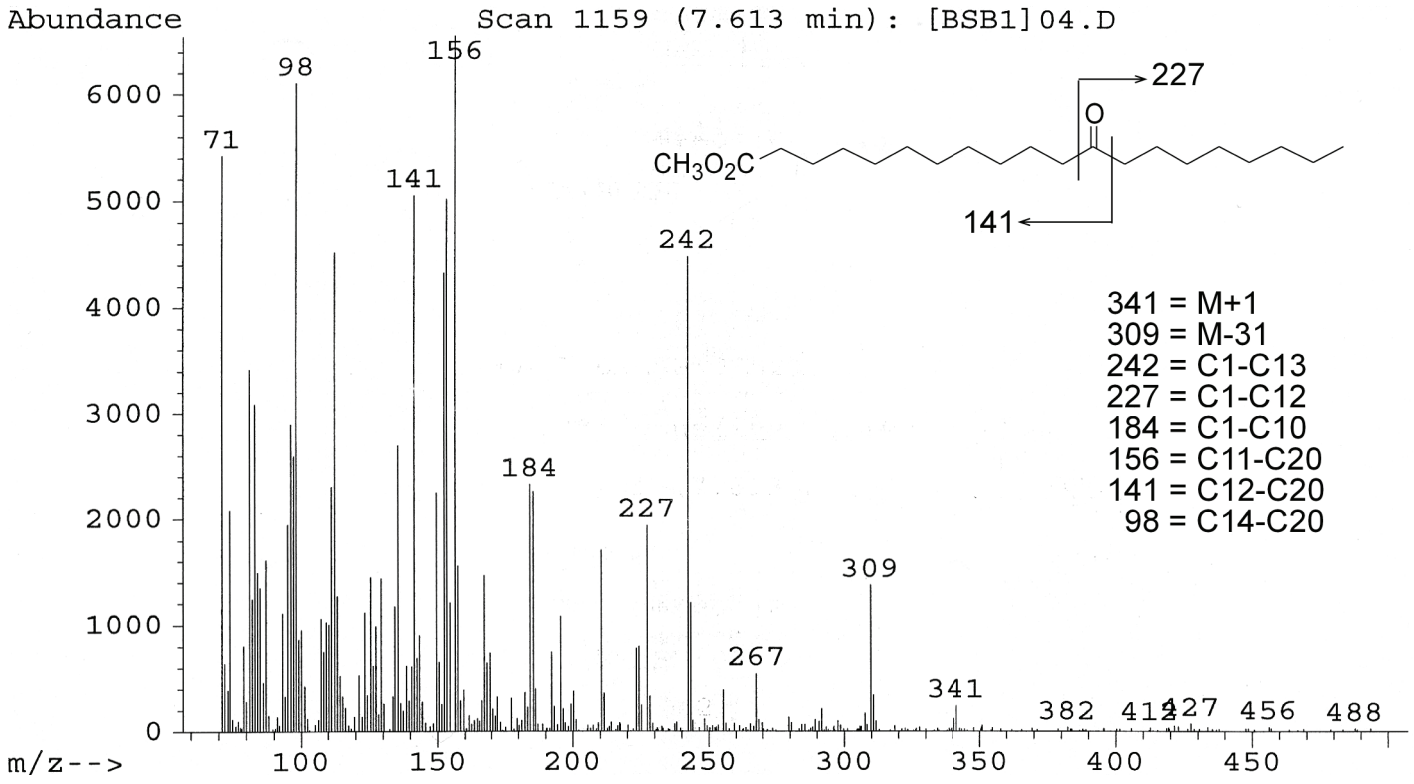

Figure 9. EI mass spectrum of the hydrogenated methyl ester derivative of the keto product formed from the reaction of 12*R*-HPETE with human eLOX3.

12-KETE (identified as above) near 17 min. The very small peaks at 7 - 8 min retention time had the UV spectra of conjugated trienes, whereas the peaks at 9 - 12 min, including the two major products, showed only end absorbance in the UV.

The chromatogram from the 15*S*-HPETE incubation (Figure 8, panel C) showed a main product at ≈10 min with additional earlier peaks at 7.5 - 9 min, all displaying only end absorbance in the UV. A minor peak at ≈15 min was identified as 15-ketoeicosa-5*Z*,8*Z*,11*Z*,13*E*-tetraenoic acid (15-KETE) by comparison to an authentic standard and by its conversion to 15-HETE upon treatment with $NaBH_4$. Some unreacted 15*S*-HPETE is also seen as the last eluting peak on the chromatogram. The corresponding HETE was not a product in any of the eLOX3 reactions analyzed.

Identification of the main product from 12*R*-HPETE

To prepare sufficient product for NMR analysis, 1.5 mg 12*R*-HPETE was incubated in 25 ml incubation buffer with 0.1 μM eLOX3. After collection of the main product from RP-HPLC, it was re-purified using SP-HPLC, where it also chromatographed as a single peak.

GC-MS analysis of the purified main product from 12*R*-HPETE was associated with issues of stability on GC, including the appearance of multiple GC peaks with very similar mass spectra. We attribute this to isomerization of the sample. (From the proposed configuration of this product as shown in Figure 12A, it is very possible that this isomerization occurs on the 9,10*trans* double bond and/or the 11,12*trans* epoxide moieties.) GC-MS of the methyl ester trimethylsilyl (TMS) ether derivative on a ThermoFinnigan Trace DSQ instrument equipped with a Restek Corporation (Bellefonte,

PA) Rtx-1 15 meter non-polar GC column (injection port temperature 260°C, initial column temperature 150°C, after 1 min temperature programmed at 10°C/min) showed three GC peaks with very similar mass spectra eluting at 11-12 minutes, with approximate peak areas of 1:1:4, respectively, in order of elution. Their retention times measured as C-values in comparison to fatty acid methyl esters, were 22.2, 22.8 and 23.0, as determined on a separate isothermal run at 200°C. Use of a lower injection port temperature (200°C) and isothermal GC conditions (200°C) reduced the prominence of the two earlier-eluting peaks. (On a different GC-MS system, HP5989A, with even more evidence of thermal instability, the early-eluting peak was the most prominent.) We conclude that the last eluting peak is most likely the non-isomerized product. The electron impact mass spectrum of this major GC peak is shown in Figure 10. The other two peaks showed the identical major diagnostic ions and almost indistinguishable mass spectra with the exception of a rearrangement ion at m/z 171. The ion at m/z 171 is retained at 171 in the ethyl ester TMS ether derivative, it is shifted to m/z 180 in the d_9-TMS derivative; it is formed by rearrangement, is not structurally diagnostic, and may have a formula of $[C_6H_{10}\text{-OTMS}]^+$. In the earliest eluting GC peak, m/z 171 was the base peak of the mass spectrum. In the second peak, eluting just before the main peak, m/z 171 has less than 30% relative abundance, while in the main peak, as shown in Figure 10, it is of medium prominence.

GC-MS analysis (electron impact mode) of the main peak gave a mass spectrum of the methyl ester trimethylsilyl ether derivative with structurally significant ions (with assignment and relative abundance in brackets) at *m/z* 422 (M^+, 0.1%), 407 (M-15, 3%), 281 {C8-C20, $[HCOSi(CH_3)_3\ C_2H_2C_2H_2OC_8H_{15}]^+$, 74%}, and 243 {C1-C8, $[CH_3CO_2$

$C_6H_{10}CHOSi(CH_3)_3]^+$, 14%}, the two together indicating a C-8 hydroxyl and a base peak at *m/z* 73 (100%) (Figure 10). After hydrogenation, the high-mass ions shifted by 6 mass units (*m/z* 413, M-15, 10% abundance; and *m/z* 397, M-31, 0.5%), whereas the two α-cleavage ions around C-8 appeared at *m/z* 285 (281 + 4) (100%), and 245 (243 + 2) (98%) (Figure 11). When considered together with the (lack of) UV spectral characteristics, the structure based on the GC-MS data is compatible with a C20 fatty acid methyl ester containing a C-8 hydroxyl, an epoxide moiety, and three double bonds. The spectrum of the nonhydrogenated product showed the same major cleavage ions as an uncharacterized isomer of 8-hydroxy-11,12-epoxyeicosa-5,9,14-trienoic acid (hepoxilin A_3) (Pace-Asciak, C.R. *et al.*, 1983).

GC-MS of the hydrogenated product, as the methyl ester TMS ether derivative, gave a second GC peak which eluted shortly after the epoxyalcohol on the non-polar GC column. Its mass spectrum showed diagnostic ions at m/z 502 (M+, <0.1% relative abundance), m/z 487 (M-15, <0.5%), and major α-cleavage ions at m/z 389 (C1-C12, 22%), 359 (C8-C20, 22%), 245 (C1-C8, 70%), and 215 (C12-C20, 60%), with the base peak at m/z 73. The spectrum clearly indicates a structure of an 8,12-dihydroxyeicosanaote as the methyl ester TMS ether derivative, as expected from opening of the epoxide during hydrogenation (Anton *et al.*, 1998).

^{1}H-NMR (400 MHz, in deuterated benzene), Figure 12B and Table 2, defined the complete covalent structure of the product as a single diastereomer of 8-hydroxy-11*R*,12*R*-epoxyeicosa-5,9*E*,14-trienoic acid (Figure 12A). All proton signals were assigned by H,H-COSY analysis (Figure 12C). The coupling constant between the epoxide protons H11 and H12 (J ≈ 2 Hz) indicates the *trans* configuration of the 11,12-

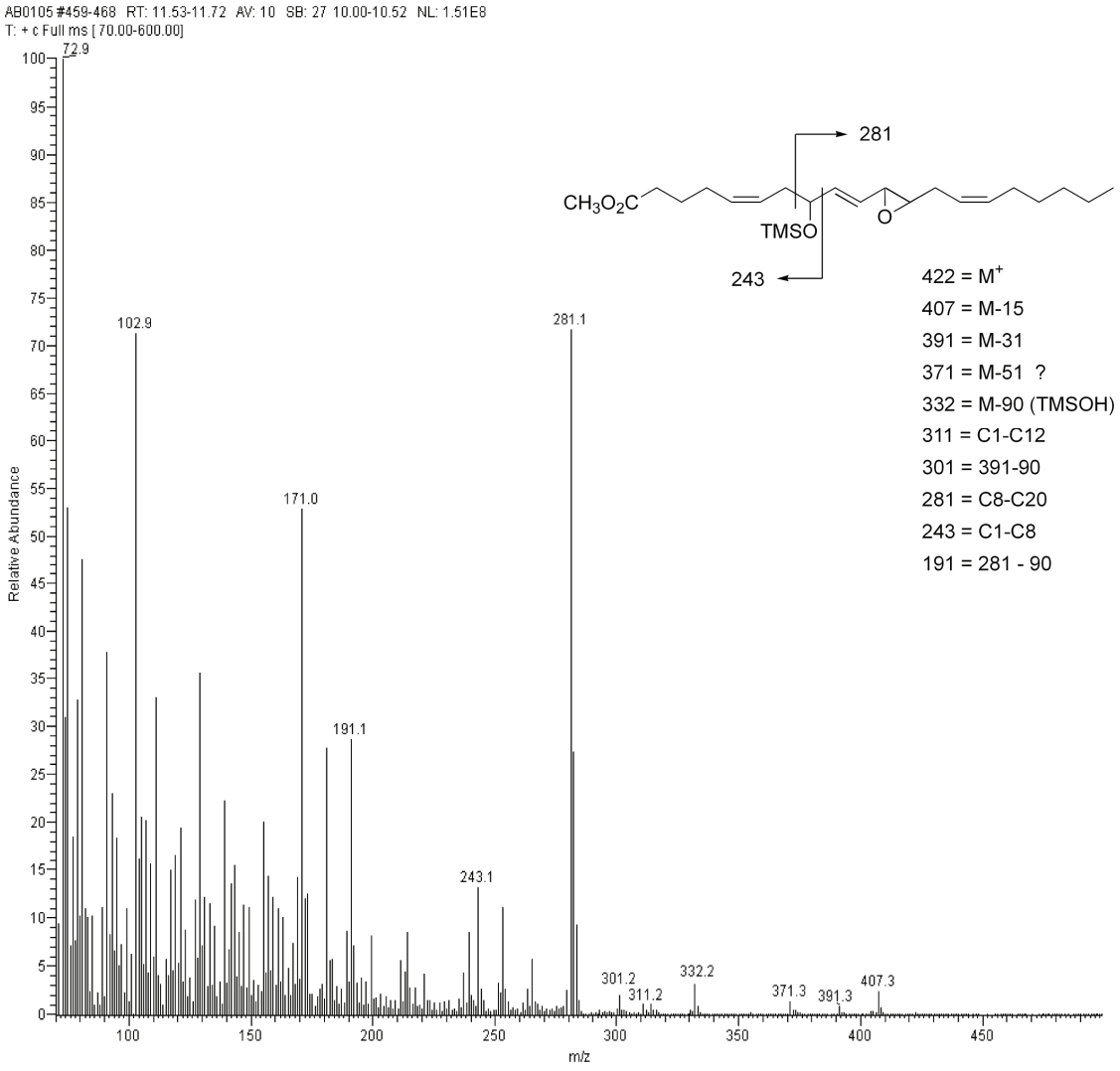

Figure 10. EI mass spectrum of the methyl ester TMS ether derivative of the main eLOX3 product formed from 12*R*-HPETE.

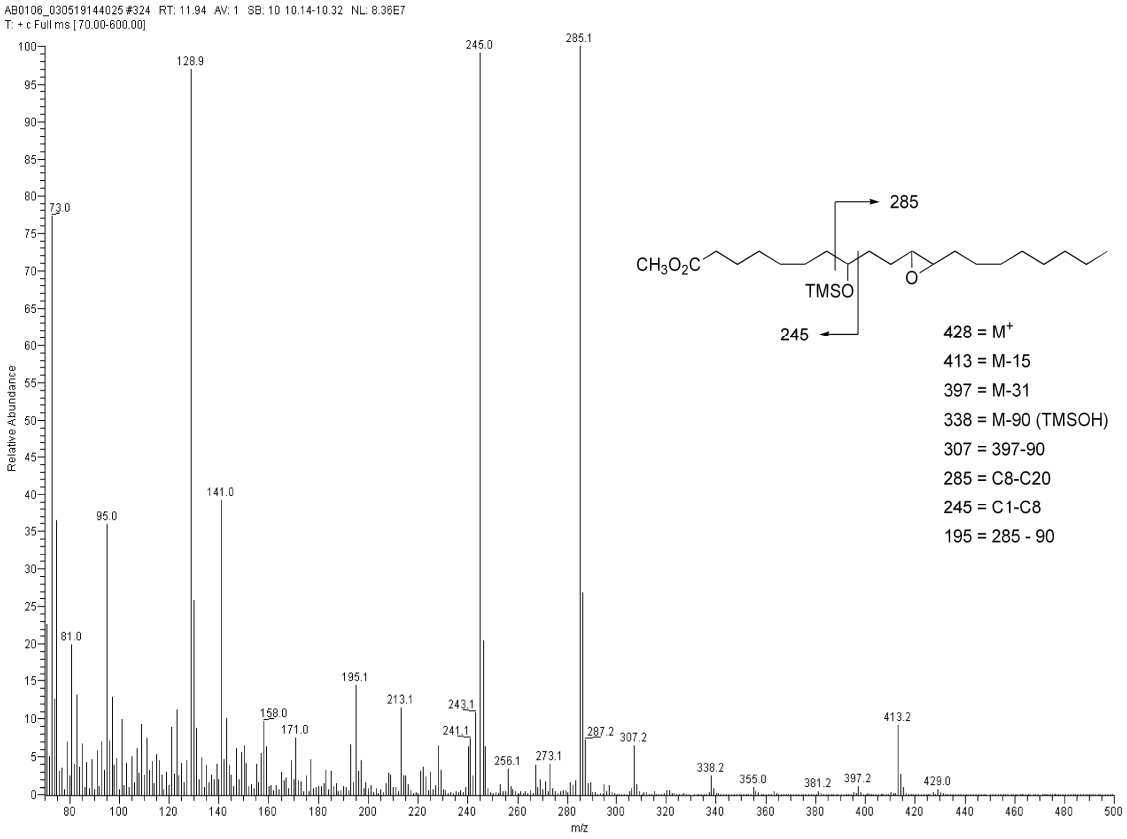

Figure 11. EI mass spectrum of the hydrogenated methyl ester TMS ether derivative of the main eLOX3 product formed from 12*R*-HPETE.

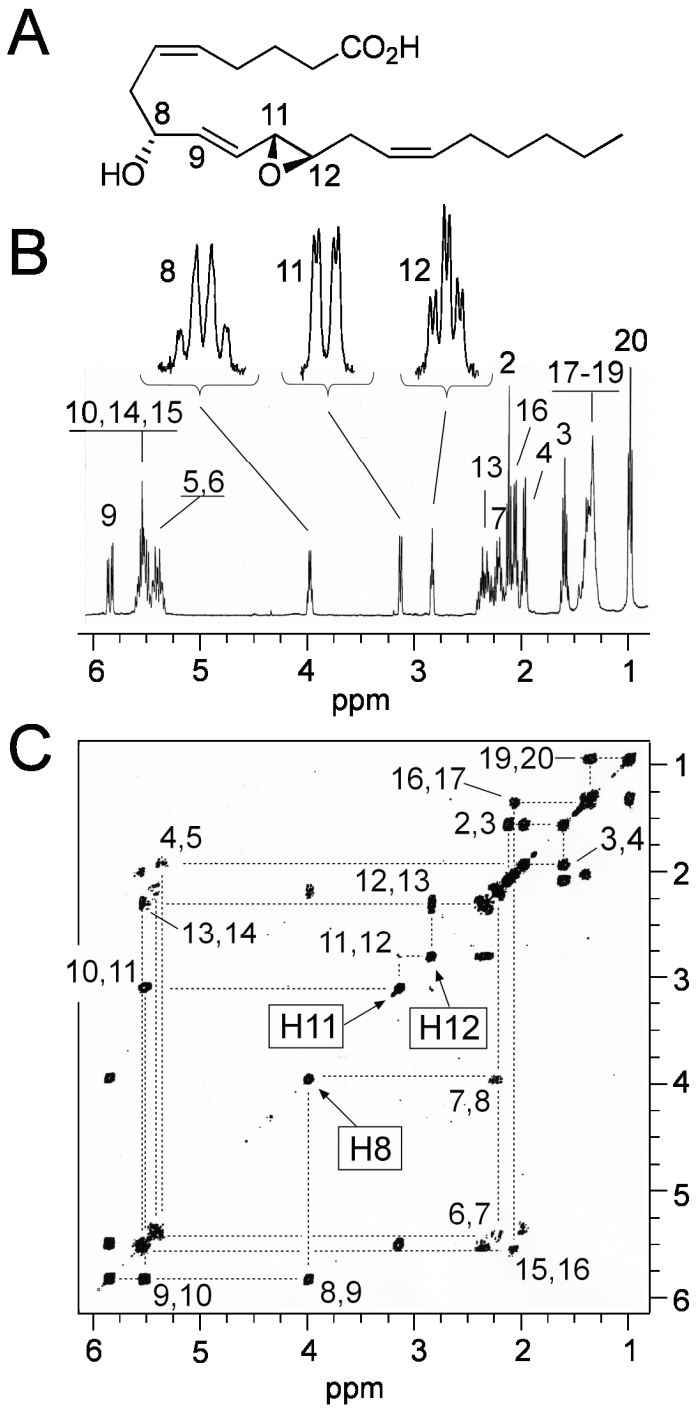

Figure 12. NMR analysis of the main product of eLOX3 reacted with 12*R*-HPETE. The proton spectrum is shown in the middle with an expanded view of the geminal hydroxyl and epoxide protons (H8, H11, and H12) above and the chemical structure at the top; below is shown the H,H-COSY analysis with the main couplings indicated.

Table 2. ^{1}H-NMR (400 MHz, in deuterated benzene) of the main product from the reaction of eLOX3 with 12*R*-HPETE (8*R*-hydroxy-11*R*,12*R*-epoxyeicosa-5*Z*,9*E*,14*Z*-trienoic acid).

Chemical shift (ppm)	Multiplicity	Proton(s) [carbon no.]	Coupling constants (Hz)
0.97	t	H20	$J_{19,20}$ = 7.0
1.3-1.4	m	H17, H18, H19	
1.58	m	H3	
1.96	q	H4	J = 7.2
2.05	q	H16	J = 6.9
2.11	t	H2	$J_{2,3}$ = 7.3
2.19-2.36	m	H7, H13	
2.82	dt	H12	$J_{11,12}$ = 2
			$J_{12,13}$ = 5.2
3.12	dd	H11	$J_{10,11}$ = 7.6
			$J_{11,12}$ = 2
3.97	m	H8	
5.32-5.64	m	H5, H6, H10, H14, H15	
5.86	dd	H9	$J_{9,10}$ = 15.6
			$J_{8,9}$ = 5.5

epoxide, i.e. 11*R*,12*R*-epoxy, assuming, as expected, that the original 12*R* configuration is retained. The 9,10 double bond is *trans* ($J_{9,10}$ = 15.6 Hz); the 5,6 and 14,15 double bonds do not participate in the transformation from 12*R*-HPETE and should retain the original *cis* configurations.

Based on published NMR data it is difficult to make an assignment of the 8-hydroxyl configuration due to chemical shifts or coupling constants (Corey and Su, 1984; Lumin *et al.*, 1992). Therefore the stereo-configuration of the 8-hydroxyl was determined by CD spectroscopy (Schneider *et al.*, 1997; Schneider *et al.*, 2001b). This method requires the presence of two suitable chromophores at the asymmetric carbon, one being provided by the 9,10 double bond and the other introduced at C-8 by derivatization to the benzoate ester. The through-space coupling of the two chromophores gives rise to Cotton effects in the CD spectrum that allows assignment of the absolute configuration (Schneider *et al.*, 1997). To record the CD spectra, the methyl ester benzonate derivative of the main product from 12*R*-HPETE (25 μg) was prepared. Its structure was confirmed by ^{1}H-NMR (400 MHz, in CD_3CN) gave in ppm (relative to residual CH_3CN at δ = 1.92 ppm): 7.80 (d, J = 7.1 Hz, 2H, Ar), 7.41 (dd, J = 6.2 Hz, 1H, Ar), 7.28 (dd, J = 7.4/7.9 Hz, 2H, Ar), 5.81 (dd, J = 15.5/6.4 Hz, 1H, H9), 5.35 – 5.14 (m, 6H, H5, H6, H8, H10, H14, H15), 3.86 (s, 3H, $-OCH_3$), 2.95 (dd, J = 7.8/1.9 Hz, 1H, H11), 2.63 (dt, J = 5.4/2.0, 1H, H12). The existence of the conformer in which the hydrogen at C-8 is eclipsed with the C9-C10 double bond was evident from the large coupling constant of 6.4 Hz between H8 and H9.The CD spectrum showed a negative Cotton effect at 227 nm (Δε -12.5) indicating negative chirality between the two chromophores and therefore the absolute configuration can be assigned as 8*R* (Figure 13). Thus, the product of the eLOX3 reaction

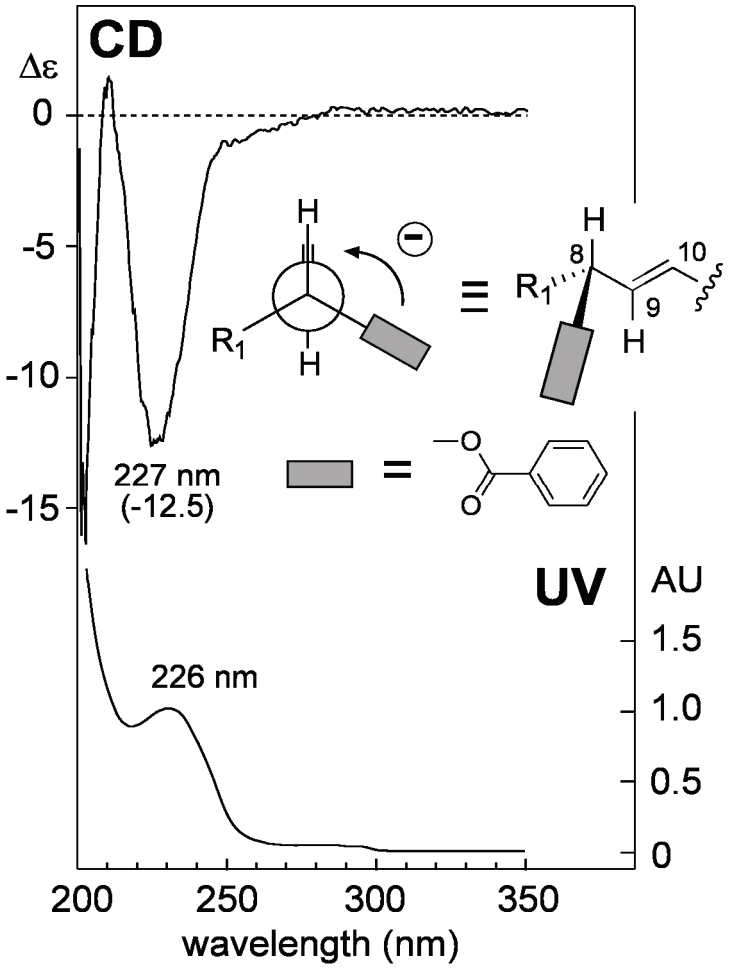

Figure 13. Chiral analysis of the hydroxyl configuration in the 12*R*-HPETE-derived epoxyalcohol. CD and UV spectra of the benzoate derivative of the methyl ester of 8-hydroxy-11*R*,12*R*-epoxyeicosa-5*Z*,9*E*,14*Z*-trienoate were recorded in acetonitrile. As determined from the ^{1}H NMR coupling constant, the preferred conformer of the benzoate derivative has H8 and H9 in the anti position as shown in the Newman projection. The CD spectrum showed a negative first Cotton effect at 227 nm and, therefore, the chirality between the two chromophores as shown in the Newman projection is negative. This allowed designation of the C-8 configuration as 8*R*.

with 12*R*-HPETE was identified as 8*R*-hydroxy-11*R*,12*R*-epoxyeicosa-5*Z*,9*E*,14*Z*-trienoic acid (Figure 12A).

An EI mass spectrum is published for the methyl ester TMS ether derivative of "hepoxilin A3" isolated from incubations with rat lung (Pace-Asciak, C.R. *et al.*, 1983). This product formed from 12*S*-HPETE may be a mixture of diastereomers. On GC-MS analysis the reported product eluted from the GC with a C-value of 23.1 on a non-polar SE-30 packed column. The published mass spectrum shows structurally significant ions at m/z 311 (C1 through C12, ~5-10% abundance), m/z 281 (C8-C20, base peak) and m/z 243 (C1-C8, ~25% abundance), with no other prominent ions above m/z 150 and no higher mass ions discernable (Pace-Asciak, C.R. *et al.*, 1983). Our spectrum of the same derivative of the main eLOX3 product from 12*R*-HPETE has the same major fragment ions but significant differences in ion abundances. In particular, although our spectra do exhibit an ion at m/z 311, (which, as expected, does shift to m/z 325 in the ethyl ester derivative), it is only of 1-2% abundance in the spectrum of each of the three isomeric GC peaks. Also, in the published spectrum the m/z 243 ion stands out much more prominently. It is difficult to account for the differences in character of our spectra and this one published in 1983 (Pace-Asciak, C.R. *et al.*, 1983). The instrumentation conditions of the 1983 report (on a packed SE-30 GC column, with a separator and different transfer line and mass spectrometer instrumentation) differ from ours, and possibly a different hepoxilin A3 diastereomer was being analyzed.

Identification of the two main products from 12*S*-HPETE

The most prominent of the mixture of products from 12*S*-HPETE analyzed on RP-HPLC (Figure 8, panel B, ≈12 min retention time) gave a single peak when further purified on SP-HPLC (data not shown). GC-MS analysis of the methyl ester trimethylsilyl ether derivative gave a mass spectrum (*m/z* 407 $[M\text{-}CH_3]^+$, 311 $[CH_3CO_2C_8H_{12}CHOSi(CH_3)_3C_2H_2O]^+$, 282 $[CH_3CO_2C_8H_{12}CHOSi(CH_3)_3\ CH]^+$, and 269 $[CH_3CO_2C_8H_{12}CHOSi(CH_3)_3]^+$) that was very similar to a published spectrum of the same derivative of hepoxilin B_3 (10-hydroxy-11,12-epoxyeicosa-5,9,14-trienoic acid) (Pace-Asciak, C.R. *et al.*, 1983). ^{1}H-NMR (400 MHz, in deuterated benzene), assigned from the H,H-COSY analysis, defined the covalent structure and provided key details of the stereochemistry (Table 3). For the proton signals from the 10-hydroxy-11,12-epoxy moiety, it was clear that our product from the reaction of 12*S*-HPETE with eLOX3 has a similar visual appearance and similar coupling constants to the 10*R* diastereomer (Vasiljeva *et al.*, 1993; Bernart and Gerwick, 1994). The coupling constant between H11 and H12 (≈2.2 Hz) indicates the 11,12-*trans* epoxide configuration, i.e. 11*S*,12*S*-epoxy in this case. Assuming that the double bonds not involved in the reaction retain their original *cis* configuration, we assign the structure as 10*R*-hydroxy, 11*S*,12*S*-epoxyeicosa-5*Z*,8*Z*,14*Z*-trienoic acid (Figure 14).

GC-MS analysis of the second most prominent product (10.5 min retention time on RP-HPLC, Figure 8) as the hydrogenated methyl ester trimethylsilyl ether derivative gave a mass spectrum with structurally significant ions at *m/z* 413 $[M\text{-}CH_3]^+$, 285 (C8 – C20, $[HCOSi(CH_3)_3C_2H_4C_2H_2OC_8H_{17}]^+$), 245 (C1 – C8, $[CH_3CO_2C_6H_{12}CHOSi(CH_3)_3]^+$), and 315 (C1 – C12, $[CH_3CO_2C_6H_{12}CHOSi(CH_3)_3C_2H_4C_2H_2O]^+$), which is consistent with

the reported mass spectrum of hydrogenated hepoxilin A_3 (Pace-Asciak, C.R. *et al.*, 1983). Although we did not obtain further structural data on this second most prominent product from 12*S*-HPETE, we can make some likely deductions. Based on its chromatographic properties, it is a diastereomer (not the enantiomer) of the major 12*R*-HPETE-derived epoxyalcohol – the two separate on RP-HPLC. If it is assumed that the 12*S*-HPETE product is a *trans* 11*S*,12*S* epoxide, then this would make the predicted structure 8*R*-hydroxy-11*S*,12*S*-epoxyeicosa-5*Z*,9*E*,14*Z*-trienoic acid (Figure 14).

Identification of the main product from 15*S*-HPETE

By using the same lines of evidence from GC-MS and NMR, and comparison to published data (Corey and Mehrotra, 1983; Chang *et al.*, 1996), the main product from the reaction of 15*S*-HPETE with eLOX3 was identified as an analog of the main 12*S*-HPETE product, i.e. 13*R*-hydroxy-14*S*,15*S*-epoxyeicosa-5*Z*,8*Z*,11*Z*-trienoic acid. The mass spectrum of the methyl ester trimethylsilyl ether derivative showed characteristic ions at *m*/*z* 407 $[M\text{-}CH_3]^+$, 309$[CH_3CO_2C_{11}H_{22}CHOSi(CH_3)_3]^+$ and 351 $[CH_3CO_2C_{11}H_{22}CHOSi(CH_3)_3C_2H_2O]^+$ (indicating the C-13 hydroxyl). After hydrogenation, the main structurally significant ions shifted to *m*/*z* 413 $[M\text{-}CH_3]^+$, 315 $[CH_3CO_2C_{11}H_{16}CHOSi(CH_3)_3]^+$ and 215 $[HCOSi(CH_3)_3C_2H_2OC_5H_{11}]^+$. Both spectra are essentially identical to the published spectra (Narumiya *et al.*, 1981). The NMR data are summarized in Table 4. We also compared this product with the products from the hematin-catalyzed transformation of 15*S*-HPETE, which we have previously characterized by oxidative ozonolysis, GC-MS, and ^{1}H-NMR (Chang *et al.*, 1996). This

Table 3. ^{1}H-NMR (400 MHz, in deuterated benzene) of the main product from the reaction of eLOX3 with 12*S*-HPETE (10*R*-hydroxy, 11*S*,12*S*-epoxyeicosa-5*Z*,8*Z*,14*Z*-trienoic acid).[1]

Chemical shift (ppm)	Multiplicity	Proton(s) [carbon no.]	Coupling constants (Hz)
0.96	t	H20	$J_{19,20}$ = 7.0
1.30-1.36	m	H17, H18, H19	
1.47-1.67	m	H3a, H3b	
1.92-2.04	m	H2a, H16	
2.08-2.17	m	H2b, H4	
2.20-2.28	m	H13a	
2.33-2.43	m	H13b	
2.64-2.71	m	H7a	
2.88	dd	H11	$J_{10,11}$ = 5.2
			$J_{11,12}$ = 2.2

(Continued in next page.)

Table 3. continued.

Chemical shift (ppm)	Multiplicity	Proton(s) [carbon no.]	Coupling constants (Hz)
2.96	q	H7b	J = 7.9
3.01	dt	H12	$J_{11,12}$ = 2.2
			$J_{12,13}$ = 5.4
4.42	dd	H10	$J_{9,10}$ = 8.0
			$J_{10,11}$ = 5.2
5.29	m	H5	
5.43	m	H6	
5.47-5.60	m	H8, H9, H14, H15	

[1]FOOTNOTE: Upon transfer of this product into the non-polar NMR solvent (benzene) the free carboxylate lactonized to the hydroxy group at C-10. Lactonization was apparent from loss of the signal of the 10-O<u>H</u> proton, and from splitting of the pairs of protons for H2, H3 and H7 into two separate signals with different chemical shifts.

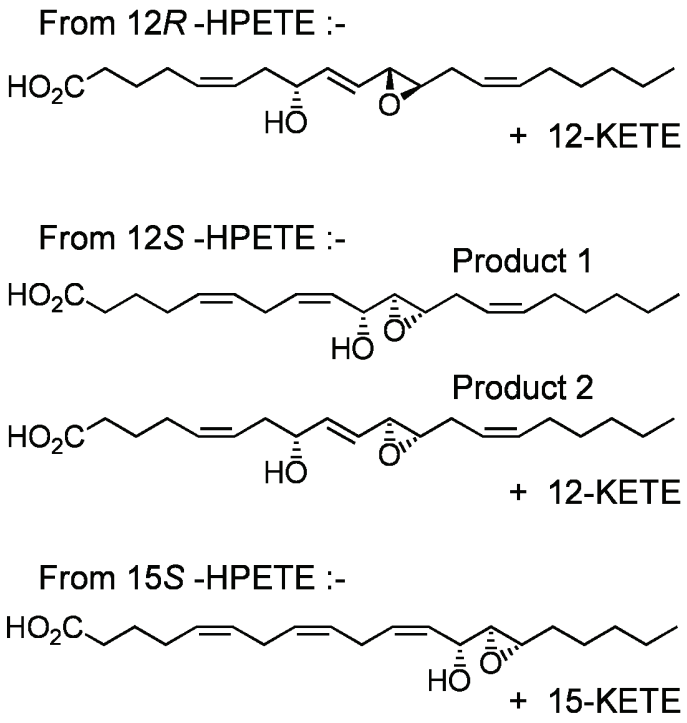

Figure 14. Structures of the epoxyalcohol products. The products shown are from 12*R*-HPETE: 8*R*-hydroxy-11*R*,12*R*-epoxyeicosa-5*Z*,9*E*,14*Z*-trienoic acid; from 12*S*-HPETE: 10*R*-hydroxy, 11*S*,12*S*-epoxyeicosa-5*Z*,8*Z*,14*Z*-trienoic acid (product 1) and 8*R*-hydroxy-11*S*,12*S*-epoxyeicosa-5*Z*,9*E*,14*Z*-trienoic acid (product 2); and from 15*S*-HPETE: 13*R*-hydroxy-14*S*,15*S*-epoxyeicosa-5*Z*,8*Z*,11*Z*-trienoic acid.

confirmed that the main product from the eLOX3 reaction with 15*S*-HPETE is 13*R*-hydroxy-14*S*,15*S*-epoxyeicosa-5*Z*,8*Z*,11*Z*-trienoic acid (Figure 14).

Reaction of eLOX3 with ^{18}O-labeled hydroperoxy substrate

[^{18}O]15*S*-HPETE, with the two oxygens of the hydroperoxide labeled with ^{18}O, was reacted with eLOX3 and the epoxyalcohol product was collected from HPLC and analyzed for ^{18}O content by negative ion chemical ionization GC-MS. A corresponding GC-MS analysis of 15-HETE derived from the starting material indicated it comprised

92.4% ^{18}O and 7.6% unlabeled molecules; as nearly all the molecules contain either 2 ^{16}O or 2 ^{18}O, the ^{18}O-labeled 15-HPETE, with two heavy oxygens, is calculated to have a 92% content of two atoms of ^{18}O. GC-MS analysis of the epoxyalcohol demonstrated that 91.6% of the product molecules contained 2 atoms of ^{18}O; (2% contained one ^{18}O, and 6.4% of the molecules were unlabeled). These results indicate that there was essentially complete retention of the original hydroperoxide oxygens in the epoxyalcohol product. eLOX3, therefore, is a hydroperoxide isomerase. Although, other ^{18}O-labeled hydroperoxide substrates were not available, we were able to show using an oxygen electrode that exogenous molecular oxygen made no significant contribution to the eLOX3-catalyzed transformations of the hydroperoxide substrates.

The effect of NDGA on eLOX3 reaction

In the conventional Fe^{2+}/Fe^{3+} redox cycle of normal LOX catalysis, the Fe^{3+} enzyme is the active form. Thus a reducing agent such as nordihydroguaiaretic acid (NDGA) is frequently used as a non-specific inhibitor for typical lipoxygenases. Reducing agent also can be used as a co-substrate to support the pseudoperoxidase activity of the LOX enzymes that permits cycling of the active site iron with concomitant metabolism of HPETE (Kemal *et al.*, 1987; Riendeau *et al.*, 1991). The characteristics of eLOX3 in reacting with HPETE substrates resemble the pseudoperoxidase activity of the LOX enzymes. To investigate the mechanism of eLOX3 reaction, we tested the effect of NDGA. Submicromolar concentrations of NDGA caused a dose-dependent increase in reaction rates of eLOX3 with HPETE substrates. The addition of NDGA increased the

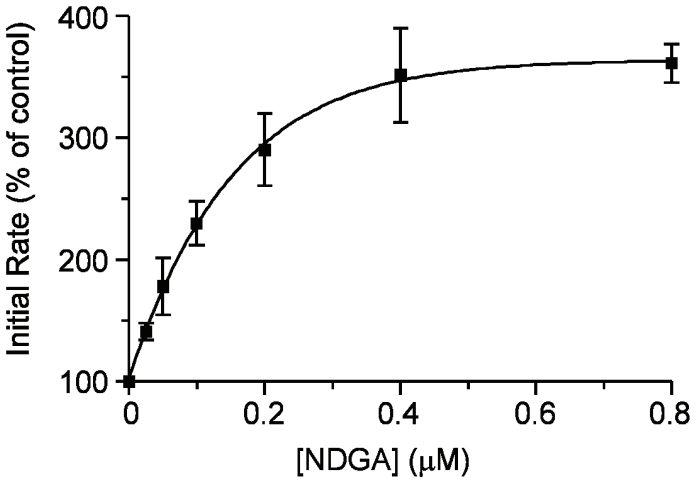

Figure 15. Effect of NDGA on eLOX3 rate of reaction. The dose-dependent effects of NDGA are shown for the reaction of 12*R*-HPETE with eLOX3. Rates were determined by following the decrease in absorbance at 235 nm.

rate of eLOX3 reaction with 12*R*-HPETE by 3-4 fold (Figure 15), and with 15*S*-HPETE by up to 6-fold.

Table 4. ^{1}H-NMR (400 MHz, in deuterated benzene) of the methyl ester of the main product from the reaction of eLOX3 with 15*S*-HPETE (13*R*-hydroxy-14*S*,15*S*-epoxyeicosa-5*Z*,8*Z*,11*Z*-trienoic acid methyl ester).

Chemical shift (ppm)	Multiplicity	Proton(s) [carbon no.]	Coupling constants (Hz)
0.93	t	H20	$J_{19,20}$ = 6.9
1.21-1.52	m	H16, H17, H18, H19	
1.67	p	H3	J = 7.4
1.92	d	13-OH	$J_{13,13\text{-OH}}$ = 5.2
2.06	q	H4	J = 7.4
2.18	t	H2	$J_{2,3}$ = 7.3
2.80	dd	H14	$J_{13,14}$ = 5.1
			$J_{14,15}$ = 2.0
2.83-2.99	m	H7, H10, H15	
3.44	s	-OCH_3	
4.37	ddd	H13	$J_{12,13}$ = 7.8
			$J_{13,14}$ = 5.0
			$J_{13,13\text{-OH}}$ = 5.2
5.34-5.64	m	H5, H6, H8, H9, H11, H12	

Discussion

Fatty acid epoxyalcohols are produced from unsaturated fatty acid hydroperoxides, which are the products of the LOX enzymes in plant and animal tissues. Epoxyalcohols are readily formed via non-enzymatic transformations. For example, it has been reported that heat-insensitive heme catalysis of 12*S*-HPETE produce 8- and 10-hydroxy-11,12-epoxyeicosatrienoic acids, while 11- and 13-hydroxy-14,15-epoxyeicosatrienoic acids, can be formed from 15*R*- and 15*S*-HPETE by hematin reaction. In general these reactions lack stereo-control and they do not lead to the synthesis of the distinct diastereomers that are likely to be involved in cell signaling or other biological functions.

The enzymatic formation of epoxyalcohols in plant tissues is catalyzed by hydroperoxide isomerases. These enzymes are hydroperoxide-metabolizing enzymes which have formal similarities to cytochrome P450. So far, an enzyme with epoxyalcohol synthase activity in mammalian tissues has not been characterized, but there are reports about the detection of this activity in rat and human skin and appearance of the products in human psoriatic lesions (Nugteren *et al.*, 1985; Anton *et al.*, 1998; Anton and Vila, 2000). It also has been reported that human platelet-type 12-LOX catalyzes the transformation of AA into epoxyalcohols (Anton *et al.*, 1995). However, this epoxyalcohol synthase activity of 12-LOX is still questionable since no any products other than 12-HETE was formed when recombinant 12-LOX was incubated with 12*S*-HPETE.

In this study we showed a novel epidermal LOX, human eLOX3, is a functional and specific epoxyalcohol synthase. Although eLOX3 is clearly a member of the LOX gene family it does not have the LOX activity predicted from proteomic analysis. Our

hypothesis on its catalytic activity came from the genetic finding that mutations in the coding sequence of either eLOX3 or its co-localized protein 12*R*-LOX can cause an inherited skin disease, NCIE, which suggested that both enzymes might participate in the same metabolic pathway. Here we provide biochemical evidence that eLOX3 exhibits potent enzymatic activity toward the transformation of the 12*R*-LOX derived product, 12*R*-HPETE, into a specific epoxyalcohol product, 8*R*-hydroxy-11*R*,12*R*-epoxyeicosa-5*Z*,9*E*,14*Z*-trienoic acid. We also have shown that the LOX-products 12*S*-HPETE and 15*S*-HPETE are converted to specific epoxyalcohol products of related structure, albeit with lower catalytic efficiency.

The term "hepoxilin" is generally used to refer to groups of 12-HPETE-derived epoxyalcohol fatty acids that have been detected in skin and other tissues (Pace-Asciak, C.R. *et al.*, 1995). Hepoxilin A_3 is used for any stereoisomer with an 8-hydroxy-11,12-epoxy structure, while hepoxilin B_3 refers to the isomers with a 10-hydroxy-11,12-epoxyeicosatrienoic acid structure. Thus the recombinant human eLOX3 forms one particular stereoisomer of hepoxilin A_3 from 12*R*-HPETE, and mainly one isomer of hepoxilin B_3 from the substrate 12*S*-HPETE. It remains to be elucidated the extent to which the eLOX3 activity is responsible for the formation of hepoxilin isomers that have been detected in human skin or whether additional activities or non-enzymatic reactions have to be considered.

In terms of mechanism, the facets of eLOX3 reactivity that make it stand out are the complete absence of typical lipoxygenase (oxygenase) activity under any of the variety of conditions that have been explored, and also the unusual autocatalytic nature of the reaction with HPETE substrates. Equivalent hydroperoxide rearrangements by other

LOX enzymes are limited to single turnovers, unless promoted by a reducing cofactor (Garssen *et al.*, 1976; Riendeau *et al.*, 1991). In the conventional Fe^{2+}/Fe^{3+} redox cycle of normal LOX catalysis (Figure 4), the Fe^{3+} enzyme is the active form that performs the hydrogen abstraction from the *bis*-allylic methylene of the fatty acid substrate. Oxygenation of the fatty acid radical and reduction of the peroxyl radical to the fatty acid hydroperoxide completes the cycle. So NDGA and other reducing agents can reduce Fe^{3+}-enzyme to Fe^{2+}-enzyme and inhibit the LOX catalyzed reaction. By contrast, in the reaction of eLOX3 with HPETE substrates, I found that NDGA speed up the catalysis by 6 fold. It can be assumed that the Fe^{2+} enzyme is the active species, and reducing agent converts the pool of enzyme molecules from predominantly ferric (Fe^{3+}) to the active ferrous (Fe^{2+}) state.

Based on this, we propose a mechanism for epoxyalcohol formation by eLOX3 as depicted in Figure 16. The Fe^{2+} enzyme initiates a homolytic cleavage of the hydroperoxide O-O bond (Figure 16, step 1), the resulting alkoxyl radical cyclizes to an epoxyallylic carbon radical (step 2) while the other oxygen of the original hydroperoxide is retained in a Fe^{3+}-OH complex. The cycle is completed by an oxygen rebound type of reaction that forms the epoxyalcohol product (step 3) while the iron is restored to the active Fe^{2+} form. The corresponding ketoeicosatetraenoic acid is formed as a by-product in some of the catalytic cycles (step 4).

Since the reaction mechanism in Figure 16 could be proposed "on paper" for any LOX, why is such a self-sufficient catalytic cycling observed only with eLOX3? We speculate that the redox state of eLOX3 may make the ferric enzyme incapable of performing a hydrogen abstraction from a typical lipoxygenase substrate, and thus the

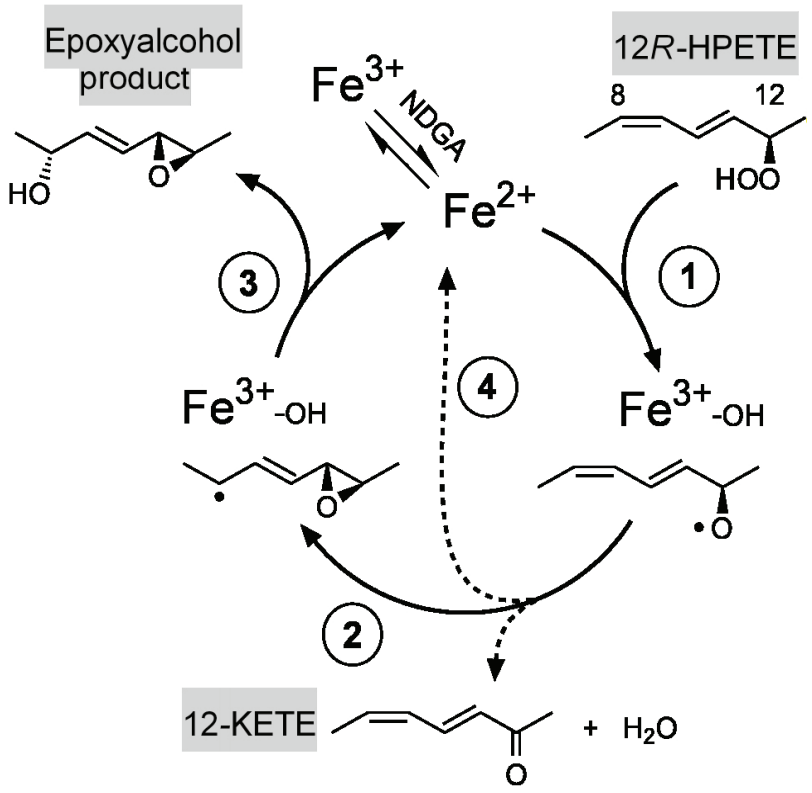

Figure 16. Proposed mechanism for eLOX3 catalysis.

protein is incapable of oxygenating a polyunsaturated fatty acid. This shift in balance of redox potential may, in turn, favor the reduction reaction that constitutes the basis of the catalytic activity we describe with HPETE substrates.

CHAPTER III

IDENTIFICATION OF A NOVEL LIPOXYGENASE PATHWAY IN SKIN AND ITS MUTATION IN ICHTHYOSIS

Introduction

The formation of a bioactive eicosanoid usually occurs through the actions of a cascade of interrelated enzymes. Data reported in Chapter II provide evidence for the identification of a novel catalytic activity of eLOX3 in the conversion of HPETE substrates to specific epoxyalcohols (hepoxilins or hepoxilin-type products). eLOX3 preferentially transforms the 12*R*-LOX derived product, 12*R*-HPETE, into a specific epoxyalcohol product, 8*R*-hydroxy-11*R*,12*R*-epoxyeicosa-5*Z*,9*E*,14*Z*-trienoic acid. This provides biochemical support that the two epidermal enzymes work together.

The concept that 12*R*-LOX and eLOX3 function in the same metabolic pathway was proposed first in a recent genetic study which showed that mutations in one or the other enzyme are associated with the development of an inherited skin disease, non-bullous congenital ichthyosiform erythroderma (NCIE) (Jobard *et al.*, 2002). NCIE represents the first example in which mutations in the coding region of a LOX gene have been associated with a disease. This suggests that the products of both enzymes might serve as novel lipid mediators in normal skin physiology. Thus, identification of the biologically active product and its further metabolism are required to help elucidate this normal function. Herein I described the further enzymatic transformation of the epoxyalcohol product of eLOX3.

Although the genetic study links mutations in the coding sequence of eLOX3 or 12*R*-LOX genes to the inherited skin disease NCIE, the functional impact of these mutations on enzyme activities has not been defined. To explore whether the mutations reported in NCIE patients may be associated with alteration of 12*R*-LOX and eLOX3 functionality, in the current study we have mutated the corresponding amino acids in 12*R*-LOX and eLOX3. After overexpressing the wild-type and mutant proteins in *E. coli* and COS7 cells, we have characterized the essential catalytic properties.

Experimental Procedures

Materials

[1-^{14}C]arachidonic acid was purchased from PerkinElmer Life Sciences. [1-^{14}C]15*S*-HPETE was prepared by reaction of [1-^{14}C]arachidonic acid with soybean lipoxygenase type V (Sigma, St. Louis, MO). 12*R*-HPETE was prepared by arachidonic acid autoxidation as described previously in Chapter II. [1-^{14}C]12*R*-HPETE was prepared by reaction of [1-^{14}C]arachidonic acid with human 12*R*-LOX (Boeglin *et al.*, 1998). 8*R*-hydroxy-11*R*,12*R*-epoxyeicosa-5*Z*,9*E*,14*Z*-trienoic acid (8*R*,11*R*,12*R*-epoxyalcohol) was prepared by the reaction of 12*R*-HPETE with human eLOX3 in pH 6.0 Tris buffer (Chapter II).

Cell culture

The human epidermal keratinocytes isolated from human newborn foreskins were purchased from Vanderbilt Skin Disease Research Center and passaged three or four

times. Proliferating cultures were fed every other day with complete Epi-life medium (0.06 mM Ca^{2+}; Cascade).

The COS-7 (ATCC CRL-1651) cells were routinely cultured in Dulbecco's modified Eagle's medium containing 10% fetal bovine serum (BioWhittaker, Walkersville, MD) at 37 °C, 5% CO_2. They were typically split 1:6 every 3 days.

Cellular hydrolysis of 8*R*,11*R*,12*R*-epoxyalcohol

For incubations of the 8*R*,11*R*,12*R*-epoxyalcohol with COS7 cells and keratinocytes, a 100 mm plate (90% confluent) each was homogenized in incubation buffer. 4 μg of the epoxyalcohol were added to 200 μl of cellular lysate and incubated at 37°C for 45 min. The products were extracted and analyzed by RP-HPLC and diode array detection using a Waters Symmetry C18 5-μm column (0.46 x 25 cm) eluted at a flow rate of 1 ml/min with methanol/water/acetic acid (80/20/0.01, by volume). Heat-inactivated lysates were prepared by boiling for 10 min (COS7 cells) or 45 min (keratinocytes).

Acid-catalyzed hydrolysis of 8*R*,11*R*,12*R*-epoxyalcohol

The non-enzymatic hydrolysis of epoxyalcohol was done by treating the epoxyalcohol with 1% acetic acid at room temperature for 30 min. This will hydrolyze the epoxide and yield a series of diastereomeric isomers of trihydroxy-eicosatrienoic acids (triols). The mixture was analyzed by RP-HPLC using a Waters Symmetry C18 5-μm column (0.46 x 25 cm) eluted at a flow rate of 1 ml/min with methanol/water/acetic acid (80/20/0.01, by volume) and monitoring at UV 205 nm. The diastereomers eluted

between 5 – 6 min were collected and further separated by SP-HPLC using a Beckman Ultrasphere Silica column (0.46 x 25 cm) eluted at a flow rate of 1 ml/min with hexane/IPA/ acetic acid (90/10/0.1, by volume). Further purification was done by chiral-HPLC using Chiralpak AD column (0.46 x 25 cm) eluted at a flow rate of 0.5 ml/min with hexane/methanol/ethanol/acetic acid (95/5/10/0.1, by volume). The position of the hydroxy groups along the carbon chain was determined by GC-MS after hydrogenation (Pd/Al) and derivatization to the methyl esters TMS ethers as described previously in Chapter II.

LC-ESI-MS analysis

A Thermo Finnigan LC Quantum system was used. Samples were introduced via a Waters Symmetry C18 3-μm column (0.2 x 10 cm) eluted with a water/acetonitrile gradient containing 10 mM ammonium acetate at a flow rate of 0.2 ml/min. The heated capillary ion lens was operated at 220°C. Nitrogen was used as a nebulization and desolvation gas. The electrospray potential was held at 4 kV. Mass spectra were acquired over the mass range *m/z* 200 to 750 at 2 sec/scan.

GC-MS analysis

Analysis of the methyl ester trimethylsilyl ether derivatives of the products was carried out in the positive-ion electron impact mode (70 eV) using a Hewlett–Packard 5989A mass spectrometer coupled to a Hewlett–Packard 5890 gas chromatograph equipped with an RTX-1701 fused silica capillary column (17 m x 0.25 mm internal

diameter). Samples were injected at 150°C, and after 1 min the temperature was programmed to 300°C at 10 or 20°C/min.

NMR analysis

^{1}H NMR spectra were recorded in $CDCl_3$ using a Bruker Avance DRX 400 MHz instrument. Chemical shifts are reported relative to $CHCl_3$ (δ = 7.24 ppm).

Expression and purification of human soluble epoxide hydrolase (sEH)

The cDNA for human sEH was cloned by PCR with cDNA prepared from human keratinocytes. To prepare the sEH protein with an N-terminal $(His)_6$ tag, the sEH cDNA was subcloned into the pET3a expression vector (Novagen, Madison, WI) with the 5' sequence encoded as ATG CAT CAC CAT CAC CAT CAC ACG-, with the last codon representing the start of the wild type enzyme. The human sEH was expressed in *E. coli* BL21 (DE3) cells (Novagen, Madison, WI) and the $(His)_6$ tagged protein was purified on Ni-NTA agarose (Qiagen, Valencia, CA) according to the manufacturer's instructions. Fractions of 0.5 ml were collected off the affinity column and assayed by using SDS/PAGE. Fractions containing eLOX3 were pooled and dialyzed against a buffer of 50 mM Tris (pH 7.5) containing 300 mM NaCl to remove the imidazole. The activity of human sEH was determined by the reaction with 14,15-EET.

Plasmids and Site-Directed Mutagenesis

The cDNAs for human 12*R*-LOX and eLOX3 were subcloned into the pcDNA3.1 expression vector (Invitrogen, Carlsbad, CA). Site-directed mutagenesis was carried out

using the Quickchange site-directed mutagenesis kit (Stratagene, La Jolla, CA) following the manufacturer's instructions. Site-directed mutants were selected by sequencing.

Transfection and Harvesting of COS7 Cells

Subconfluent COS7 cells in 100 mm dishes were transfected with 7 μg of wild-type and mutant human 12*R*-LOX and eLOX3 plasmids or vector control using FuGENE 6 (Roche Molecular Biochemicals). Forty-eight hours after transfection, cells were harvested and washed with phosphate-buffered saline, and sonicated for 5 s in incubation buffer (100 mM KH_2PO_4, 200 mM NaCl, pH 6.5). Cell lysates were assayed for protein content using Bio-Rad protein assay dye reagent (Bio-Rad, Hercules, CA).

Western Blot Analysis

Aliquots of cell lysates from each sample (20 μg total protein) were boiled in sample buffer and separated on 10% SDS-PAGE followed by transferring to a nitrocellulose membrane. The primary antibody used in 12*R*-LOX detection was rabbit antiserum raised against the human 12*R*-LOX. To analyze eLOX3 expression, the membranes were probed using a primary rabbit antiserum raised against human 15-LOX-2, which will also detect human eLOX3 with sufficient sensitivity to allow evaluation of its expression level in the current experiments. The blots were developed with alkaline phosphatase-conjugated donkey anti-rabbit IgG antibodies.

12*R*-LOX and eLOX3 Activity Assays

Aliquots of cell lysates from each sample (normalized to a similar amount of wild-type and mutant enzymes) were used in the incubations. The total incubation volume was 200 μl. For 12*R*-LOX activity assays, the cell lysates were incubated with 25 μM [1-^{14}C]arachidonic acid at 37 °C for 45 min. For eLOX3 activity assay, the cell lysates were incubated with 25 μM [1-^{14}C]15*S*-HPETE or [1-^{14}C]12*R*-HPETE at 37 °C for 45 min. After the incubation, protein was removed by precipitation with 500 μl of methanol and 250 μl of methylene chloride and subsequent centrifugation. After evaporation of the organic solvents, the products were recovered by extraction using a 100-mg Oasis HLB cartridge (Waters) essentially as described by Powell (Powell, 1982). Product analysis was performed by RP-HPLC using a Waters Symmetry C18 5-μm column (0.46 x 25 cm) eluted at a flow rate of 1 ml/min with methanol/water/acetic acid (90/10/0.01, by volume) for incubation with 12*R*-LOX or methanol/water/acetic acid (80/20/0.01, by volume) for eLOX3. Peaks were monitored using an Agilent 1100 diode array detector. To detect radiolabeled products, a Packard A100 Flo-One Radiomatic liquid scintillation detector was connected to the Agilent 1100 diode array detector. The incubations with 15*S*-HPETE and 12*R*-HPETE were repeated twice with identical results.

Results

Incubation of eLOX3 product with cell lysates

To test the further metabolism of eLOX3 product in the cellular environment, we incubated the eLOX3 product 8*R*-hydroxy-11*R*,12*R*-epoxyeicosa-5*Z*,9*E*,14*Z*-trienoic acid (8*R*,11*R*,12*R*-epoxyalcohol) with homogenates of human keratinocytes. After extraction, the products were analyzed by RP-HPLC (Figure 17A). The keratinocyte lysate converted the epoxyalcohol substrate to a major product eluting at about 5.5 min on RP-HPLC. This product is significantly more polar than the epoxyalcohol, which elutes at about 9.5 min using the same RP-HPLC solvent. This suggests that, in contrast to the reaction of purified eLOX3 with 12*R*-HPETE in Tris buffer (in which the epoxyalcohol product is stable for analysis as described in Chapter II), in the cell lysate the epoxyalcohol product is further converted to more polar product. This metabolism is due to an inherent enzymatic activity in keratinocytes as it was markedly inhibited by prior boiling of the keratinocyte homogenate: heat inactivation almost completely eliminated the formation of the polar product as judged by the appearance of the peak detected at 205 nm on RP-HPLC (Figure 17B). The small amount of the 5.5 min peak formed is likely due to incomplete inactivation of the enzymatic activity or due to non-enzymatic conversion. Analysis of incubations of the 8*R*,11*R*,12*R*-epoxyalcohol with COS7 cell lysates or 12*R*-HPETE with COS7 cell lysate expressing wild-type human eLOX3 demonstrated the same transformation (Page 87, Figure 25A). The polar peaks we detected in these incubations co-chromatographed on RP-HPLC with the product that was formed in the keratinocytes.

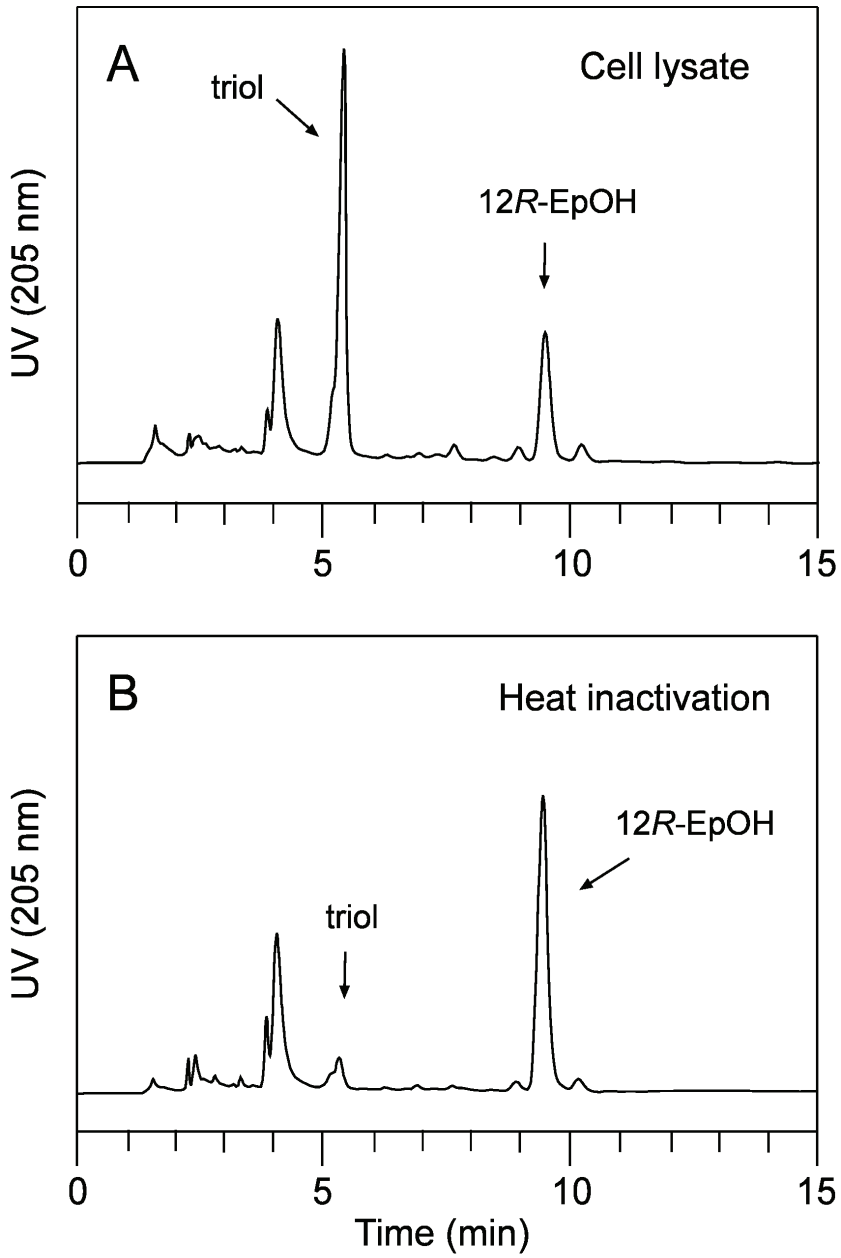

Figure 17. RP-HPLC analysis of the incubation of the 8*R*-hydroxy-11*R*,12*R*-epoxyeicosa-5*Z*,9*E*,14*Z*-trienoic acid (8*R*,11*R*,12*R*-epoxyalcohol) with homogenates of human keratinocytes. (A) The untreated keratinocyte lysate converted the 8*R*,11*R*,12*R*-epoxyalcohol mainly to one isomer of 8,11,12-trihydroxyeicosa-5*Z*,9*E*,14*Z*-trienoic acid (triol, retention time 5.5 min). (B) Heat-inactivation of the keratinocyte lysate greatly abolished the formation of the triol product. The products were analyzed by RP-HPLC with a Waters Symmetry C18 5 μm column (0.46 x 25 cm) eluted at a flow rate of 1 ml/min with methanol/water/acetic acid (80:20:0.01 by volume). The chromatograms were recorded at UV 205 nm using a diode array detector.

Identification of the polar peak from cellular incubation with the eLOX3 product

Analysis using LC-ESI-MS in the negative ion mode gave a $[M-H]^-$ ion at m/z 353 for the peak at 5.5 min (Figure 17A), corresponding to a molecular weight of 354. This is 18 mass units higher than 8*R*,11*R*,12*R*-epoxyalcohol (MW = 336), and is compatible with its identity as a trihydroxy hydrolysis product.

The 5.5 min peak was purified by RP-HPLC, converted to the methyl ester trimethylsilyl ether derivative, and analyzed by GC-MS analysis in the electron impact mode. It chromatographed as a single sharp peak on GC (Figure 18A) and gave a mass spectrum (Figure 18B, with m/z 570 $[M-CH_3]^+$, 213 $[C12-C20]^+$, 243 $[C1-C8]^+$, 371 $[C1-C11]^+$, 281 $[C1-C11]^+$-90, 383 $[C1-C12]^+$-90, and 444 $[C8-C20]^+$) consistent with the structure of the parent molecule as 8,11,12-trihydroxyeicosa-5,9,14-trienoic acid. The mass spectrum is very similar to that reported for 8,11,12-trihydroxyeicosatrieneoic acid hydrolysis products derived from 12*S*-HPETE in platelets and rabbit aorta (Jones *et al.*, 1978; Pfister, S. L. *et al.*, 2003). Furthermore, this structural identification was supported by 1D and 2D NMR analyses (diagnostic signals only: δ 5.82, broad s, 2H, H9, H10; δ 5.6-5.35, m, 4H, H5, H6, H14, H15; δ 4.21, m, 1H, H8; δ 4.16, m, 1H, H11; δ 3.71, broad s, 1H, H12).

We noted that hydrolysis of the authentic 8*R*,11*R*,12*R*-epoxyalcohol in both keratinocytes and COS7 cells gives a single 8,11,12-triol as judged by the sharp peak on RP-HPLC and GC-MS. By contrast, acid-catalyzed hydrolysis of the 8*R*,11*R*,12*R*-epoxyalcohol gave a mixture of products with the two main peaks running as a broad partially resolved peak at ~6 min retention time on the RP-HPLC chromatogram (Figure 19A). In SP-HPLC, these peaks were separated into 4 peaks eluted between 10 min and

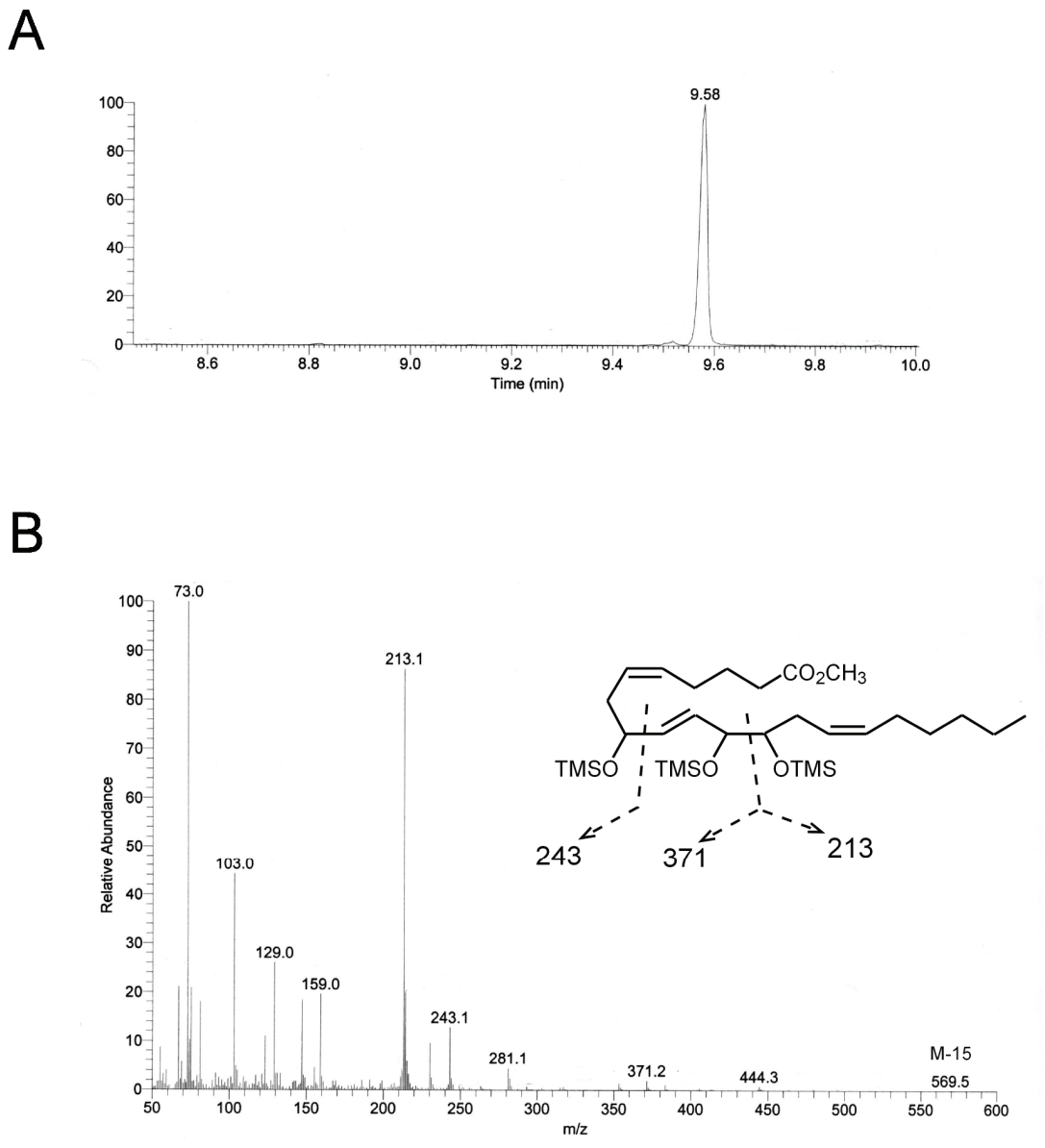

Figure 18. GC-MS analysis of the trihydroxy hydrolysis product in the incubation of 12*R*-HPETE with COS7 cell lysate expressing wild-type human eLOX3. (A) Total ion chromatogram of the methyl ester TMS ether derivative. (B) EI-mass spectrum of the peak at 9.58 min retention time.

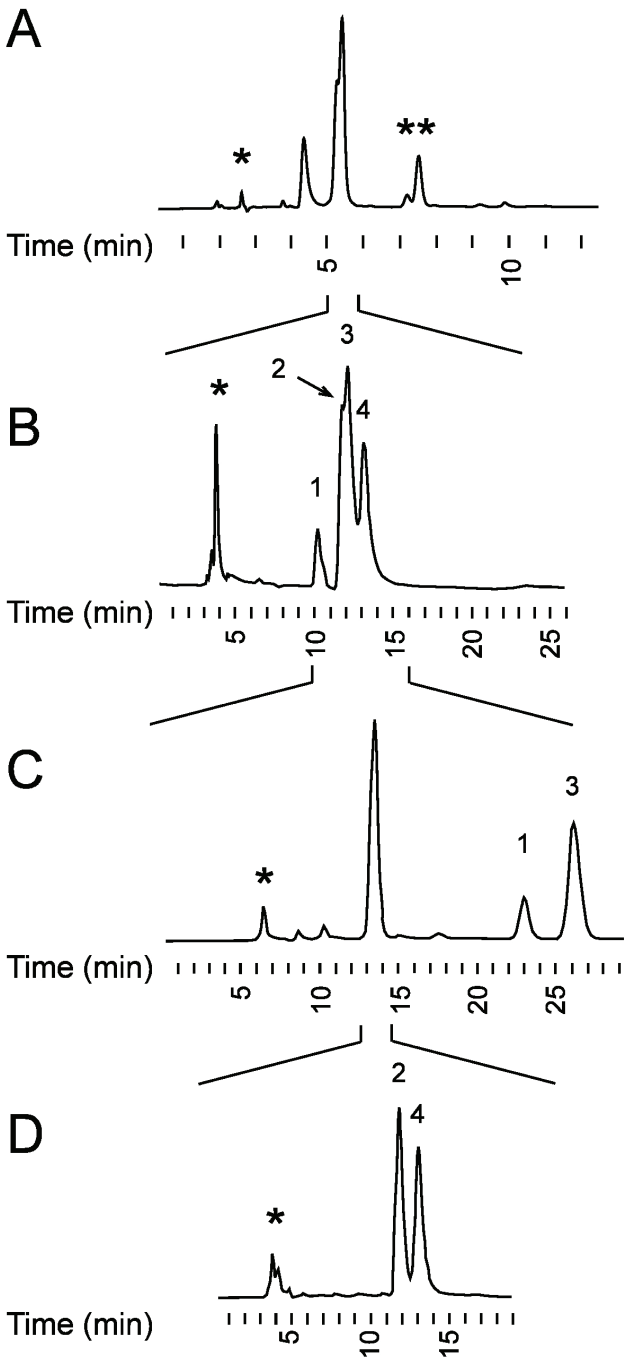

Figure 19. Purification of the triols from the acid-catalyzed hydrolysis of 8*R*,11*R*,12*R*-epoxyalcohol. (A) RP-HPLC. (B) SP-HPLC. (C) Chiral-HPLC. (D) SP-HPLC. The HPLC conditions were described in the Experimental Procedures. *, solvent artifact. **, unknown compounds with m/z =335. The peaks 1, 2, 3, 4 were identified in Figure 20. The cellular hydrolysis product co-eluted with peak 4 under all of these HPLC conditions.

15 min, and assigned 1-4, respectively (Figure 19B). A better purification of these 4 peaks was achieved by running a chiral-HPLC first and then SP-HPLC (Figure 19C and D). GC-MS analysis suggests all of these 4 peaks are triols (two 8,9,12-triols and two 8,11,12-triols). A tentative setero-configuration assignment of these triols was made based on the observations by M. Hamburg (Hamberg, 1991) and L.J. Morris (Morris, 1963). M. Hamburg's results suggested that in the hydrolysis of epoxyalcohol containing a 1-hydroxy-2,3-enonoic-4,5-epoxy structure, the solvent attack only occurs on carbon 2 and 4 of this structure. As a result, the stereo-configurations on carbon 1 and 5 are always retained. Thus all of these four triols which are formed from acid hydrolysis of 8*R*,11*R*,12*R*-epoxyalcohol remain the 8*R* and 12*R* configuration. As expected, *threo* trihydroxy fatty acid was less polar than the corresponding *erythro* compound (Morris, 1963). So *threo* compound elutes earlier than *erythro* compound in SP-HPLC. This was used here to assign the stereo-configuration of the third hydroxy group. The assignment of the stereo-configurations of all four non-enzymatic hydrolysis products was shown in Figure 20. The cellular hydrolysis product from 8*R*,11*R*,12*R*-epoxyalcohol co-chromatographed on SP-HPLC with triol 4 in Figure 20, which is 8*R*,11*S*,12*R*-trihydroxy-5*Z*,9*E*,14*Z*-trienoic acid (8*R*,11*S*,12*R*-triol).

Molecular cloning of human soluble epoxide hydrolase and its reaction with epoxyalcohol

The stereo-specific hydrolysis of 8*R*,11*R*,12*R*-epoxyalcohol in keratinocyte and COS7 cell lysates indicates human soluble epoxide hydrolase (sEH) might be the possible enzyme in this transformation. To test this hypothesis, we cloned human sEH gene from keratinocyte cDNA and expressed it in *E. coli* with His_6-tag. The epoxide hydrolase

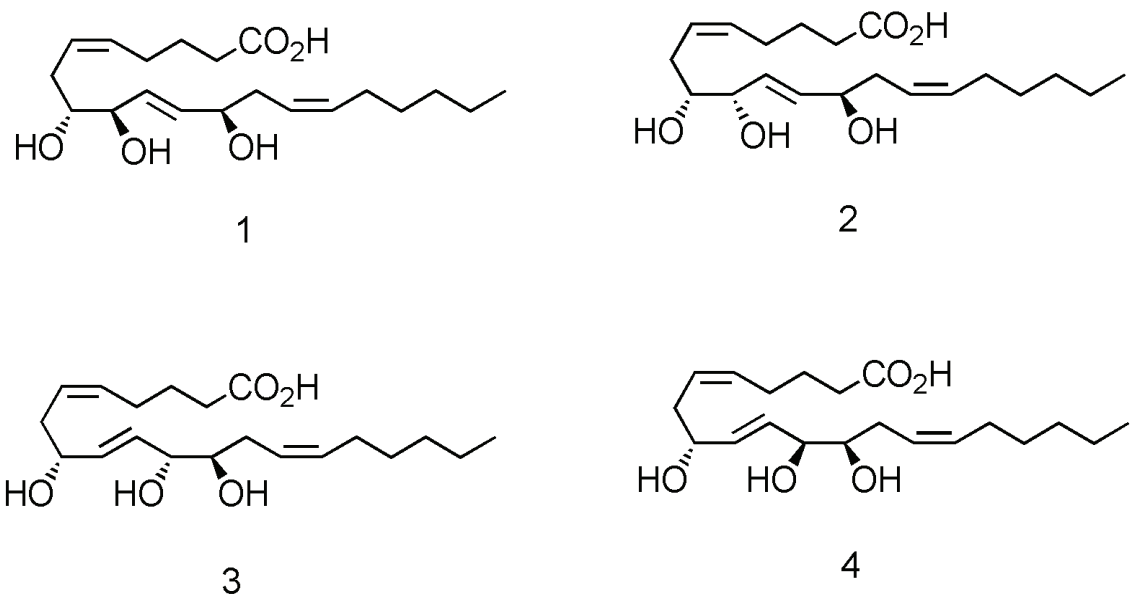

Figure 20. Stereo-configuration of the triol products from acid-catalyzed hydrolysis of the 8*R*,11*R*,12*R*-epoxyalcohol. (1) 8*R*,9*R*,12*R*-trihydroxy-5*Z*,10*E*,14*Z*-trienoic acid. (2) 8*R*,9*S*,12*R*-trihydroxy-5*Z*,10*E*,14*Z*-trienoic acid. (3) 8*R*,11*R*,12*R*-trihydroxy-5*Z*,9*E*,14*Z*-trienoic acid. (4) 8*R*,11*S*,12*R*-trihydroxy-5*Z*,9*E*,14*Z*-trienoic acid. The cellular hydrolysis product is the same as 4.

activity of purified sEH was determined and confirmed by the reaction of sEH with 14,15-EET (Zeldin *et al.*, 1995).

The active sEH was incubated with 8*R*,11*R*,12*R*-epoxyalcohol. The products was extracted and analyzed in RP-HPLC (Figure 21A). The epoxyalcohol peak decreased and the major product peak eluted at about 5.5 min on RP-HPLC. This RP-HPLC spectrum is very similar to that of cellular hydrolysis product (Figure 21B). This suggests that 8*R*,11*R*,12*R*-epoxyalcohol is a suitable substrate for human sEH. The same stereoconfiguration of formed triols from either sEH hydrolysis or cellular hydrolysis indicates sEH is the candidate enzyme catalyzed this hydrolysis reaction in keratinocytes and COS7 cells.

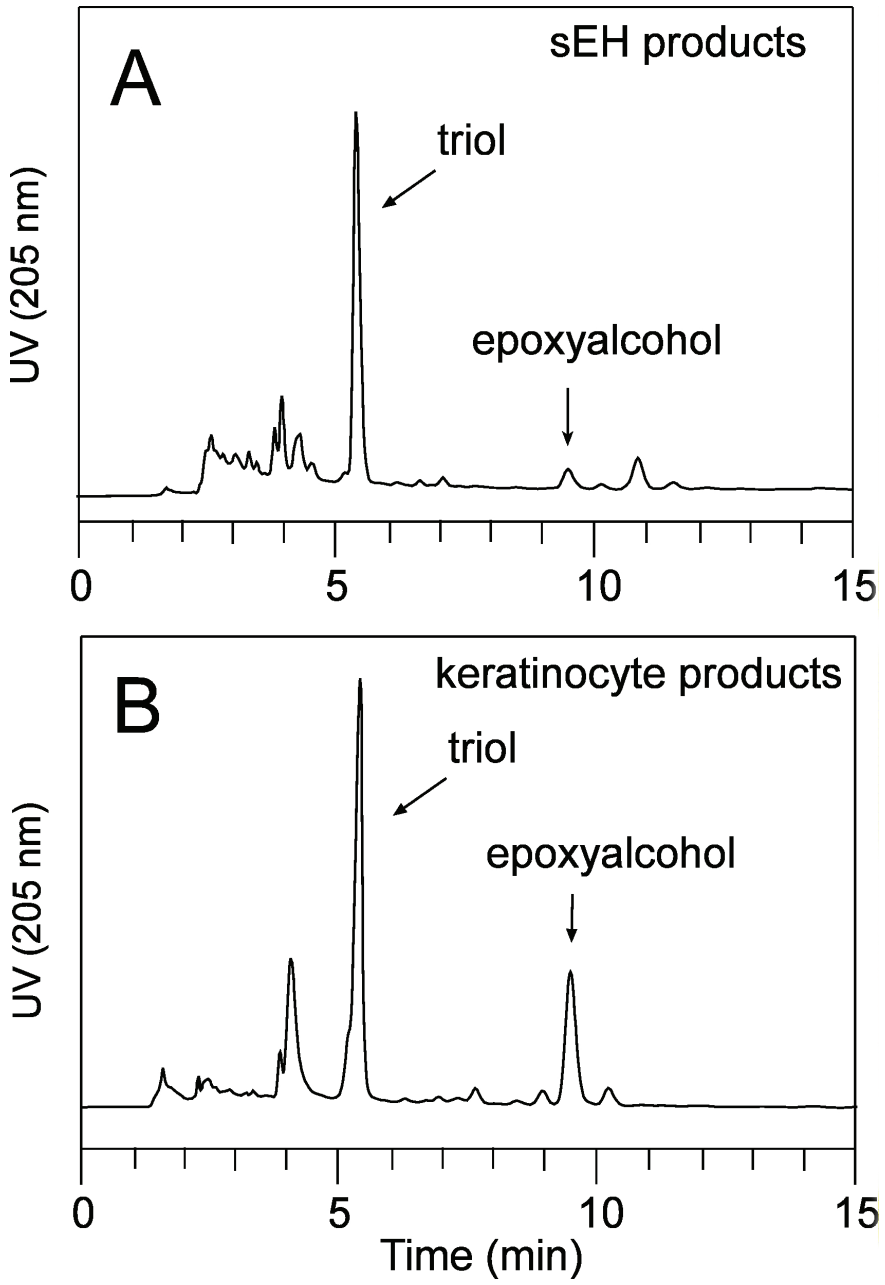

Figure 21. Human soluble epoxide hydrolase is the possible enzyme in 8*R*,11*R*,12*R*-epoxyalcohol hydrolysis in keratinocytes. RP-HPLC analysis of 8*R*,11*R*,12*R*-epoxyalcohol incubations with recombinant human sEH (A) or keratinocyte cell lysate (B).

Site-directed mutagenesis and expression of 12*R*-LOX and eLOX3 mutants

In NCIE patients, two point mutations in 12*R*-LOX (L426P and H578Q) and a frameshift mutation were reported, and two point mutations (R396S and V500F) and a truncation (change arginine 234 to a premature stop codon) were found in eLOX3 (Jobard *et al.*, 2002). The frameshift mutation and the truncation would be anticipated to eliminate the catalytic activities. To explore whether the other naturally occurring mutations in 12*R*-LOX and eLOX3 may be associated with alterations of enzyme activities, we constructed all of these point mutations (12*R*-LOX L426P, 12*R*-LOX H578Q, eLOX3 R396S, and eLOX3 V500F) by site-directed mutagenesis. All mutations were confirmed by sequencing of the cDNAs.

When we expressed the His_6-tagged mutants in *E. coli*, in contrast to the wild-type enzymes, none of the four mutant proteins were recovered at the nickel affinity column step (data not shown), suggesting to us that these mutated proteins are unstable and fail to accumulate in the bacteria. In COS7 cells, both the wild-type and mutant enzymes were expressed, as observed by western blotting (Figure 22). No eLOX3 or 12*R*-LOX could be detected in COS7 cells transfected with pcDNA3.1 vector alone. Because of slight expression variability in the wild-type and mutant enzymes (Figure 22), in the activity assays we used aliquots of cell lysates containing similar amount of eLOX3 or 12*R*-LOX proteins as determined by the western blotting.

Activities of wild-type and mutant 12*R*-LOX

The wild-type human 12*R*-LOX expressed in COS7 cells metabolized [1-^{14}C]arachidonic acid to a single product, 12*R*-HPETE, which was detected as its hydroxy

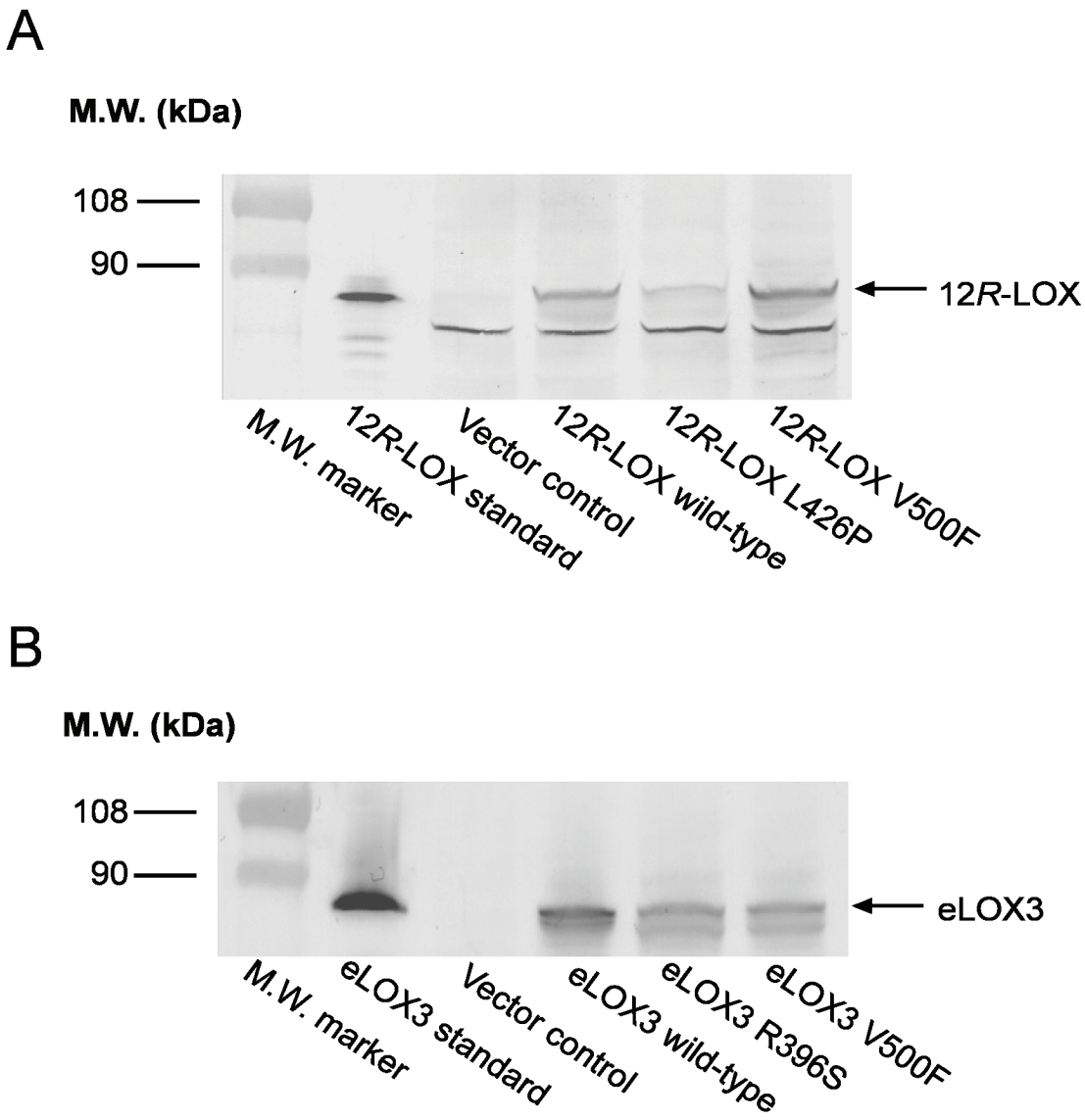

Figure 22. Expression of eLOX3 and 12*R*-LOX mutants in COS7 cells. COS7 cells expressing the different 12*R*-LOX (A) or eLOX3 (B) wild-type and mutants were grown and lysis supernatants were prepared. About 20 µg of total lysis proteins were applied to SDS-PAGE. The Western blot was developed either using a polyclonal anti-human 12*R*-LOX antibody (A) or a polyclonal antibody raised against human 15-LOX-2 that also detects human eLOX3 with sufficient sensitivity (B). As reference proteins, about 50 ng of purified His_6-tagged human eLOX3 and 12*R*-LOX were used. The transfection of pcDNA3.1 vector was used as control. The results shown are representative of three independent experiments.

derivative 12*R*-HETE as a peak at about 6.5 min on RP-HPLC (Figure 23, panel A); additional more polar peaks in the chromatogram are attributed to breakdown of the 12*R*-HPETE during the course of the 45 min incubation. RP-HPLC analysis of incubations with the L426P and H578Q 12*R*-LOX mutants, by contrast, revealed complete elimination of the catalytic activity (Figure 23, panels B and C), giving a similar profile to the vector control (panel D).

Activities of wild-type and mutant eLOX3: experiments with 15*S*-HPETE substrate

eLOX3 lacks conventional lipoxygenase activity, and instead functions as a hydroperoxide isomerase (Yu, Z. *et al.*, 2003). In our first series of experiments we tested its activity using [1-^{14}C]15*S*-HPETE as substrate as this is more readily available than [1-^{14}C]12*R*-HPETE. RP-HPLC analysis of the products formed from [1-^{14}C]15*S*-HPETE by wild-type eLOX3 expressed in COS7 cells showed a main product peak at about 10 min (Figure 24, panel A). In Chapter II we identified this product, prepared using purified recombinant human eLOX3 protein, as the epoxyalcohol 13*R*-hydroxy-14*S*,15*S*-epoxyeicosa-5*Z*,8*Z*,11*Z*-trienoic acid. As with the purified human eLOX3, eLOX3 expressed in COS7 cells also produced a minor product, 15-KETE, which eluted at about 15 min in RP-HPLC. When using 15*S*-HPETE as substrate, the only difference between incubation with cell lysates and the wild-type purified protein is that cell lysates reduced all the remaining 15*S*-HPETE to 15*S*-HETE. Upon incubation of 15*S*-HPETE with the R396S and V500F eLOX3 mutants, most of the substrate was reduced to 15*S*-HETE (Figure 24, panels B and C) and the profiles were indistinguishable from the vector control (panel D). A small peak of radioactivity was present at the retention time

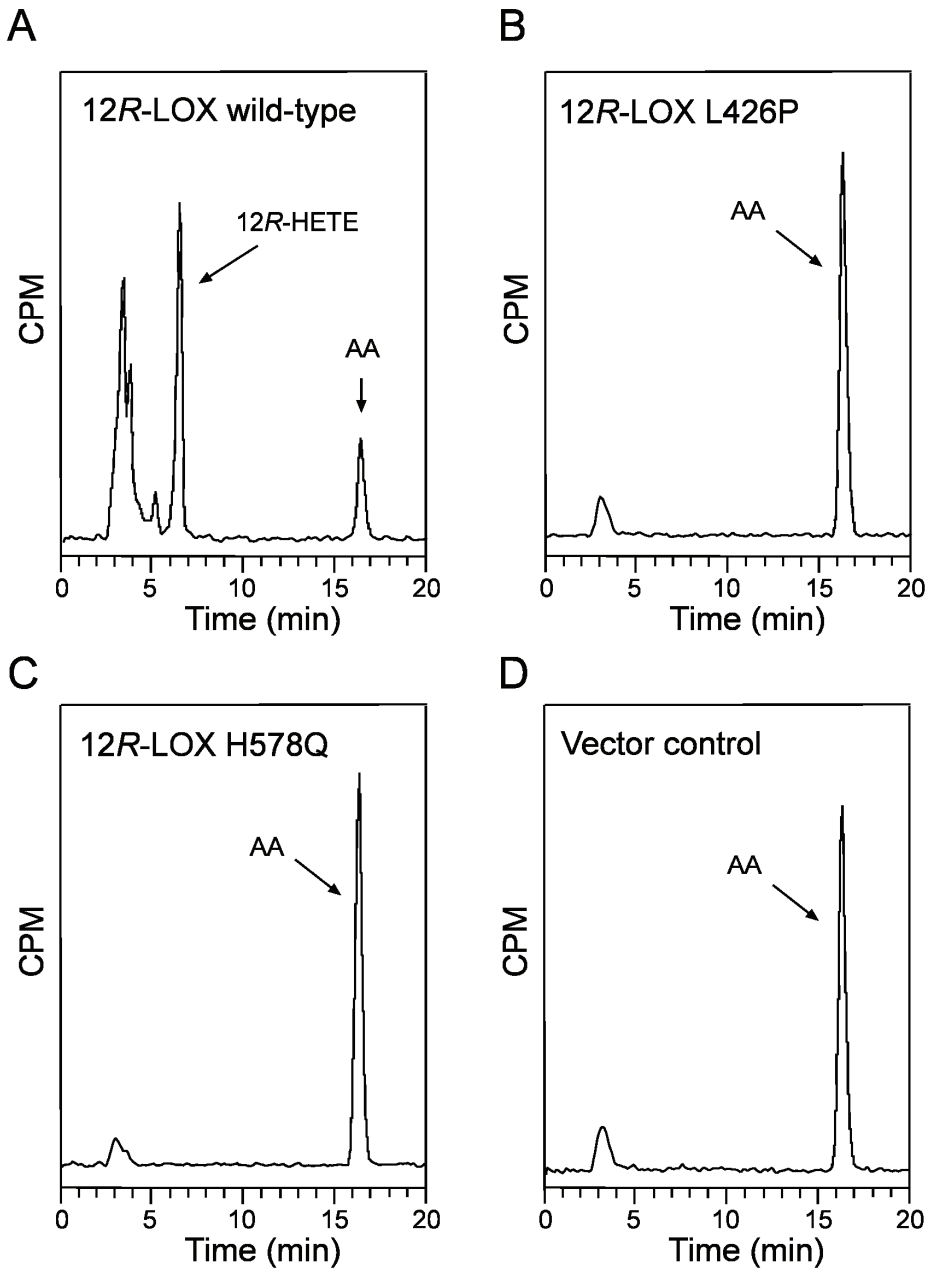

Figure 23. RP-HPLC analysis of the reaction of 12*R*-LOX wild-type or mutants with [1-^{14}C]arachidonic acid. COS7 cells transfected with (A) 12*R*-LOX wild-type, (B) 12*R* L426P (C) 12*R* H578Q and (D) pcDNA3.1 vector were grown and harvested. Aliquots of the COS7 lysis supernatants were incubated with [1-^{14}C]arachidonic acid in pH 6.0 Tris buffer. The products were analyzed by RP-HPLC with a Waters Symmetry C18 5 μm column (0.46 x 25 cm) eluted at a flow rate of 1 ml/min with methanol/water/acetic acid (90:10:0.01 by volume). The results shown are representative of three independent experiments.

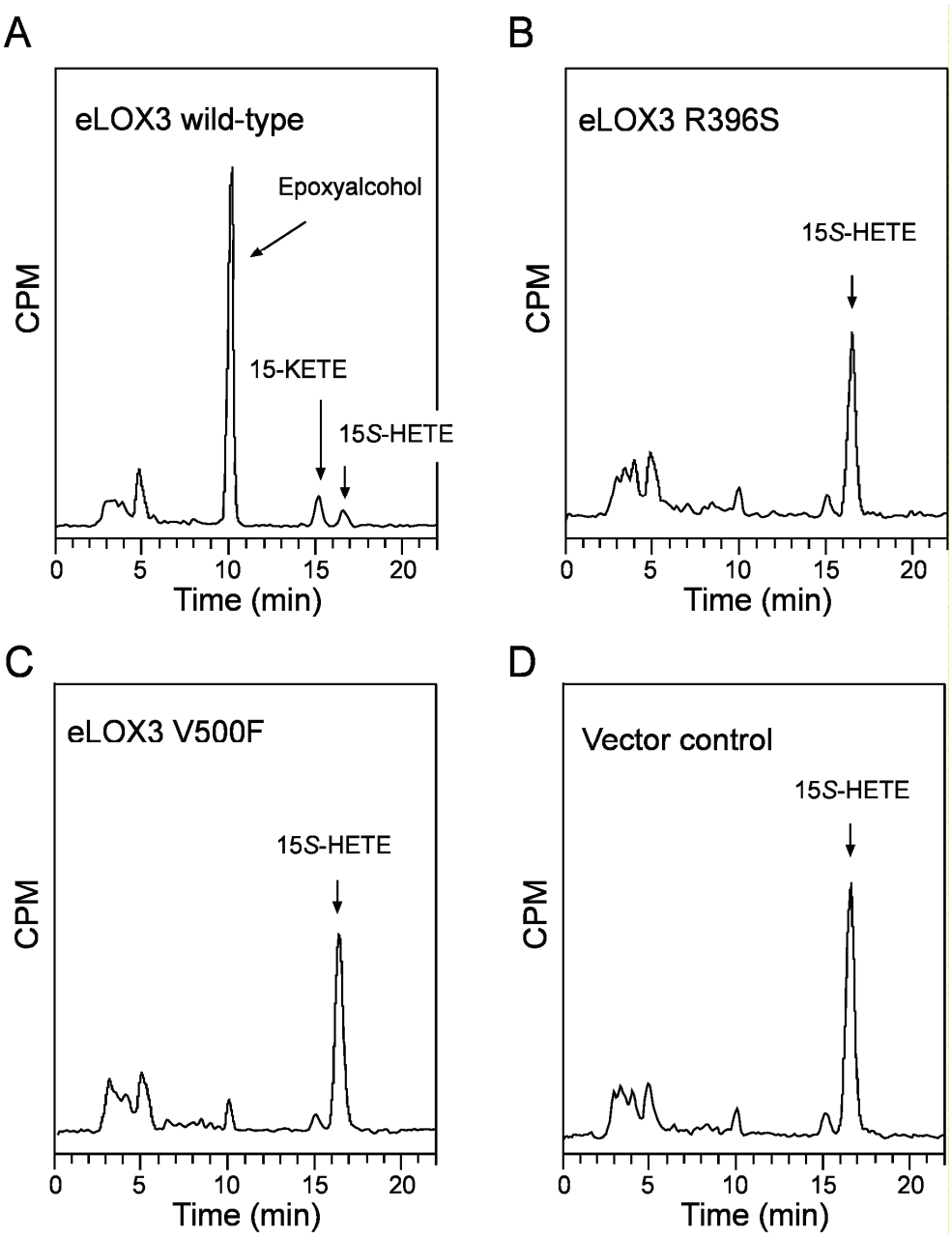

Figure 24. RP-HPLC analysis of the reaction of eLOX3 wild-type or mutants with [1-^{14}C]15*S*-HPETE. COS7 cells transfected with (A) eLOX3 wild-type, (B) eLOX3 R396S, (C) eLOX3 V500F and (D) pcDNA3.1 vector were grown and harvested. Aliquots of the COS7 lysis supernatants were incubated with [1-^{14}C]15*S*-HPETE. The products were analyzed by RP-HPLC with a Waters Symmetry C18 5 μm column (0.46 x 25 cm) eluted at a flow rate of 1 ml/min with methanol/water/ acetic acid (80:20:0.01 by volume). The results shown are representative of three independent experiments.

of the epoxyalcohol product (7% or less of wild-type peak of epoxyalcohol), but it was of similar prominence in the vector only control. The same was true for a peak of 15-KETE (panels B, C and D). It is well known that epoxyalcohols and keto derivatives can be formed through non-enzymatic transformations of HPETEs (Gardner, 1989), and most likely this accounts for the small peaks seen with the vector control and mutant eLOX3. We conclude that the mutant eLOX3 enzymes had no detectable activity in these analyses.

Activities of wild-type eLOX3: experiments with 12*R*-HPETE substrate

As we reported previously, eLOX3 uses 12*R*-HPETE as the preferred substrate and converts it to one of the isomers of hepoxilin A_3, 8*R*-hydroxy-11*R*,12*R*-epoxyeicosa-5*Z*,9*E*,14*Z*-trienoic acid. When we incubated [1-^{14}C]12*R*-HPETE with wild-type eLOX3 expressed in the COS7 cells, the substrate was consumed. As described earlier in this study, incubation of [1-^{14}C]12*R*-HPETE with cell lysate expressing wild-type eLOX3 protein formed one major product eluting at about 5.5 min on RP-HPLC, which is the hydrolysis metabolite of epoxyalcohol (Figure 25, panel A). Cell lysates expressing only the vector control converted [1-^{14}C]12*R*-HPETE to a mixture of products (Figure 25, panel D). One peak is 12*R*-HETE, the reduced metabolite of 12*R*-HPETE. The prominent early peak at 4 min on RP-HPLC was tentatively identified, based on its retention time and characteristic conjugated dienone chromophore (λmax at 282 nm in RP-HPLC column solvent) as the C_{12} trienal acid, 12-oxo-dodeca-5*Z*,8*Z*,10*E*-trienoic acid. This type of aldehyde is formed by a hydroperoxide cleavage reaction that can be promoted by heme and other non-enzymatic catalysts (Dix and Marnett, 1985; Gardner, 1989).

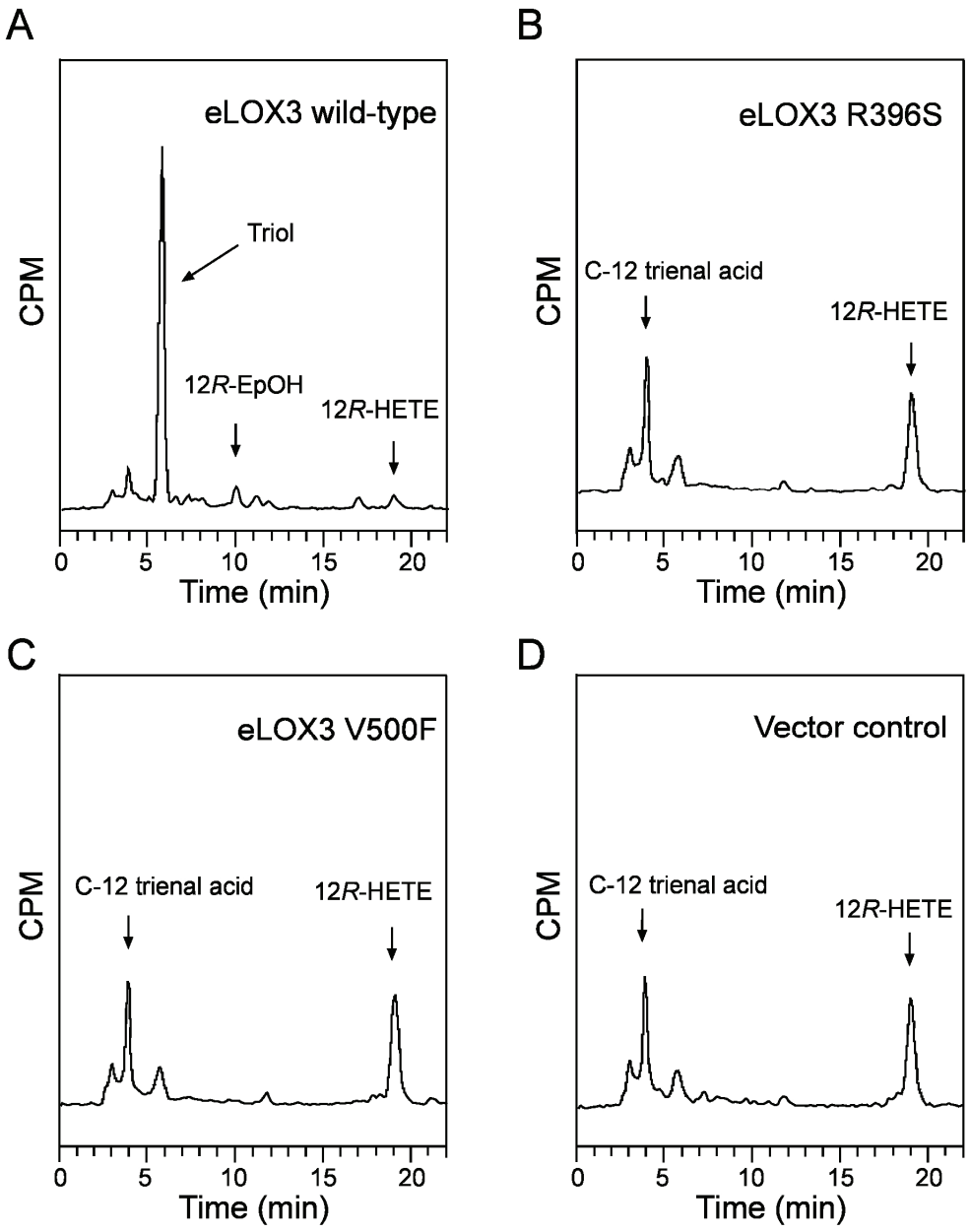

Figure 25. RP-HPLC analysis of the reaction of eLOX3 wild-type or mutants with [1-^{14}C]12*R*-HPETE. COS7 cells transfected with (A) eLOX3 wild-type, (B) eLOX3 R396S, (C) eLOX3 V500F, and (B) pcDNA3.1 vector were grown and harvested. Aliquots of the COS7 lysis supernatants were incubated with [1-^{14}C]12*R*-HPETE. The products were analyzed by RP-HPLC with a Waters Symmetry C18 5 μm column (0.46 x 25 cm) eluted at a flow rate of 1 ml/min with methanol/water/ acetic acid (80:20:0.01 by volume). The results shown are representative of three independent experiments.

Interaction with LOX can also give rise to this cleavage product (Garssen *et al.*, 1971; Glasgow *et al.*, 1986), but there is no LOX activity in vector-transformed COS7 cells. In the incubations of [1-^{14}C]12*R*-HPETE with both eLOX3 R396S and V500F mutations expressed in COS7 cells (Figure 25, panels B and C), the RP-HPLC results were very similar to the vector control (Figure 25, panel D). Neither epoxyalcohol nor a specific trihydroxy peak was detected. Both the vector control and the mutants showed a small broad peak at the retention time of the trihydroxy metabolite (~6 min). This may be composed of a mixture of products formed non-enzymatically from 12*R*-HPETE.

Discussion

Our results show that the 8*R*,11*R*,12*R*-epoxyalcohol (isomer of hepoxilin A_3) from the reaction of eLOX3 with 12*R*-HPETE is easily hydrolyzed to a single 8*R*,11*S*, 12*R*-triol (trioxilin A_3 isomer) in both keratinocytes and COS7 cells. In buffer alone, the 8*R*,11*R*,12*R*-epoxyalcohol is stable under the conditions of incubation (Tris, pH 6, 45 min incubation at 37 ºC) and also during extraction and HPLC. In COS7 cells or human keratinocytes it is converted to a single product as determined by RP-HPLC and GC-MS. In contrast, acid-catalyzed transformation gives a mixture of trihydroxy isomers. There is prior evidence that 8,11,12-trihydroxyeicosa-5,9,14-trienoic acids are formed in incubations of human epidermal fragments in the presence of arachidonic acid (Anton *et al.*, 1995; Anton and Vila, 2000); three isomers of 8,11,12-triols as well as isomers of 8,9,12-triols and 10,11,12-triols were identified by GC-MS (Anton *et al.*, 1995; Anton and Vila, 2000). These were almost certainly derived from 12-HPETE, although the contributions of 12*R*-HPETE and 12*S*-HPETE are unknown. Our observations on the

appearance of a single isomer of 8,11,12-triol formed from the 12*R*-LOX/eLOX3-derived 8*R*,11*R*,12*R*-epoxyalcohol point to the involvement of a specific enzyme, likely an epoxide hydrolase, in formation of this trihydroxy derivative. This enzymatic hydrolysis is also supported by the thermal instability of the activity in COS7 cells and keratinocytes. Boiling the cell lysate for 10 min prior to incubation with the epoxyalcohol largely eliminated the transformation. Candidate enzymes involved in the hydrolysis include cytosolic and microsomal epoxide hydrolases (Armstrong and Cassidy, 2000) or the hepoxilin epoxide hydrolase activity partially characterized by Pace-Asciak and Lee (Pace-Asciak, C. R. and Lee, 1989). We also tentatively assigned the stereochemistry of the triol hydrolysis product as the structure 8*R*,11*S*,12*R*-trihydroxyeicosa-5*Z*,9*E*,14*Z*-trienoic acid formed by SN2 hydrolysis of the epoxide at C-11. Based on the specific catalytic activity of human epoxide hydrolases (Ota and Hammock, 1980; Armstrong, 1999), the soluble epoxide hydrolase which can use cis-disubstituted epoxides as substrates is the possible enzyme involved in this hydrolysis. Our result using the recombinant enzyme also strongly supported this hypothesis. In human keratinocytes, this hydrolase activity may be the downstream enzyme in the pathway consisting of 12*R*-LOX and eLOX3 to form an active mediator in the regulation of keratinocyte differentiation. Figure 26 summarizes all the transformations of arachidonic acid discussed in this study.

NCIE is an autosomal recessive form of ichthyosis with an incidence of about 1 in 100,000-200,000. The best characterized mutations inactivate the transglutaminase 1 gene, with resultant defects in formation of the skin permeability barrier (Huber *et al.*, 1995). So far, NCIE with mutations in LOX genes has been reported in a small number of

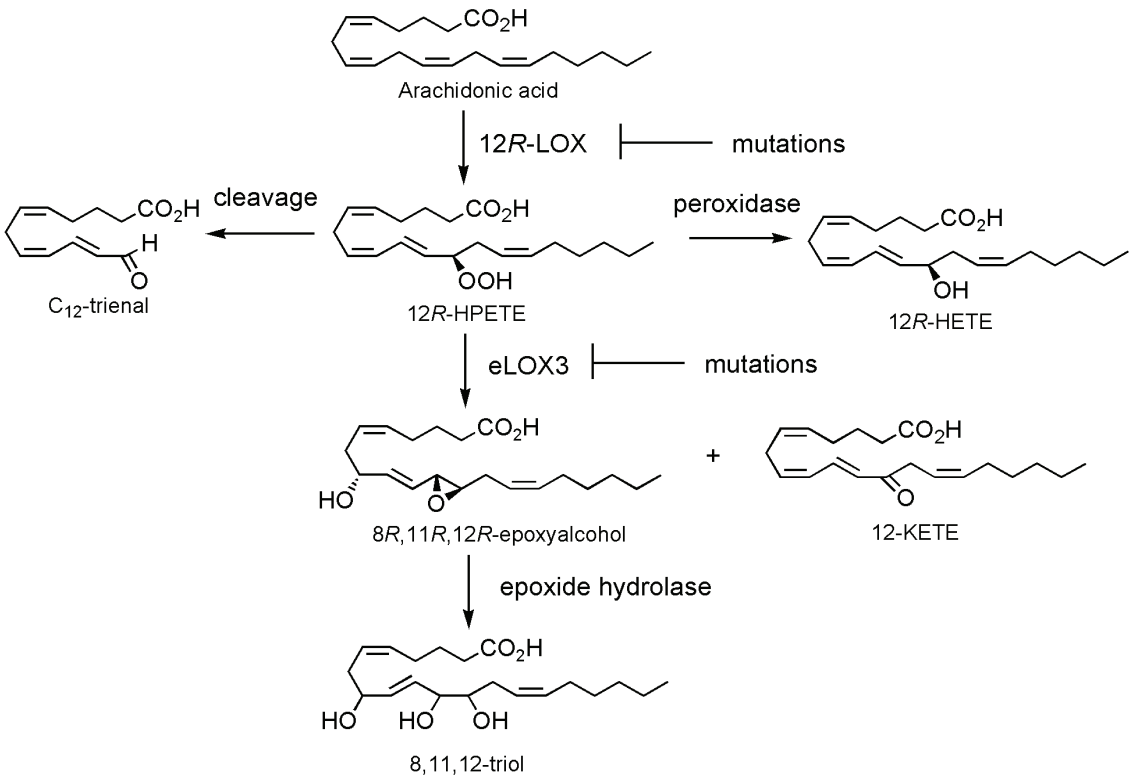

Figure 26. Transformations of arachidonic acid and 12*R*-HPETE observed in this study.

consanguineous families in the Mediterranean by Jobard et al. (Jobard *et al.*, 2002) and in additional patients from an independent study in Germany (Eckl *et al.*, 2005). In the present study, we show that the point mutations identified by Jobard et al. in the coding region of human eLOX3 and 12*R*-LOX completely eliminate the enzyme activities. These data are consistent with the concept that this loss of function of eLOX3 or 12*R*-LOX is fundamental to the pathogenesis of the LOX-dependent form of NCIE. The findings further imply that eLOX3 and 12*R*-LOX activities normally are involved in the biochemistry underlying the process of development of an intact epidermis. This possibility is reinforced by the recent suggestion that a novel gene, ichthyin, may encode

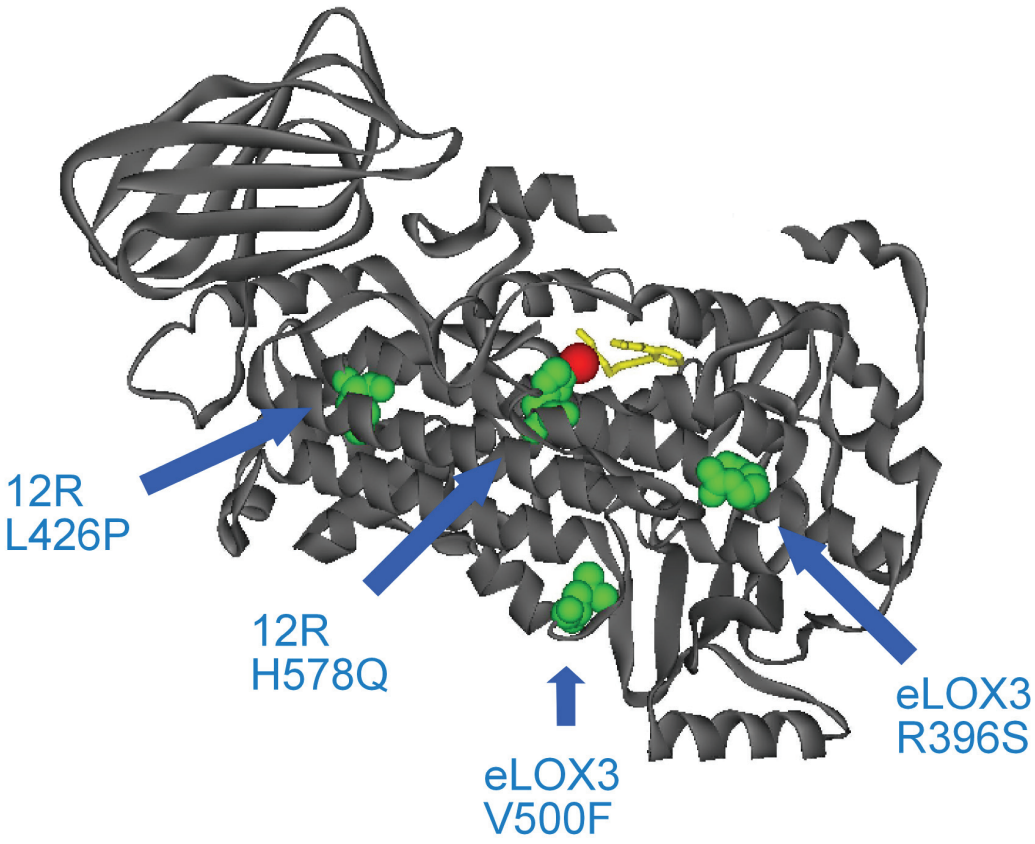

Figure 27. Location of point mutations identified in 12*R*-LOX or eLOX3 genes of NCIE patients. Positions equivalent to the mutated residues in eLOX3 or 12*R*-LOX are shown on the crystal structure of rabbit reticulocyte 15-LOX. Red: iron. Yellow: inhibitor co-crystallized in the 15-LOX active site. Green, mutated residues.

for a putative receptor for the epoxyalcohol pathway product (Lefevre *et al.*, 2004). Taken together, the genetic and biochemical insights provide new evidence of the involvement of LOX enzymes in the formation of the skin permeability barrier. It remains to be established that one can detect these specific product(s) and their physiological activities in normal keratinocytes. The products should ameliorate the symptoms of the forms of NCIE involving LOX mutations, and presumably be ineffective in the patients lacking the putative signaling receptor.

Based on the alignment of eLOX3 and 12*R*-LOX with rabbit 15-LOX, (the only mammalian LOX for which the 3-D structure is available), one of the mutations in 12*R*-LOX, His578, is a ligand to the iron in the lipoxygenase active site. As expected, its mutation eliminates catalytic activity. The locations of other point mutations (Arg396 and Val500 in eLOX3 and Leu426 in 12*R*-LOX) are far away from the iron ligands and the substrate binding pocket, having no obvious connection to the active site (Figure 27). Mutations of these residues also rendered the enzymes completely inactive. Although these three mutations may not interfere with substrate binding or catalysis directly, they may disrupt the correct folding of the catalytic domain of the proteins. This is suggested by our observation that the mutated proteins failed to accumulate when expressed in *E. coli*.

CHAPTER IV

COMPARISON OF THE CATALYTIC ACTIVITY OF MOUSE AND HUMAN EPIDERMAL LIPOXYGENASE 3

Introduction

One remarkable aspect of mammalian LOX enzymes is that although their homologs in various species share high amino acid sequence identity, some of them show differences in expression pattern, catalytic activity and biological function across species. For example, mouse has three isoforms of 12-LOX that form 12*S*-HPETE: platelet-type, leukocyte-type and epidermis-type. In human, only platelet-type 12-LOX expressed. The homolog of mouse leukocyte-type 12-LOX in human (15-LOX-1) mainly forms 15*S*-HPETE as well as 12*S*-HPETE. The counterpart of mouse epidermal-type 12-LOX gene in human is a pseudo-gene. The mRNA transcribed from this gene contains a premature stop codon in sequence.

A pertinent example here is human and mouse 12*R*-LOX. They share about 85% amino acid sequence identity but have different substrate selectivity. Human 12*R*-LOX forms 12*R*-HPETE from arachidonic acid and exhibit a slightly acidic pH-optimum (Schneider *et al.*, 2001a). The mouse ortholog does not use free acid as substrate. *In vitro* experiment showed that only arachidonic acid methyl ester is its substrate. Also in mouse, no 12*R*-HETE has been described as an endogenous product. Mouse 12*R*-LOX may use a yet unknown natural substrate and has different functions compared to human 12*R*-LOX.

In Chapter II we showed that human eLOX3 exhibits hydroperoxide isomerase activity and it preferentially transforms the human 12*R*-LOX-derived product, 12*R*-

HPETE, into a specific epoxyalcohol product. In this study we will investigate the catalytic activity of its mouse homolog. Mouse eLOX3 is expressed in the stratified epithelia of skin, tongue, and forestomach, but has no detectable oxygenase activity (Kinzig *et al.*, 1999). If it has similar activity as human eLOX3, the situation that the coupling of human 12*R*-LOX and eLOX3 as described in Chapter II and III may not exist in mouse since mouse 12*R*-LOX does not supply a fatty acid hydroperoxide substrate for eLOX3. Does mouse eLOX3 also exhibit hydroperoxide isomerase activity? If so, which hydroperoxide is the preferred substrate for mouse eLOX3? Is there a specific LOX functionally linked to mouse eLOX3 in mouse skin? The present work in this study is aimed to answer these questions.

Experimental Procedures

Expression and purification of mouse eLOX3

The cDNA for mouse eLOX3 was cloned by PCR using cDNA prepared from mouse keratinocytes. To prepare the eLOX3 protein with an N-terminal 6×His tag, the eLOX3 cDNA was subcloned into the pCW expression vector (a generous gift from Dr. Michael R. Waterman, Vanderbilt University, Nashville, TN) with the 5' sequence encoded as ATG CAT CAC CAT CAC CAT CAC GCA-, with the last codon representing the start of the wild type enzyme. The mouse eLOX3 was expressed in *E. coli* BL21 (DE3) cells (Novagen) and the His_6-tagged protein was purified on Ni-NTA agarose (Qiagen, Valencia, CA) according to the manufacturer's instructions. Fractions of 0.5 ml were collected off the affinity column and assayed using SDS-PAGE. Fractions

containing mouse eLOX3 were pooled and dialyzed against a buffer of 50 mM Tris (pH 7.5) containing 150 mM NaCl to remove the imidazole.

Preparation of hydroperoxides

HPETEs with specific positional and stereo configurations were prepared from the autoxidation of arachidonate methyl ester as described previously in Chapter II. 13*S*-HPODE was synthesized from linoleic acid using soybean lipoxygenase (Sigma, Type V) and purified by preparative SP-HPLC (Alltech Econosil silica, 1.0 × 25 cm, hexane/ isopropanol/acetic acid 100:1.5:0.1 by volume at 4 ml/min). 9*S*-HPODE was synthesized using a lipoxygenase preparation from tomato fruit (Matthew *et al.*, 1977) and purified using the same SP-HPLC conditions as above. The hydroperoxides were stored as a 5 mg/ml stock solution in acetonitrile or methanol under argon at -80 °C.

eLOX3 activity assay

Incubation with the purified human or mouse eLOX3 were typically conducted in 500 μl incubation buffer (50 mM Tris, 150 mM NaCl, pH 6.0) using 0.01 – 0.1 μM enzyme concentration in a 1 cm path length microcuvette. Each HPETE at the concentration of 30 μM was added and incubated at room temperature for 10 min. The HPETE concentration used here is around the Km of human eLOX3 reaction with 12*R*-HPETE as described previously in Chapter II. eLOX3 activity was measured by monitoring the disappearance of the UV absorbance at 235 nm in the time-drive mode and the reaction rate was calculated from the initial linear part of the curve.

HPLC analysis

Products of the eLOX3 reactions with HPETE substrates were analyzed initially by RP-HPLC using a Waters Symmetry C18 5μm column (0.46 × 25 cm) eluted at a flow rate of 1 ml/min with methanol/water/acetic acid (80:20:0.01 by volume), and UV detection at 205, 220, 235, and 270 nm using an Agilent 1100 series diode array detector. The main products were recovered from the reversed-phase solvent by addition of water and extraction with dichloromethane. Further purification was carried out by SP-HPLC using an Alltech Econosil Silica column (0.46 × 25 cm), a solvent system of hexane/isopropanol/acetic acid (100:2:0.1 by volume), and a flow rate of 1 ml/min.

The conjugated trienes from mouse eLOX3 and 8*S*-HPETE reaction were recovered using the same RP-HPLC conditions as above. Purified peaks were treated by triphenyl phosphine (TPP) to reduce the hydroperoxide to hydroxide, and then analyzed by RP-HPLC using a Waters Symmetry C18 5μm column (0.46 × 25 cm) eluted at a flow rate of 1 ml/min with methanol/water/acetic acid (75:25:0.01 by volume), and UV detection at 270 nm.

Derivatization

Methyl esters of the products were prepared using ethereal diazomethane/ methanol (5:1). Catalytic hydrogenations were performed in 100 μl of ethanol using about 1 mg of palladium on alumina and bubbling with hydrogen for 2 min at room temperature. Reactions were terminated by the addition of water and extraction with ethyl acetate. Trimethylsilyl ester and trimethylsilyl ether derivatives were prepared by treatment overnight with bis(trimethylsilyl)trifluoracetamide (10 μl) and pyridine (5 μl)

at room temperature. Subsequently, the reagents were evaporated under a stream of nitrogen and the samples were dissolved in hexane for GC-MS.

GC-MS analysis

Analysis of the methyl ester trimethylsilyl ether derivatives of the products was carried out in the positive ion electron impact mode (70 eV) using a Hewlett-Packard 5989A mass spectrometer coupled to a Hewlett-Packard 5890 gas chromatograph equipped with a RTX-1701 fused silica capillary column (17 m × 0.25 mm, internal diameter). Samples were injected at 150°C, and after 1 min the temperature was programmed to 300°C at 12 or 20°C/min.

NMR

1H NMR and 2D (H,H-COSY) NMR spectra were recorded on a Bruker DRX 400 MHz spectrometer. The ppm values are reported relative to residual non-deuterated solvent (δ = 7.24 ppm for C_6H_6).

Results

Reaction of human and mouse eLOX3 with natural HPETEs and HPODEs

To compare the substrate selectivity of human and mouse eLOX3, purified human and mouse enzymes (about 0.01–0.1 μM) were incubated with different natural HPETEs or HPODEs (30 μM, which is around the Km of human eLOX3 reaction with 12*R*-HPETE) at room temperature in 500 μl incubation buffer (50 mM Tris, 150 mM NaCl, pH 7.5) in a 1-cm path length microcuvette. The reaction rates were measured by monitoring disappearance of the signal at 235 nm in the time-drive mode and calculated from the initial linear part of the curve. The relative activities (rates of 12*R*-HPETE were set as 100) are shown in Figure 28. As described previously in Chapter II, 12*R*-HPETE is the best substrate for human eLOX3. For mouse eLOX3, 8*S*-HPETE is the best substrate.

RP-HPLC analysis of mouse eLOX3 reaction with 8*S*-HPETE

The product of mouse eLOX3 reaction with 8*S*-HPETE was extracted and analyzed by RP-HPLC using a Waters Symmetry C18 5-μm column (0.46 × 25 cm) eluted at a flow rate of 1 ml/min with methanol/water/acetic acid (80:20:0.01 by volume) (Figure 29). The main product with retention time of 12 min displayed maximum UV absorbance at 205 nm. A minor product that eluted near 20 min had the UV spectrum of a conjugated dienone with λ_{max} at 285 nm in the reversed-phase column solvent. Treatment of this product with $NaBH_4$ yielded a product that cochromatographed on RP-HPLC with an 8-HETE standard, which, in accord with the UV spectrum and the mobility on RP-HPLC, points to the original product being 8-ketoeicosa-5*Z*,9*E*,11*Z*,14*Z*-tetraenoic acid

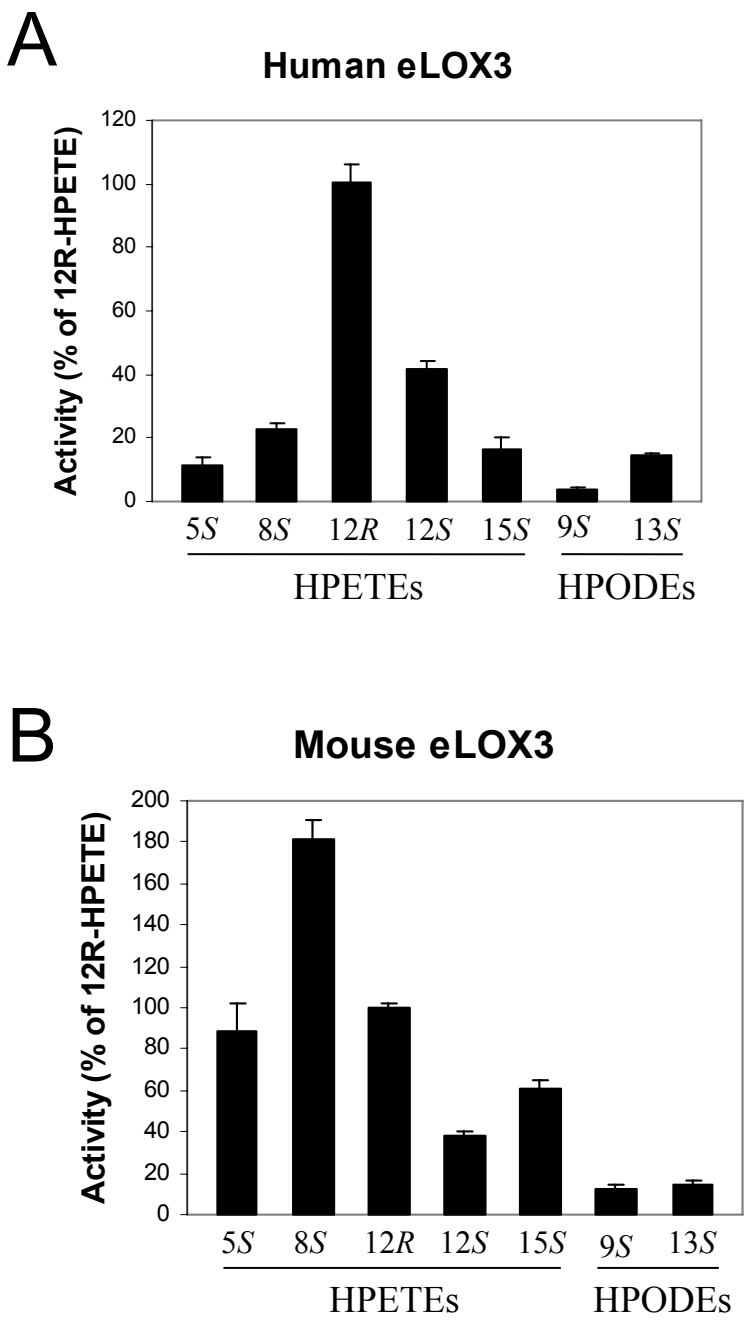

Figure 28. Substrate selectivity of human and mouse eLOX3. Purified human and mouse eLOX3 (about 0.01–0.1 μM) were incubated with different natural HPETEs (30 μM) at room temperature in 500 μl incubation buffer (50 mM Tris, 150 mM NaCl, pH 7.5) in a 1-cm path length microcuvette. Rates were measured by monitoring disappearance of the signal at 235 nm in the time-drive mode and calculated from the initial linear part of the curve. (A) Human eLOX3 reactions. (B) Mouse eLOX3 reactions. Rates for 12*R*-HPETE were set as 100% and all the other reactions were compared with 12*R*-HPETE reaction.

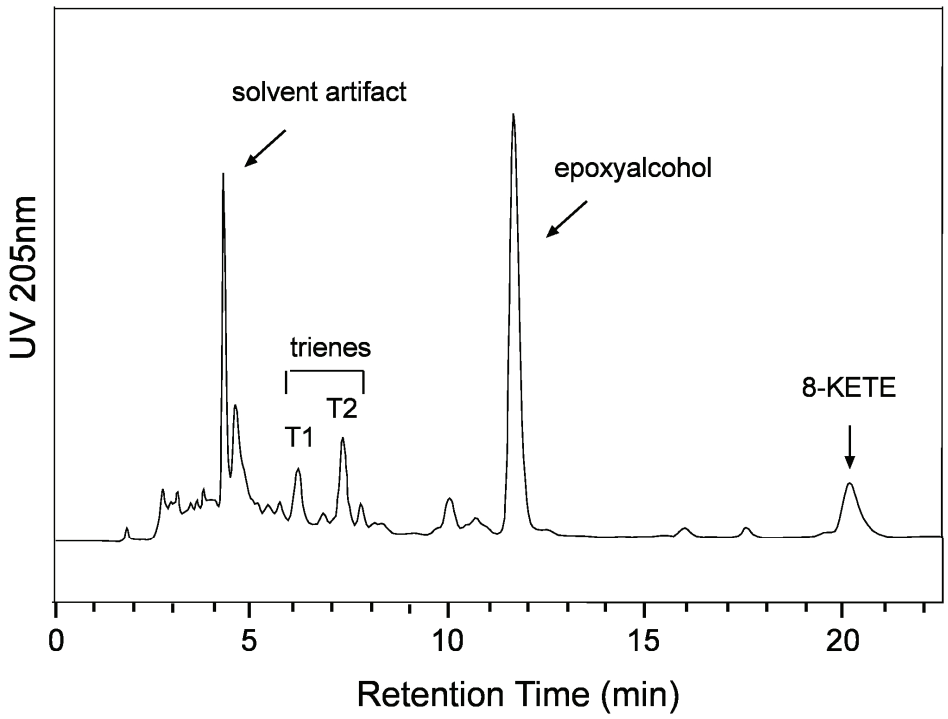

Figure 29. RP-HPLC analysis of the products in mouse eLOX3 reaction with 8*S*-HPETE. The products were analyzed by RP-HPLC using a Waters Symmetry C18 5-μm column (0.46 x 25 cm) eluted at a flow rate of 1 ml/min with methanol/water/acetic acid (80:20:0.01 by volume), and UV detection at 205 nm.

(8-KETE). There are several minor products eluted between 5 and 10 min. Two prominent peaks T1 and T2 (Figure 29) had the UV spectrum of a conjugated triene with λ_{max} at 270 nm in the same reversed-phase column solvent.

Identification of the main product from 8*S*-HPETE and mouse eLOX3 reaction

To prepare sufficient product for NMR analysis, 1.0 mg of 8*S*-HPETE was incubated in 25 ml of incubation buffer with 0.1 μM mouse eLOX3. The main product was purified from RP-HPLC and then treated with ethereal CH_2N_2. The methyl ester derivative was further purified in SP-HPLC. GC-MS analysis (electron impact mode)

gave a mass spectrum of the methyl ester trimethylsilyl ether derivative with structurally significant ions (with relative abundance in parentheses) at *m/z* 407 $[M\text{-}CH_3]^+$ (<1%), 391 (M-31, <1%), 281 (C8 – C20, $[C_2H_2OCHOSi(CH_3)_3\ C_{10}H_{17}]^+$, 2.5%) and 239 (C10 – C20, $[CHOSi(CH_3)_3\ C_{10}H_{17}]^+$, 52%), indicating a C-10 hydroxyl, and a base peak at *m/z* 142 (100%) (Figure 30A). After hydrogenation, the M-15 ion peak shifted by 6 mass units (m/z 413) and the α-cleavage ions around C-10 appeared at 243 (239 + 4) and 287 (Fig. 30B). The predicted molecular weight of 422 is compatible with a C20 fatty acid methyl ester containing a C-10 hydroxyl, an epoxide moiety, and three double bonds. ^{1}H-NMR (400 MHz, in deuterated benzene) and all proton signals assigned by H,H-COSY analysis defined the complete covalent structure of the product as a single diastereomer of 10-hydroxy-8,9-epoxyeicosa-5,11,14-trienoic acid (Figure 31).. The coupling constant between the epoxide protons H8 and H9 (J=2.16 Hz) indicates the *trans* configuration of the 8,9-epoxide, i.e. 8*S*,9*S*-epoxy, assuming, as expected, that the original 8*S* configuration is retained. The coupling constant between H9 and H10 (J=4.9 Hz) indicates *threo* diasteromer of 10-hydroxy-8*S*,9*S*-epoxy, i.e., 10*R*-hydroxy-8*S*,9*S*-epoxy. All the three double bonds do not participate in the transformation from 8*S*-HPETE and should retain the original *cis* configurations. Overall, the structure of the main product from mouse eLOX3 reaction with 8*S*-HPETE is 10*R*-hydroxy-8*S*,9*S*-epoxyeicosa-5*Z*,11*Z*,14*Z*-trienoic acid (Figure 31A).

Production of trienes from mouse elox3 reaction with 8S-HPETE

The mixture of products from 8*S*-HPETE analyzed on RP-HPLC using a Waters Symmetry C18 5-μm column (0.46 × 25 cm) eluted at a flow rate of 1 ml/min with

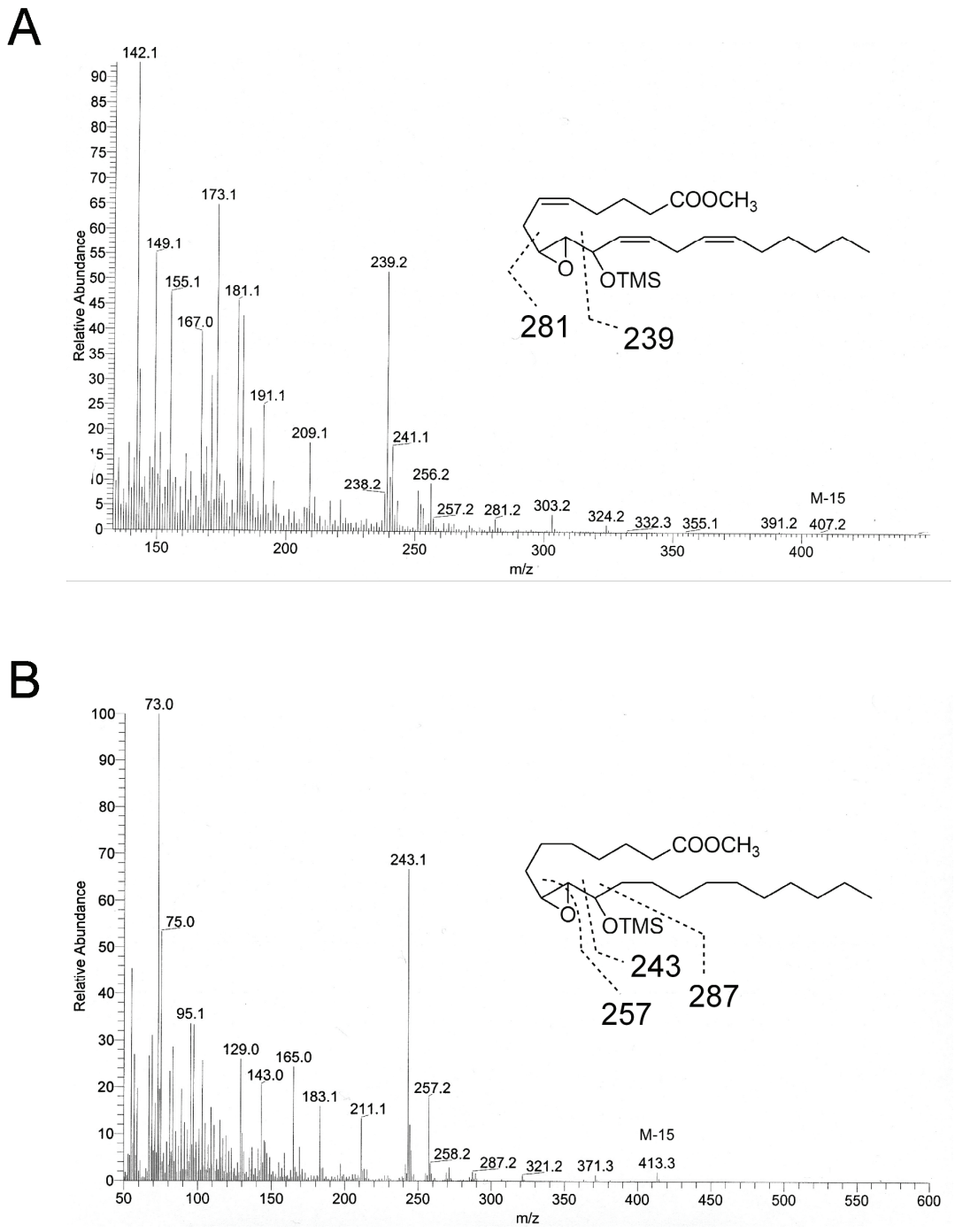

Figure 30. GC-MS analysis of the main product of mouse eLOX3 reacted with 8*S*-HPETE. (A) EI-mass spectrum of the methyl ester TMS ether derivative. (B) EI-mass spectrum of the hydrogenated methyl ester TMS ether derivative.

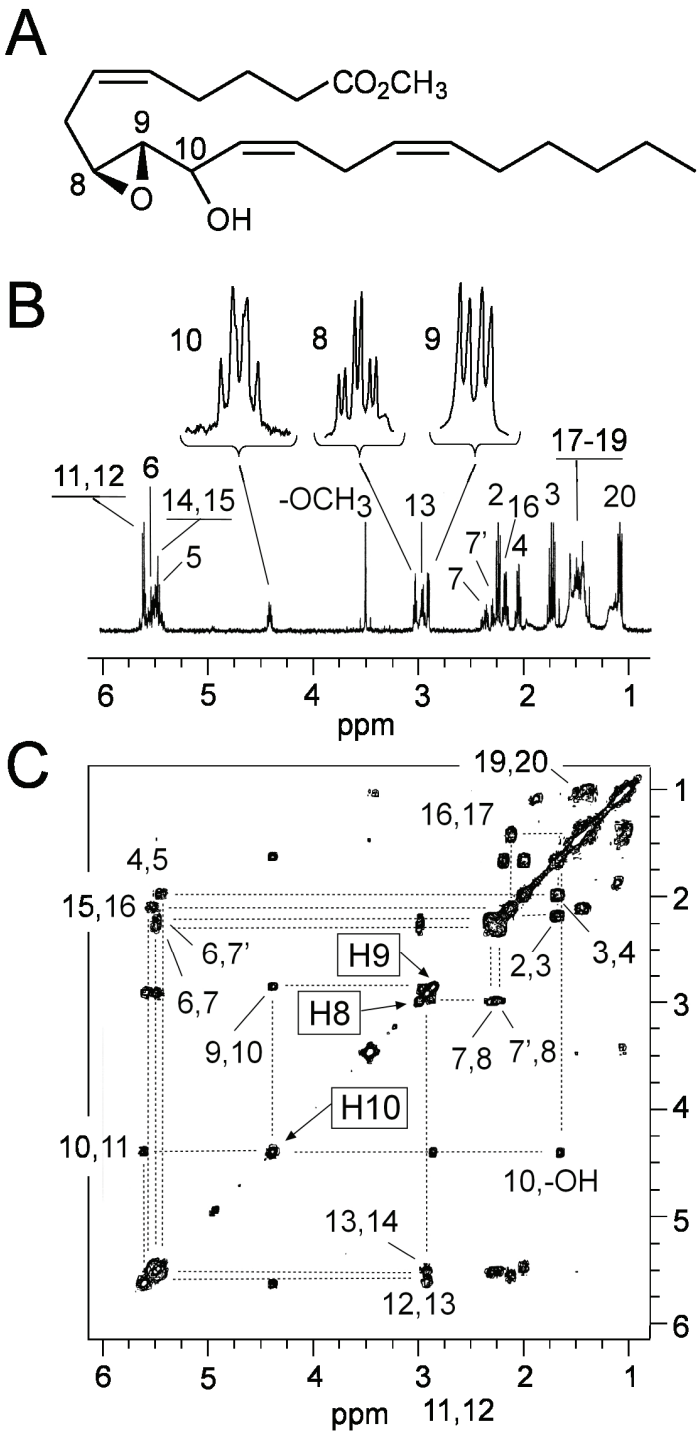

Figure 31. NMR analysis of the main product of mouse eLOX3 reacted with 8*S*-HPETE. The proton spectrum is shown in the middle with an expanded view of the geminal hydroxyl and epoxide protons (H8, H9, and H10) above and the chemical structure at the top; below is shown the H,H-COSY analysis with the main couplings indicated.

methanol/water/acetic acid (80:20:0.01 by volume) gave multiple peaks between 5 to 10 min. To identify their structures, we purified the two prominent peaks T1 and T2 (Figure 29) in the same RP-HPLC system. Based on the maximum UV absorbance at 270 nm and UV spectra, T1 and T2 are the mixtures of conjugated trienes. The purified peaks were treated respectively by TPP and then analyzed on RP-HPLC with methanol/water/acetic acid (75:25:0.01 by volume). Both T1 and T2 were separated into two peaks (I and II on Figure 32 panel A, and III and IV on Figure 32 panel B, respectively). GC-MS analysis (electron impact mode) gave very similar mass spectrum of the methyl ester trimethylsilyl ether derivatives from these 4 products with structurally significant ions at *m*/*z* 404 (M-90), 173 (C15 – C20), 353 (C8 – C20), 263 (353-90), and hydrogenated products at m/z 487 (M-15), 431 (C1 – C15), 359 (C8 – C20), 341 (431-90), 269 (359-90), 245 (C1 – C8) and 173 (C15 – C20), indicating the four parent molecules are all 8, 15-dihydroxy-5,9,11,13-tetraenoic acids. There are two possible pathways to form these conjugated trienes from 8*S*-HPETE (Figure 33). One pathway is from further oxygenation of 8*S*-HPETE at carbon 15, which will form 8*S*,15*R*/*S*-dihydroperoxy-5*Z*,9*E*,11*Z*,13*E*-tetraenoic acids. Via this route, the formed conjugated triene has trans-cis-trans conformation. After TPP treatment, they will be reduced to dihydroxy fatty acid products and thus change the retention time in RP-HPLC (peak II and IV on Figure 32). The other pathway is through a LTA4-like epoxide intermediate followed by its hydration to give 8*S*,15*R*/*S*-dihydroxy-5*Z*,9*E*,11*E*,13*E*-tetraenoic acids (trans-trans-trans conformation for the conjugated triene). TPP treatment does not affect their retention time in RP-HPLC (Peak I and III in Figure 32), indicating that the products were formed as hydroxy derivatives, not hydroperoxides.

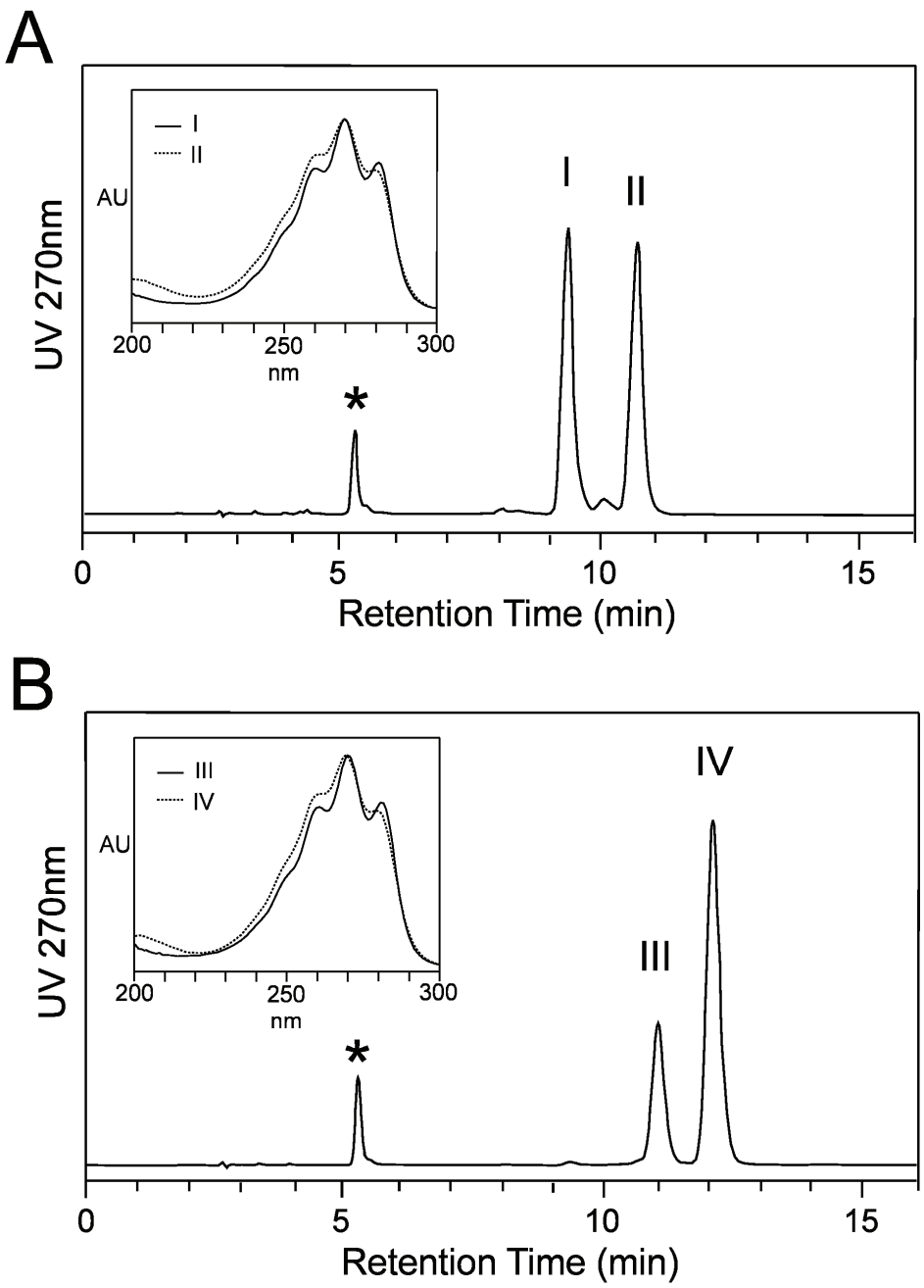

Figure 32. Production of conjugated trienes from the mouse eLOX3 reaction with 8*S*-HPETE. (A) Peak T1 and (B) peak T2 in Figure 29 were purified and treated respectively by TPP and then analyzed on RP-HPLC with methanol/water/acetic acid (75:25:0.01 by volume). The UV spectra of each separated peaks (I to IV) were shown in inset. The conjugated trienes which have trans-trans-trans double bond conformation were shown in solid line (——) and which have trans-cis-trans double bond conformation were shown in dashed line (……).The oxidized TPP was marked as *.

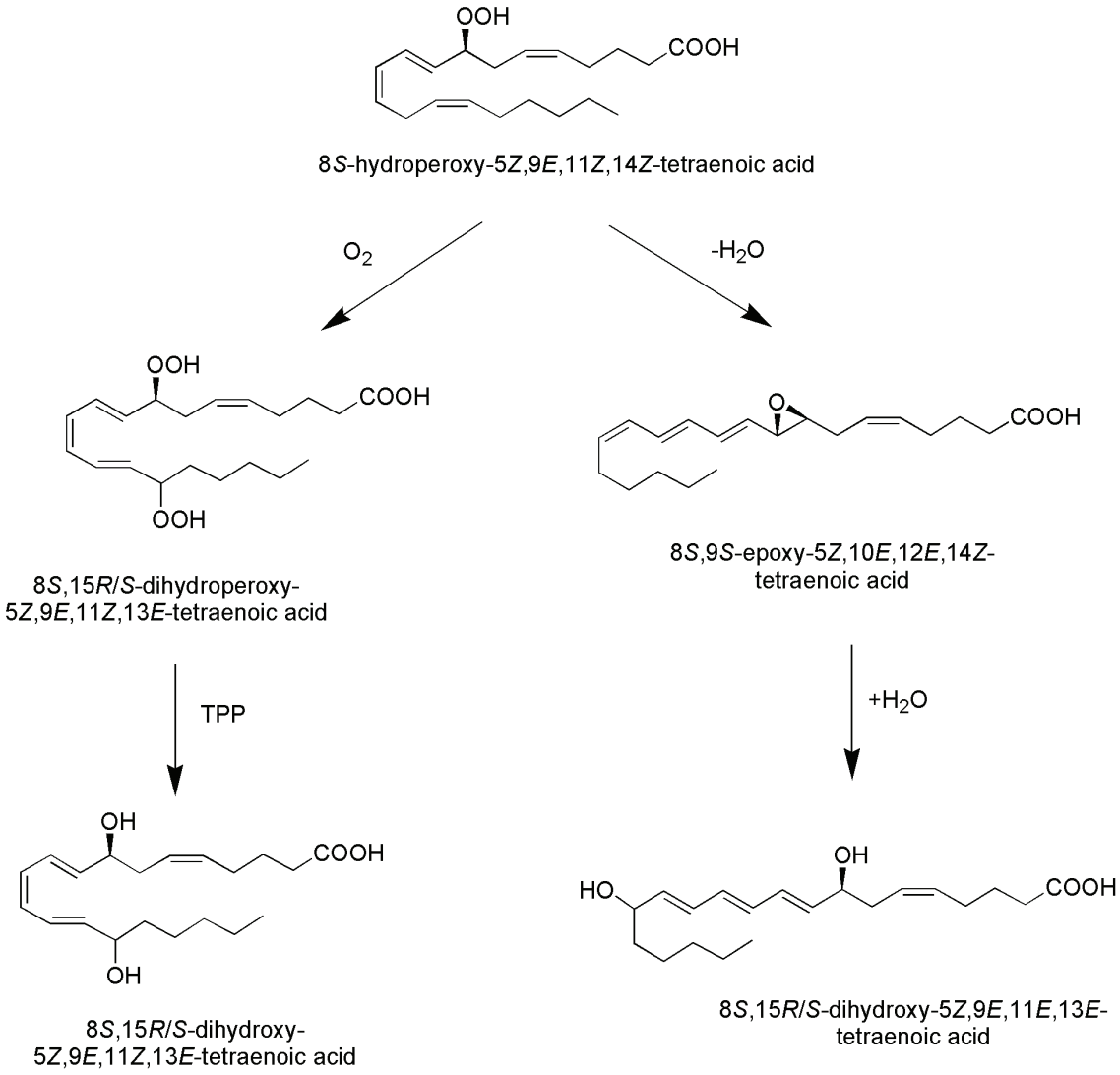

Figure 33. Possible pathways to form conjugated trienes from 8*S*-HPETE.

Reaction of mouse eLOX3 with 8*R*-HPETE

Unlike human eLOX3 reaction, in which 12*R*-HPETE is the best substrate among all the natural and non-natural HPETEs and HPODEs, mouse eLOX3 prefer to react with the non-natural HPETE, 8*R*-HPETE. The reaction rate of 8*R*-HPETE with mouse eLOX3 is about twice the reaction rate of 8*S*-HPETE with mouse eLOX3 in the same pH6.0 reaction buffer (Figure 34A). The product of 8*R*-HPETE reaction with mouse eLOX3 was analyzed in RP-HPLC using a Waters Symmetry C18 5-μm column (0.46 x 25 cm) eluted at a flow rate of 1 ml/min with methanol/water/acetic acid (80:20:0.01 by volume) (Figure 34B). The main product in this reaction was eluted at 19.5 min. This product is 8-KETE, as identified by the UV spectrum, the mobility on RP-HPLC and the treatment with $NaBH_4$. In this reaction complex minor products were also formed. Based on the UV spectra and the retention time in RP-HPLC, the products eluted between 9 and 13 min are epoxyalcohols and eluted between 6 and 8 min are conjugated trienes.

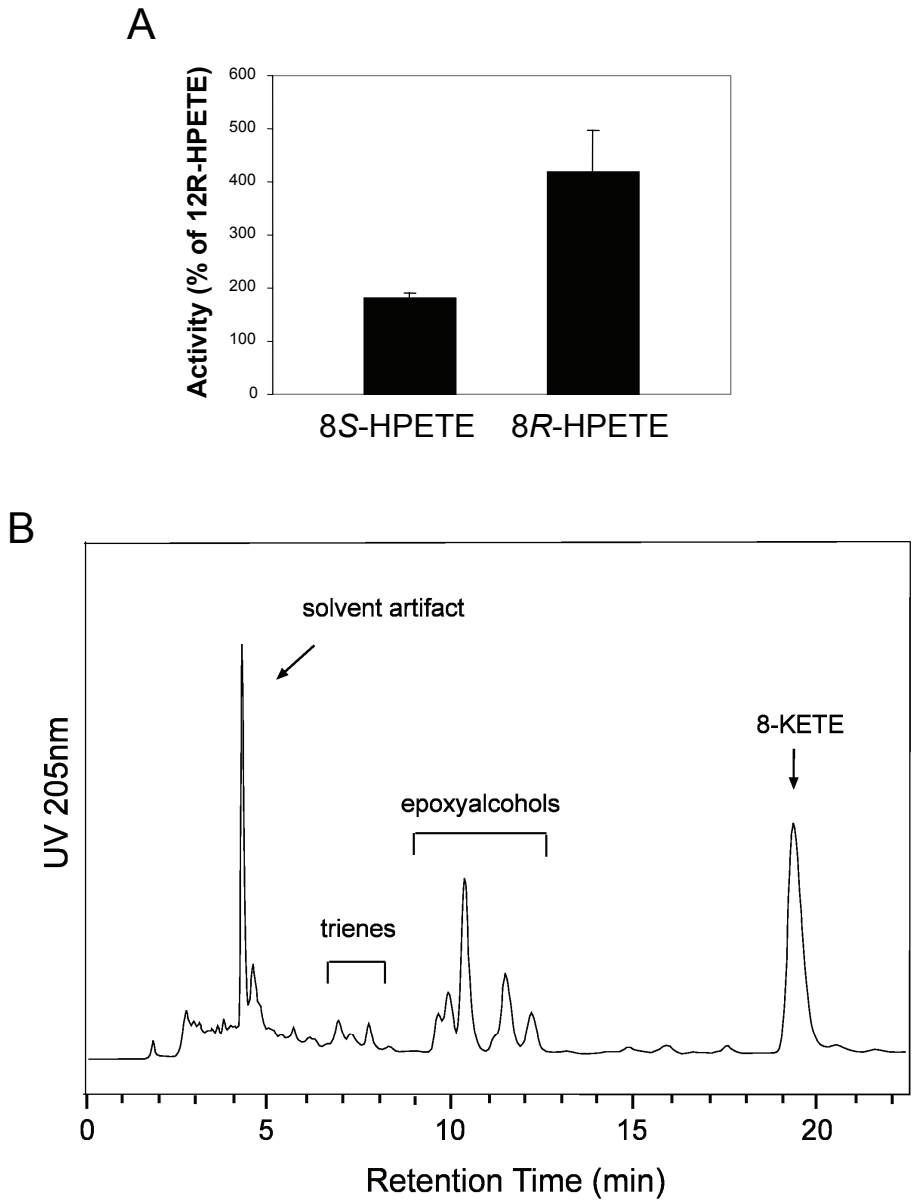

Figure 34. Reaction of mouse eLOX3 with 8*R*-HPETE. (A) Compare the rate of mouse eLOX3 with 8*S*-HPETE and 8*R*-HPETE. The incubation condition and measurement are the same as those used in Figure 28. (B) RP-HPLC analysis of the products in mouse eLOX3 reaction with 8*R*-HPETE. The products were analyzed by RP-HPLC using a Waters Symmetry C18 5-μm column (0.46 x 25 cm) eluted at a flow rate of 1 ml/min with methanol/water/acetic acid (80:20:0.01 by volume), and UV detection at 205 nm.

Discussion

Results shown here suggest that substrate specificity of mouse eLOX3 is different from the human enzyme. Among all the naturally occurring hydroperoxy fatty acids, 8*S*-HPETE is the preferred substrates for mouse eLOX3. 8*S*-HPETE is not a natural product in humans, but it can be abundant in differentiating mouse epidermis and is formed by mouse 8-LOX (Furstenberger *et al.*, 1991; Lehmann *et al.*, 1992). Thus our results provide biochemical evidence for the coupling of mouse 8-LOX and mouse eLOX3, just like that described in Chapter II for human 12*R*-LOX and human eLOX3.

No human LOX enzymes have 8-LOX activity. The homolog of mouse 8-LOX in human is 15-LOX-2. They share about 78% amino acid identity. However, the expression of mouse 8-LOX in skin is mainly in the differentiated epidermal layer, the stratum granulosum (Jisaka *et al.*, 1997), which is similar to 12*R*-LOX expression in human skin (Keeney DS, unpublished data), while the expression of human 15-LOX-2 in skin was restricted to basal keratinocytes (Shappell, S.B. *et al.*, 2001b). This indicates that the biological function of mouse 8-LOX might be more similar to human 12*R*-LOX, rather than its human homolog 15-LOX-2.

Interestingly, the possibility that mouse 8-LOX may take over the functions of human 12*R*-LOX which is suggested by their expression is also indicated in skin diseases. In humans, the metabolism of arachidonic acid in psoriasis and other proliferative dermatoses is characterized by the accumulation of 12*R*-HETE (Hammarstrom *et al.*, 1975; Woollard, 1986). The enzyme to form 12*R*-HETE, 12*R*-LOX, shows almost undetectable activity in normal human skin (Boeglin *et al.*, 1998). However, its mRNA expression in the psoriatic lesions is up-regulated (Keeney DS, unpublished data). Similar

to human 12*R*-LOX, in a dermatitis/psoriasis model mouse 8-LOX expression is much higher than that in normal control (Schneider *et al.*, 2004).

Our results also show that for the hydroperoxy fatty acids with the same positional configuration, both human and mouse eLOX3 prefer "*R*" rather than "*S*" stereoconfiguration. As a result, mouse eLOX3 reacts with 8*R*-HPETE at a much faster rate than 8*S*-HPETE. 8*R*-LOX enzymes have been identified in coral and starfish, and the product 8*R*-HETE, not 8*S*-HETE, was reported to induce starfish oocyte maturation (Meijer *et al.*, 1986). However, 8*R*-HPETE is not a natural metabolite in mouse. No mouse enzyme can form this unusual eicosanoid. Thus this substrate selectivity for mouse eLOX3 may not relate to any biological function. Further more, the reaction of mouse eLOX3 with 8*R*-HPETE produce mostly 8-KETE. Very little epoxyalcohol production also suggests the reaction of mouse eLOX3 and 8*R*-HPETE is different with human eLOX3, which function is indicated by the genetic findings in NCIE patients.

CHAPTER V

PRODUCTION OF PPARα SPECIFIC LIGANDS FROM 12*R*-LOX/eLOX3/sEH PATHWAY

Introduction

In chapter II and III, I identified a novel eicosanoid formation pathway in human skin. This pathway includes two LOX enzymes, 12*R*-LOX and eLOX3, and a possible soluble epoxide hydrolase (sEH). 12*R*-LOX can oxygenate arachidonic acid to form 12*R*-HPETE, which is used by eLOX3 as a preferred substrate to synthesize a 8*R*,11*R*,12*R*-epoxyalcohol. The epoxyalcohol is readily hydrolyzed by sEH to form a specific triol, 8*R*,11*S*,12*R*-triol.

The biological importance of one or some of these metabolites was indicated by the genetic evidence that either 12*R*-LOX or eLOX3 is mutated in a rare type of ichthyosis, NCIE (Jobard *et al.*, 2002; Yu, Z. *et al.*, 2005). This suggests that the products of both enzymes might serve as novel lipid mediators in the physiology of normal skin. Since NCIE patients are deficient in the formation of a normal epithelial water barrier, a reasonable hypothesis is that these metabolites might serve as an inducer of late-stage keratinocyte differentiation.

Of the six LOX enzymes in the human genome, 15-LOX-2, 12*R*-LOX and eLOX3 form a subgroup with preferential expression in epithelial tissues (Krieg *et al.*, 2001). Their genes are located as a gene cluster on human chromosome 17p13.1, and the proteins share about 50% amino acid identity. A common physiological role of these epithelial LOX enzymes was suggested in the regulation or modulation of normal

proliferation and differentiation of epithelial cells and keratinocytes (Krieg *et al.*, 2001). 12*R*-LOX is expressed almost exclusively in skin. Synthesis of its product, 12*R*-HETE, is upregulated in psoriasis while it is almost undetectable in normal human skin (Hammarstrom *et al.*, 1975; Woollard, 1986). 15-LOX-2 appears to modulate the differentiation of prostate epithelial cells and act as a negative regulator of the cell cycle (Tang, S. *et al.*, 2002); its expression tends to be lost in prostate cancer (Shappell, S.B. *et al.*, 1999; Shappell, S.B. *et al.*, 2001c). Changes in LOX expression in these tissues imply an important role for these enzymes in the regulation of cellular proliferation and differentiation.

Research on peroxisome proliferator-activated receptors (PPARs) has revealed that PPARs are important regulators of epidermal differentiation (Kuenzli and Saurat, 2003). PPARs are ligand-activated transcription factors that are members of the nuclear hormone receptor superfamily. There are three distinct PPAR isoforms: PPARα, PPARγ, and PPARβ/δ. They bind to sequence-specific DNA response elements as a heterodimer with the retinoic acid receptor (RXR). Research on PPARs has revealed that all three isoforms have been identified in human keratinocytes. Whereas PPARδ is the predominant subtype expressed, PPARα and PPARγ are present at lower levels but are upregulated during keratinocyte differentiation (Hanley *et al.*, 1998; Muga *et al.*, 2000). PPARβ/δ is not implicated in differentiation but is activated in inflammation and wound repair (Tan *et al.*, 2001; Tan *et al.*, 2003). Although the identity of definitive high-affinity natural ligands for PPARs is lacking, there is evidence that fatty acid/eicosanoid products are strong activators (Yu, K. *et al.*, 1995; Devchand *et al.*, 1996; Kliewer *et al.*, 1997; Cowart *et al.*, 2002).

In this study we investigated the potential activities of these LOX-derived epoxyalcohols and triols on PPAR receptors. Since as a class of molecules, epoxyalcohols of the type generated by eLOX3 have not been tested as endogenous ligands of PPARs, we tested their trans-activation effect on all three receptor subtypes.

Experimental Procedures

Materials

12*R*-HPETE and 8*S*-HPETE were prepared by arachidonic acid autoxidation as described previously in Chapter II. [1-^{14}C]12*R*-HPETE was prepared by the reaction of [1-^{14}C]arachidonic acid with human 12*R*-LOX (Boeglin *et al.*, 1998). eLOX3 product 8*R*-hydroxy-11*R*,12*R*-epoxyeicosa-5*Z*,9*E*,14*Z*-trienoic acid (8*R*,11*R*,12*R*-epoxyalcohol) was prepared by the reaction of 12*R*-HPETE with human eLOX3 in Tris buffer (pH 6.0). 8*S*-HETE was prepared by the reduction of 8*S*-HPETE using triphenyl phosphine (TPP). The synthetic PPAR ligands GW7647 (PPARα ligand), GW7845 (PPARγ ligand) and GW1516 (PPARδ ligand) were obtained from Glaxo Wellcome.

Cell culture

The PC-3 (ATCC CRL-1435) cells were routinely cultured in Ham's F12K medium containing 10% fetal bovine serum (BioWhittaker, Walkersville, MD) at 37 °C, 5% CO_2. They were typically split 1:6 every 3 days.

Plasmids

PPRE-tk-luc (PPAR reporter plasmid expressing firefly luciferase), pRL-SV40 (control plasmid expressing *Renilla* luciferase), and the expression plasmids containing full-length PPARα, PPARγ and PPARδ were kindly provided by Dr. Raymond N. DuBois (Vanderbilt University, Nashville, TN).

Quantitation of authentic 8*R*,11*R*,12*R*-epoxyalcohol

Since 8*R*,11*R*,12*R*-epoxyalcohol has very little UV absorbance and no commercially available standard, it is difficult to quantify. The method used here is to compare its relative peak height to 13*S*-hydroxyoctadeca-9*Z*,11*E*,15*Z*-trienoic acid (13*S*-OH C18.3ω3) in RP-HPLC. The quantity of 13*S*-OH C18.3ω3 can be easily determined by UV (the molar extinction coefficient is 23,000 at 235 nm). In RP-HPLC (Waters Symmetry C18 column, MeOH/H_2O/HAc=85/15/0.01, flow rate=1 ml/min), it elutes very close to the 8*R*,11*R*,12*R*-epoxyalcohol, and therefore it is used here as an internal standard. The quantity of ^{14}C-8*R*,11*R*,12*R*-epoxyalcohol was determined by radioactivity using liquid scintillation counting. The quantity of 8*R*,11*R*,12*R*-epoxyalcohol was calculated by co-injecting 8*R*,11*R*,12*R*-epoxyalcohol and13*S*-OH C18.3ω3 in the RP-HPLC and UV detection at 205 nm:

$$\text{Quantity of epoxyalcohol (ng)} = \text{Quantity of 13}S\text{-OH C18.3}\omega3\text{ (ng)} \times \frac{\text{Height of epoxyalcohol (cm)}}{\text{Height of 13}S\text{-OH C18.3}\omega3\text{ (cm)}} \times n$$

In this equation, n is the proportion of the mass extinction coefficients of 13*S*-OH C18.3ω3 and 8*R*,11*R*,12*R*-epoxyalcohol at 205 nm. It was obtained by co-injecting of ^{14}C-8*R*,11*R*,12*R*-epoxyalcohol and13*S*-OH C18.3ω3 in HPLC:

$$n = \frac{\text{Quantity of } ^{14}\text{C-epoxyalcohol (ng)} \times \text{Height of 13}S\text{-OH C18.3}\omega3 \text{ (cm)}}{\text{Quantity of 13}S\text{-OH C18.3}\omega3 \text{ (ng)} \times \text{Height of } ^{14}\text{C-epoxyalcohol (cm)}}$$

Preparation of the hydrolysis products from the 8*R*,11*R*,12*R*-epoxyalcohol

The triol products from 8*R*,11*R*,12*R*-epoxyalcohol was prepared by treating the epoxyalcohol with 1% acetic acid at room temperature for 30 min. This will hydrolyze the epoxide and yield a series of diastereomeric isomers of trihydroxy-eicosatrienoic acids. The product was recovered by extraction using a 100-mg Oasis HLB cartridge (Waters) essentially as described by Powell (Powell, 1982). The purification of each triol diastereomer was done by using SP-HPLC and chiral-HPLC as described previously in Chapter III.

Screening for PPAR Activators using a dual-luciferase assay

PC-3 cells (1.0×10^5 cells/well using 24-well plates) were transfected by using FUGENE 6 (Roche Molecular Biochemicals) at a lipid/DNA ratio of 3:1. Cells were exposed to a mix containing 150 ng/ml PPRE-tk-luc, 150 ng/ml one of the three PPAR plasmids (PPARα, PPARγ, or PPARδ), and 1.0 ng/ml pRL-SV40 in Ham's F12K medium. The transfection mix was replaced after 4-5 h with 10% charcoal-stripped FBS containing media supplemented with either 0.1% vehicle (DMSO or ethanol) or the

indicated compound. After 24 h, cells were harvested in 100 μl/well 1× luciferase lysis buffer (Promega) for 20 min at room temperature using an orbital shaker. Relative light units from firefly luciferase activity were determined using a luminometer (MGM Instruments, Hamden, CT) and normalized to the relative light units from *Renilla* luciferase which served as internal control for transfection efficiency (Promega). The effects of various compounds on activation of PPARs were presented as "fold-activation" relative to the vehicle (DMSO) control values.

Results

8*R*,11*R*,12*R*-epoxyalcohol mediated activation of PPARα

To test the possibility that the eLOX3-generated epoxyalcohol 8*R*-hydroxy-11*R*,12*R*-epoxyeicosa-5*Z*,9*E*,14*Z*-trienoic acid (8*R*,11*R*,12*R*-epoxyalcohol) could serve as an activating ligand for PPARs, a PPAR transactivation assay was used. In this assay, PC-3 cells were transiently co-transfected with PPRE-tk-luc plasmid (PPAR reporter plasmid expressing firefly luciferase), pRL-SV40 plasmid (control plasmid expressing *Renilla* luciferase)and one of the three full length PPAR (PPARα, PPARγ, or PPARδ) plasmids. Cells then were treated with vehicle (DMSO), synthetic ligand for each receptor, or different concentrations of 8*R*,11*R*,12*R*-epoxyalcohol (0.1, 1.0, 5.0 and 10 μM). PPAR transactivation was determined for each experimental condition using a dual-luciferase assay. The effects of various compounds on activation of PPARs were presented as "fold-activation" relative to the vehicle (DMSO) control values.

In the PPARα transactivation assay (Figure 35), we can see that the synthetic ligand GW7647 (1.0 μM) produces about a 5-fold activation relative to the vehicle control. It is known that 8*S*-HETE can activate PPARα (Yu, K. *et al.*, 1995). We also tested 0.1, 1.0 and 10 μM 8*S*-HETE on PPARα activation, which showed a dose-dependent activation, and the maximum value is about 3.5 fold (at 10 μM concentration). The 8*R*,11*R*,12*R*-epoxyalcohol does not show activation on PPARα at low concentrations (0.1 and 1.0 μM). However at high concentration (5 and 10 μM), 2.2- and 2.6-fold activation was observed, respectively. The lower activity of 8*R*,11*R*,12*R*-epoxyalcohol

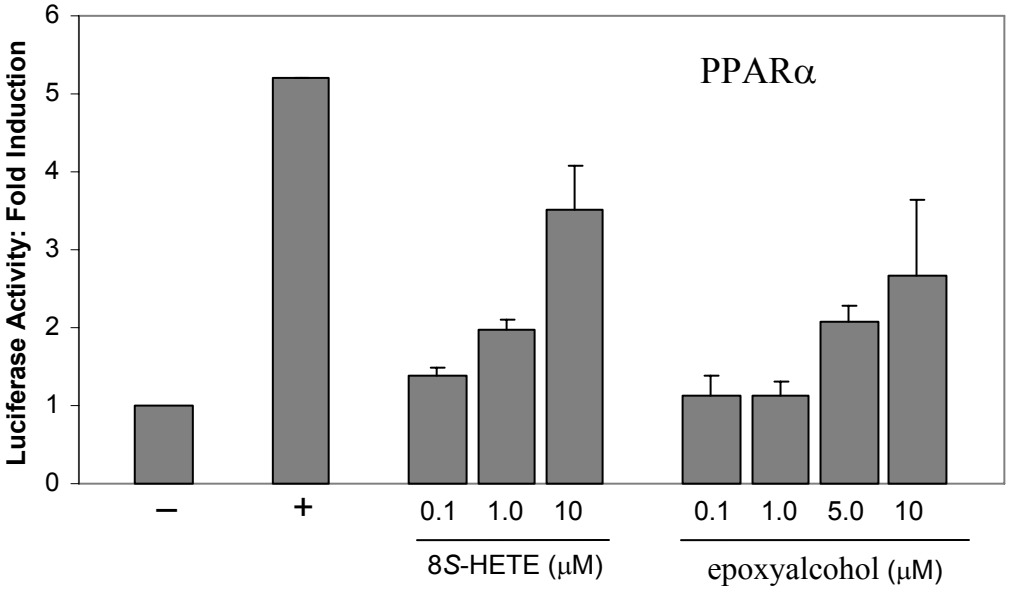

Figure 35. Activation of PPARα by the 8*R*,11*R*,12*R*-epoxyalcohol. PPRE-tk-luciferase, pRL-SV40 (control plasmid expressing *Renilla* luciferase) and PPARα plasmids were co-transfected into PC-3 cells. The transfection mix was replaced after 4-5 h with 10% charcoal-stripped fetal bovine serum-containing medium supplemented with either 0.1% vehicle or the indicated compound. After 24 h, cells were harvested in 1× luciferase lysis buffer. Relative light units from firefly luciferase activity were determined using a luminometer and normalized to the relative light units from *Renilla* luciferase using the dual luciferase kit (Promega). GW7647 (1 μM) and 8*S*-HETE were used as positive controls.

may be due to its instability in the cells comparing to the synthetic ligand and even 8*S*-HETE.

In a parallel experiment we used a chimeric receptor that contains the ligand-binding domain of PPARα fused with the DNA-binding domain of the yeast GAL4 transcription factor. We transiently co-transfected this chimeric receptor with pRL-SV40 and UAS-tk-luc (a firefly luciferase reporter gene containing GAL4 response elements) in PC-3 cells. A similar experiment was used previously to test 8*S*-HETE activation of PPARα. However, in our experiments, neither 8*S*-HETE (positive control) nor the

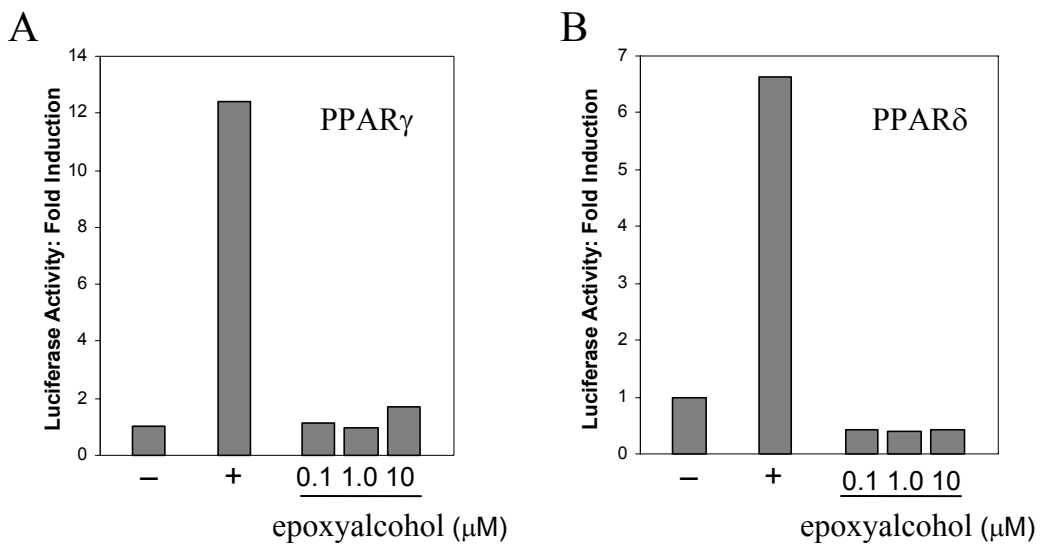

Figure 36. Effects of the 8*R*,11*R*,12*R*-epoxyalcohol on PPARγ (A) and PPARδ (B). PPRE-tk-luciferase, pRL-SV40 and PPARγ (A) or PPARδ (B) plasmids were co-transfected into PC-3 cells. The dual luciferase assay was done using the method similar in Figure 35. Positive control used here: GW7845 (PPARγ), GW1516 (PPARδ), 100 nM each.

epoxyalcohol activated the chimeric PPARα receptor in PC-3 cells, although the synthetic ligand GW7647 was active (data not shown).

We also tested 8*R*,11*R*,12*R*-epoxyalcohol in PPARγ and PPARδ transactivation assays (Figure 36). The synthetic ligand GW7845 (100 nM) activated PPARγ about 12-fold activation relative to the vehicle control. Similarly the synthetic ligand GW1516 (100 nM) activated PPARδ about 6-7 fold. However, at any concentration tested (0.1-10 μM), the epoxyalcohol failed to show any activity on PPARγ and PPARδ. This suggests that eLOX3 produced epoxyalcohol is a PPARα-specific ligand.

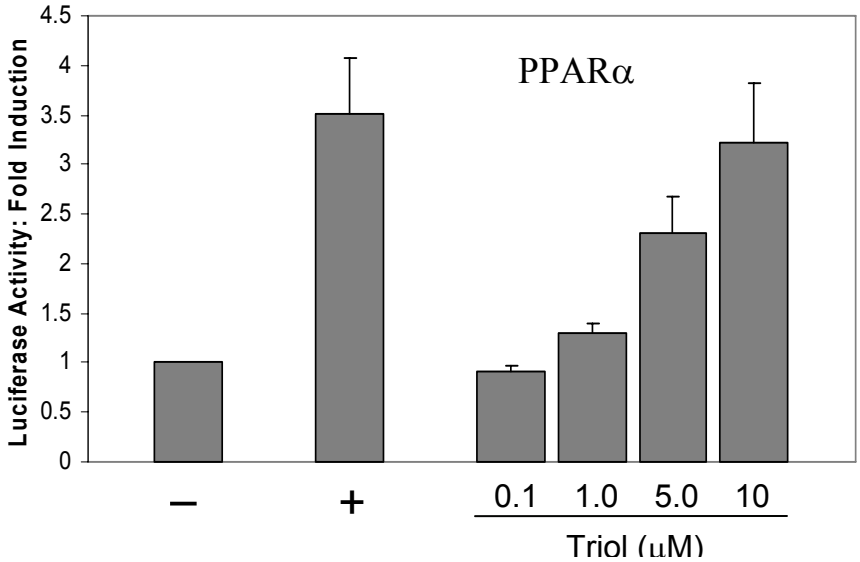

Figure 37. Activation of PPARα by the acid-catalyzed hydrolysis product from the 8*R*,11*R*,12*R*-epoxyalcohol. Co-transfection of PPRE-tk-luciferase, pRL-SV40 and PPARα plasmids and dual-luciferase assay were done using the method described in Figure 35. 8*S*-HETE (10 μM) was used as positive control.

Transactivation of PPARα by hydrolysis metabolites of the 8*R*,11*R*,12*R*-epoxyalcohol

8*R*,11*R*,12*R*-epoxyalcohol is instable in the cell. It can be hydrolyzed to form triols either enzymatically by soluble epoxide hydrolase (see Chapter III) or non-enzymatically. To investigate whether the 8*R*,11*R*,12*R*-epoxyalcohol transactivation on PPARα was the result of itself or its metabolites, I tested the effect of 8*R*,11*R*,12*R*-epoxyalcohol hydrolysis in the PPARα transactivation assay. 8*R*,11*R*,12*R*-epoxyalcohol was hydrolyzed in acidic condition. The hydrolyzed product was extracted and used in the PPARα transactivation assay (Figure 37). A dose-dependent activation of PPARα was detected. At 10 μM, the transactivation by the triols is comparable to the reported PPARα ligand 8*S*-HETE.

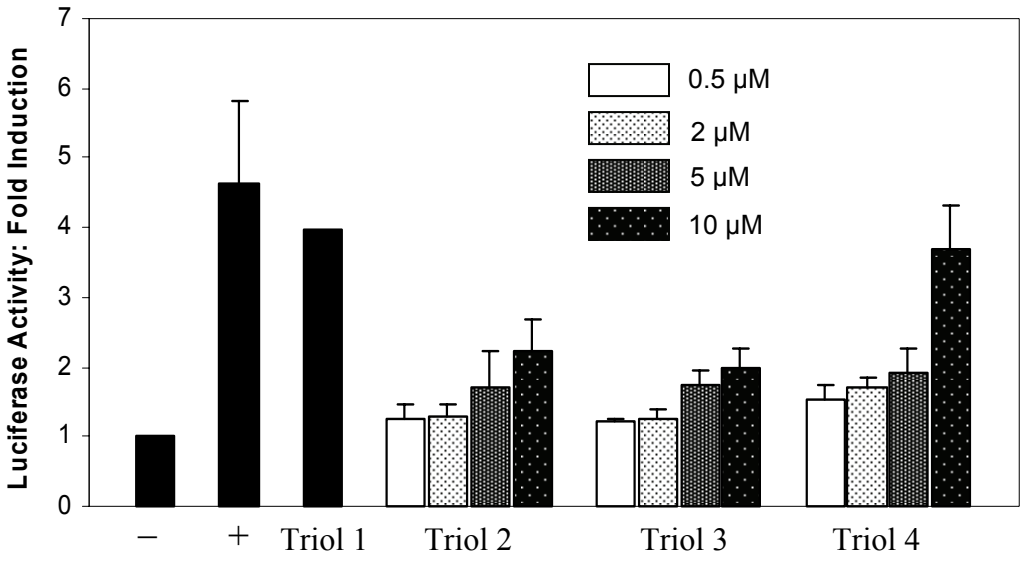

Figure 38. Activation of PPARα by different triol diastereomers. Co-transfection of PPRE-tk-luciferase, pRL-SV40 and PPARα plasmids and dual-luciferase assay were done using the method described in Figure 35. 8*S*-HETE (10 μM) was used as positive control. The triols were purified from acid-catalyzed hydrolysis of 8*R*,11*R*,12*R*-epoxyalcohol and their stereo configuration were assigned in Figure 20.

In Chapter III, I showed that the acid-catalyzed hydrolysis of 8*R*,11*R*,12*R*-epoxyalcohol produces four different triols. We also tentatively assigned the stereoconfiguration of each triol. Here I tested each triol on PPARα activation (Figure 38). We can see that each of the four triols activated PPARα. Triol 1 and triol 4 showed higher activity. During the purification of the triols, we produced very little of triol 1 sufficient for only one data point in this experiment, so its activity will need to be confirmed. The triol 4 (8*R*,11*S*,12*R*-trihydroxy-5*Z*,9*E*,14*Z*-trienoic acid) is the enzymatic product by soluble epoxide hydrolase, and its moderate activation effect on PPARα is reproducible.

Discussion

As a large class of fatty acid derivatives, the epoxyalcohols and related metabolites have not been tested previously as PPAR ligands (they are not commercially available). Here we characterized the ability of eLOX3-produced 8*R*,11*R*,12*R*-epoxyalcohol and its hydrolyzed product to transactivate PPARα, while no activity was found on PPARγ and PPARδ, suggesting that they are specific agonists for the PPARα receptor. This is the first reported biological activity of this type of epoxyalcohol or triol eicosanoids on nuclear receptors and suggests that fatty acid oxygenase metabolism by LOX enzymes might represent a novel pathway for the generation of ligands for nuclear receptors.

In our experiments, we used the full length wild type PPAR receptors and natural PPAR-response elements to test the transactivation by epoxyalcohol and triols. In some previous studies (Gupta *et al.*, 2000; Shappell, S.B. *et al.*, 2001a), chimeric PPARs in which PPAR ligand binding domains were fused to a heterologous DNA-binding domain (GAL4) were also used in similar assays. The use of GAL4 DNA-binding domain and its response element UAS can greatly reduce background when compared to assays involving transient transfection of wild type PPARs. However, the fusion receptor may lead to differences resulting from altered DNA binding and/or heterodimerization with RXR. In our experiments, we noticed that both the well established PPARα ligand 8*S*-HETE (Yu, K. *et al.*, 1995) and epoxyalcohol can not activate PPARα-GAL4 in PC-3 cells, while the synthetic ligand can. Using wild-type full length PPARα, the activations by not only the synthetic ligand, but also 8S-HETE and epoxyalcohol were observed.

This suggests that the binding of eicosanoids to PPARα may require other sequences which do not exist in our PPARα-GAL4 construct.

Since both the epoxyalcohol and the triol can activate PPARα, we still do not know whether the effect of the epoxyalcohol is direct or whether it acts through its triol metabolite. But the fact that low concentrations of epoxyalcohol have no effect might indicate that the triol is the direct ligand for PPARα. This hypothesis needs to be further tested by using radiolabeled ligand in a direct binding assay.

Although we showed that eLOX3-produced epoxyalcohol and its hydrolyzed metabolite can activate PPARα, whether signaling through this nuclear receptor is the mechanism of eLOX3 action in skin still needs to be assessed. Recently a novel gene, *ichthyin*, was found mutated in the same type of ichthyosis as 12*R*-LOX and eLOX3 mutations (Lefevre *et al.*, 2004). This gene encodes a membrane protein with seven to nine transmembrane domains. It will be interesting to investigate whether ichthyin serves as a cell surface receptor for the products from the novel eicosanoid pathway identified in this study.

The finding that the eLOX3-produced epoxyalcohol activates nuclear receptor may have important function in other tissues. Although skin is where eLOX3 is most strongly expressed as judged by RT-PCR, selected other organs give positive signals (Krieg *et al.*, 2001). A recent report has implicated eLOX3 expression in facilitating the early stages of a classic model system, the PPARγ-induced differentiation of preadipocytes (Madsen *et al.*, 2003).

CHAPTER VI

SUMMARY

The enzymatic reactions of arachidonic acid and related polyunsaturated fatty acids by COX, LOX and P450 enzymes form specific molecules in cell signaling. Their roles in inflammation have been well studied and this knowledge has led to new therapeutic advances. For example, the COX and 5-LOX enzymes are the targets of important classes of anti-inflammatory and asthma medications (Carter *et al.*, 1991; Mitchell *et al.*, 1993).

The skin displays a highly active metabolism of arachidonic acid. A complex mixture of eicosanoids is reported in human skin, and these include HETEs of both the *R* and *S* stereoconfigurations (Hammarstrom *et al.*, 1975; Woollard, 1986). Usually they are the products of LOX reactions. Among the LOX family, 15-LOX-2, 12*R*-LOX and eLOX3 form a subgroup with preferential expression in epithelial cells. The three epithelial LOX enzymes are located as a gene cluster on human chromosome 17p13.1, and the proteins share about 50% amino acid identity (Krieg *et al.*, 2001). A common physiological role of these epithelial LOX enzymes was suggested in the regulation or modulation of normal proliferation and differentiation of epithelial cells and keratinocytes (Brash, 1999; Muga *et al.*, 2000; Funk, C.D., 2001). For example, 12*R*-LOX is upregulated in psoriasis while it is almost undetectable in normal human skin (Boeglin *et al.*, 1998; Schneider *et al.*, 2001a). So far 15-LOX-2 has received most attention among the three epithelial LOX enzymes. It appears to modulate the

differentiation of prostate epithelial cells (Shappell, S.B. *et al.*, 2001a), its expression is lost in prostate neoplasia and adenocarcinoma (Shappell, S.B. *et al.*, 1999), and it acts as a negative regulator of the cell cycle in normal prostate epithelial cells (Tang, S. *et al.*, 2002).

Human eLOX3 was discovered in 2001 (Krieg *et al.*, 2001). As a member of the epithelial LOX subfamily, it contains the characteristic well-conserved amino acid residues found in all LOX enzymes, including the putative iron-binding ligands and additional structure-determining residues. The question of the catalytic activity of eLOX3 has, nonetheless, remained elusive. No conventional LOX activity has been detected. However, an important role of eLOX3 in skin pathophysiology was strongly indicated by a genetic study which linked mutations in the coding sequence of the human eLOX3 gene to the development of an inherited skin disease, non-bullous congenital ichthyosiform erythroderma (NCIE) (Jobard *et al.*, 2002). NCIE represents the first example where improper LOX expression has been shown to have direct pathophysiological consequences. The disease is characterized by hyperkeratosis and epidermal dysfunction leading to a white flaky skin with transepidermal water loss. A second group of families with NCIE showed somatic mutations in the gene of a related epithelial LOX, 12*R*-LOX (Jobard *et al.*, 2002).

The finding that mutations in *either* 12*R*-LOX *or* eLOX3 resulted in the same disease phenotype led the authors to speculate that both enzymes might participate in the same metabolic pathway, and that this pathway would have a crucial role in the normal functioning of human skin (Jobard *et al.*, 2002). From a biochemical point of view, at first glance this hypothesis seemed surprising. eLOX3 and 12*R*-LOX are both LOX

enzymes theoretically catalyzing the same type of reaction on polyunsaturated fatty acid substrates. Furthermore, recombinant eLOX3 has been shown to be lacking any demonstrable catalytic activity at all (Kinzig *et al.*, 1999).

Here we provided biochemical evidence that demonstrates a specific catalytic activity for eLOX3 and potentially provides a functional link with 12*R*-LOX. eLOX3 exhibits potent enzymatic activity toward the transformation of the 12*R*-LOX derived product, 12*R*-HPETE, into a previously undescribed epoxyalcohol product, 8*R*-hydroxy-11*R*,12*R*-epoxyeicosa-5*Z*,9*E*,14*Z*-trienoic acid (8*R*,11*R*,12*R*-epoxyalcohol) plus a minor product 12-keto-arachidonic acid (12-KETE). We also have shown that the LOX-products 12*S*-HPETE and 15*S*-HPETE are converted by eLOX3 to specific epoxyalcohol products of related structure, albeit with lower catalytic efficiency. The very fact of enzymatic conversion and especially the preference of eLOX3 for 12*R*-HPETE support the hypothesis suggested by Jobard and colleagues on the existence of a specific pathway involving the two LOX enzymes (Jobard *et al.*, 2002). An additional supportive finding is that eLOX3 and 12*R*-LOX have similar tissue expression patterns in humans (Krieg *et al.*, 2001), making the conversion of 12*R*-HPETE into the specific epoxyalcohol a reaction likely to occur *in vivo*. The platelet-type 12-LOX and the two 15-LOX enzymes (15-LOX-1 and 15-LOX-2) are also expressed in human skin potentially providing 12*S*-HPETE and 15*S*-HPETE as alternative substrates.

The transformation of fatty acid hydroperoxides to epoxyalcohol derivatives is a facile non-enzymatic reaction, the chemistry of which has been studied extensively (Gardner, 1989). Free heme or transition metals will initiate the reaction. The non-enzymatic products are a mixture of isomers with different positional and stereo

specificity. However, our results suggest that catalysis by eLOX3 has the heat-inactivation characteristics of an enzyme, and its products show stereospecificity. Thus this reaction requires the protein nature of eLOX3, not only the iron center.

Due to this unexpected catalytic activity of the novel epidermal LOX, eLOX3, it is of mechanistic interest to compare the reaction mechanism of eLOX3 with other typical LOX enzymes. The facets of eLOX3 reactivity that make it stand out are the complete absence of oxygenase activity under any of the variety of conditions that have been explored, and also the unusual autocatalytic nature of the reaction with HPETE substrates. Equivalent hydroperoxide rearrangements by other LOX enzymes are limited to single turnovers, unless promoted by a reducing cofactor (Garssen *et al.*, 1976; Riendeau *et al.*, 1991). In the conventional Fe^{2+}/Fe^{3+} redox cycle of normal LOX catalysis (Figure 4), the Fe^{3+} enzyme is the active form that performs the hydrogen abstraction from the *bis*-allylic methylene of the fatty acid substrate. Oxygenation of the fatty acid radical and reduction of the peroxyl radical to the fatty acid hydroperoxide completes the cycle. In the discussion of Chapter 2, we proposed a novel mechanism for the reaction of eLOX3 with HPETE substrates. It can be assumed that the Fe^{2+} enzyme is the active species (Figure 16). The Fe^{2+} enzyme initiates a homolytic cleavage of the hydroperoxide O-O bond, the resulting alkoxyl radical cyclizes to an epoxyallylic carbon radical while the other oxygen of the original hydroperoxide is retained in a Fe^{3+}-OH complex. The cycle is completed by an oxygen rebound type of reaction that forms the epoxyalcohol product while the iron is restored to the active Fe^{2+} form. The corresponding ketoeicosatetraenoic acid (KETE) is formed as a by-product in some of the catalytic cycles. A notable consequence of this unusual catalytic cycle is that the reducing

agent nordihydroguaiaretic acid (NDGA), a typical LOX inhibitor that reduce the catalytic iron to ferrous, actually promotes eLOX3 reactivity, as shown in our study.

Since this reaction mechanism could be proposed "on paper" for any LOX, why is such a self-sufficient catalytic cycling observed only with eLOX3? We speculate that the redox state of eLOX3 may make the ferric enzyme incapable of performing a hydrogen abstraction from a typical lipoxygenase substrate, and thus the protein is incapable of oxygenating a polyunsaturated fatty acid. This shift in balance of redox potential may, in turn, favor the reduction reaction that constitutes the basis of the catalytic activity we describe with HPETE substrates.

After identifying the novel catalytic activity of eLOX3, it was important to test whether the mutations reported in NCIE patients may be associated with alteration of eLOX3 as well as 12*R*-LOX functionality. NCIE is an autosomal recessive form of ichthyosis with an incidence of about 1 in 100,000-200,000. The best characterized mutations inactivate the transglutaminase 1 gene, with resultant defects in formation of the skin permeability barrier (Huber *et al.*, 1995; Akiyama *et al.*, 2003). So far, NCIE with mutations in lipoxygenase genes has been reported in a small number of consanguineous families in the Mediterranean (Jobard *et al.*, 2002) and more recently in Central Europe, Turkey, and the Indian subcontinent (Eckl *et al.*, 2005). In Jobard study, two point mutations (L426P and H578Q) and a frameshift mutation were reported in 12*R*-LOX and two point mutations (R396S and V500F) and a truncation (change arginine 234 to a premature stop codon) were found in eLOX3 (Jobard *et al.*, 2002). The frameshift mutation and the truncation will definitely eliminate the catalytic activities. Based on the alignment of eLOX3 and 12*R*-LOX with rabbit 15-LOX, the only

mammalian LOX for which the 3-D structure is available, one of the mutations in 12*R*-LOX, His578, is a ligand to the iron in the LOX active site. As expected, its mutation eliminates catalytic activity. The locations of other point mutations (Arg396 and Val500 in eLOX3 and Leu426 in 12*R*-LOX) are far away from the iron ligands and the substrate binding pocket, having no obvious connection to the active site. In the present study, we showed that all these point mutations completely eliminated the enzyme activities. Although these three mutations may not interfere with substrate binding or catalysis directly, they may disrupt the correct folding of the catalytic domain of the proteins. This is suggested by our observation that the mutated proteins failed to accumulate when expressed in *E. coli*. These data are consistent with the concept that loss of function of eLOX3 or 12*R*-LOX is fundamental to the pathogenesis of the LOX-dependent form of NCIE. The findings further imply that eLOX3 and 12*R*-LOX activities are involved in the biochemistry underlying the process of development of normal intact epidermis.

Our results also show that the 8*R*-hydroxy-11*R*,12*R*-epoxyeicosa-5*Z*,9*E*,14*Z*-trienoic acid (8*R*,11*R*,12*R*-epoxyalcohol) formed from the reaction of eLOX3 with 12*R*-HPETE is easily hydrolyzed to a single 8*R*,11*S*,12*R*-triol derivative in both human keratinocytes and COS7 cells. The human soluble epoxide hydrolase (sEH) is the candidate enzyme involved in this transformation, as our results show that the recombinant sEH can catalyze the same hydrolysis reaction *in vitro*. In human keratinocytes, sEH may be the downstream enzyme in the pathway consisting of 12*R*-LOX and eLOX3 to form an active mediator in the regulation of keratinocyte differentiation, or to eliminate the active metabolite.

The term “hepoxilin” is used to refer to groups of 12-HPETE-derived epoxyalcohol fatty acids that have been detected in skin and other tissues (Pace-Asciak, C.R. *et al.*, 1995). Hepoxilin A3 is used for any stereoisomer with an 8-hydroxy-11,12-epoxy structure, while hepoxilin B3 refers to the isomers with a 10-hydroxy-11,12-epoxyeicosatrienoic acid structure. Their hydrolysis products are named “trioxilin A3” and “trioxilin B3”, respectively. So far, an enzyme with hepoxilin synthase activity in human skin has not been cloned, but there are reports about the detection of this activity in rat and human skin and appearance of the hepoxilin and trioxilin products in human psoriatic lesions (Nugteren *et al.*, 1985; Anton *et al.*, 1998; Anton and Vila, 2000). In the novel eicosanoid formation pathway identified in our study, human eLOX3 converts 12*R*-HPETE to one particular stereoisomer of hepoxilin A3, which is further hydrolyzed by human sEH to produce only one stereospecific trioxilin A3. From 12*S*-HPETE, mainly one isomer of hepoxilin B3 is formed. It remains to be elucidated whether this novel pathway can account for the formation of the hepoxilin and trioxilin isomers described in human skin, whether additional activities or non-enzymatic reactions have to be considered.

The biological activity of these stereospecific hepoxilin or trioxilin-like products from this pathway remains to be assessed. Structurally related compounds have been reported as signaling molecules. For example, the bioactive principal of one of the endothelial-derived relaxing factors is a closely related trihydroxy derivative of arachidonic acid (Pfister, S.L. *et al.*, 1998; Campbell *et al.*, 2003). Another example is that hepoxilins have been shown to increase intracellular calcium levels (Reynaud *et al.*, 1999). In our study, we provide evidence of a new activity that these products are specific

ligands for the nuclear receptor PPARα. PPARα has been identified in human keratinocytes (Hanley *et al.*, 1998; Komuves *et al.*, 2000). It is present at low levels but is upregulated during keratinocyte differentiation (Hanley *et al.*, 1998; Muga *et al.*, 2000). Other eicosanoids were also reported as PPARα-specific ligands (Yu, K. *et al.*, 1995; Devchand *et al.*, 1996; Cowart *et al.*, 2002). The activation of PPAR through epoxyalcohols has not been tested previously, since these compounds are not commercially available. Our results provide the first example of such activation by epoxyalcohol or its metabolites. However, whether signaling through PPARα is the mechanism of eLOX3 action in skin still needs to be assessed. Recently a novel gene, *ichthyin*, was found mutated in a similar type of ichthyosis as associated with 12*R*-LOX and eLOX3 mutations (Lefevre *et al.*, 2004). This gene encodes a putative membrane protein with seven to nine transmembrane domains. It will be of great interest to investigate whether ichthyin serves as a cell surface receptor for the products from the novel eicosanoid pathway identified in this study.

The eLOX3-derived 12-ketoeicosatrienoic acid (12-KETE) was identified as a by-product in our *in vitro* experiments with pure enzymes. However it was not detected by HPLC analysis if the reaction was performed in cell lysates. This may be due to reduction of the keto product to the HETE or its adduction to cellular GSH. Whether such a GSH adduct from 12-KETE has distinct biological activity is not known. It has been reported that adduction of GSH to arachidonic acid derived metabolites can be used for activation of various eicosanoids in cells. The best recognized example of activation is the conjugation of GSH to the 5-LOX product LTA_4 by LTC_4 synthase (Samuelsson *et al.*, 1987a). LTC_4 and the downstream cysteinyl leukotrienes are potent mediators of asthma

and bronchoconstriction (Drazen *et al.*, 1999). Another well studied reaction is the Michael addition of GSH to the electrophilic eicosanoid 5-oxo-eicosatetraenoic acid leading to formation of 5-oxo-7-glutathionyl-8,11,14-eicosatrienoic acid (Murphy and Zarini, 2002). This adduct has distinct physiologic activity and has been found to cause a potent chemotactic response in human eosinophils and neutrophils (Bowers *et al.*, 2000).

The genetic study suggests that mutations in eLOX3 and 12*R*-LOX genes can cause ichthyosis. Thus a useful tool to study ichthyosis pathogenesis is to construct knock-out mouse models. However, for LOX enzymes, the structural homologs between mouse and human do not share functional homology. For example, the mouse 12*R*-LOX, in contrast to human 12*R*-LOX, has feeble catalytic activity and is incapable of metabolizing free arachidonic acid, although it will oxygenate arachidonate methyl ester (Krieg *et al.*, 1999). Thus gene targeting technique may not be helpful in studying the biological function of 12*R*-LOX. Here we showed that mouse eLOX3 has a different spectrum of substrate specificity compared to human eLOX3. While human eLOX3 recognized 12*R*-HPETE as its best substrate, mouse eLOX3 prefers 8*S*-HPETE. This suggests that eLOX3 might couple with the mouse 8-LOX. In other words, mouse and human eLOX3 have substrate specificities tailored to the species-specific complement of LOX enzymes in epidermis. Interestingly, similar to the up-regulation of 12*R*-LOX in human psoriasis (Hammarstrom *et al.*, 1975; Woollard, 1986), in a dermatitis/psoriasis model mouse 8-LOX expression is much higher than that in normal control animals (Schneider *et al.*, 2004). Thus the LOX enzymes involved in epidermal differentiation in the mouse are likely not equivalent to humans, although their physiological roles may be. Mouse 8-LOX may take over the functions of human 12*R*-LOX.

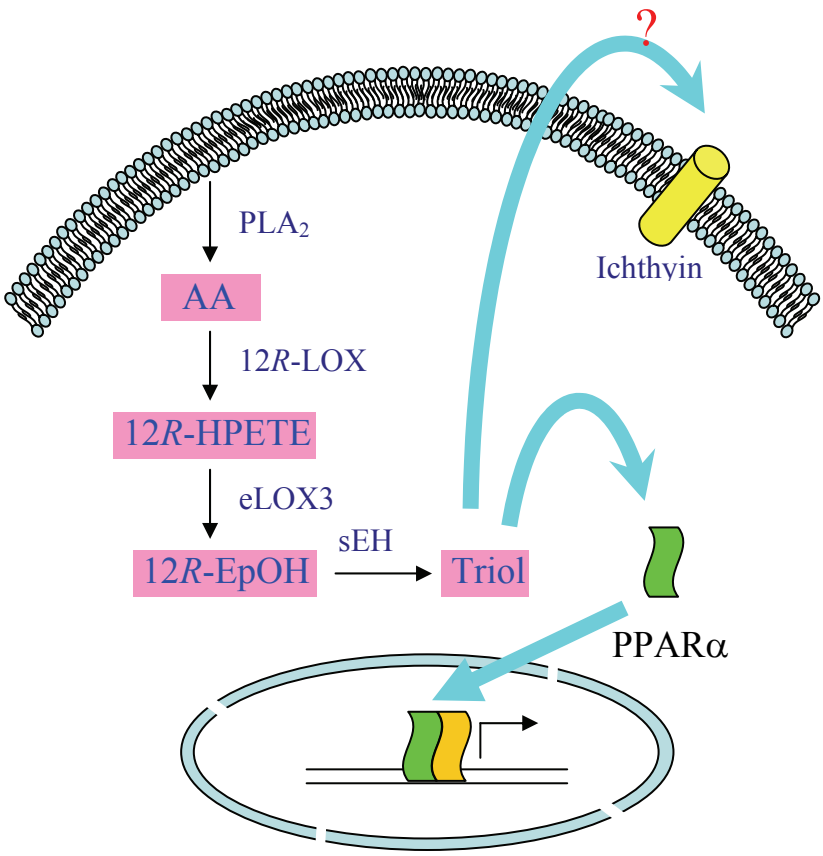

Figure 39. A novel lipoxygenase pathway in skin.

In conclusion, these studies have delineated a novel eicosanoid formation pathway including 12*R*-LOX, eLOX3 and soluble epoxide hydrolase (Figure 39). This pathway produces hepoxilin-like and trioxilin-like molecules which serve as signaling molecules in cell differentiation and proliferation. Our results may explain why mutations in either 12*R*-LOX or eLOX3 genes are detrimental to the homeostasis of human skin. While this work has answered many of the questions that initiated this project, it has generated many as well. It remains to be determined whether the epoxyalcohols or triols are active metabolites from this pathway, whether other enzymes are also involved in this pathway, how this pathway participates in epidermal differentiation, and whether such

effects contribute to the pathogenesis of ichthyosis. There are excellent prospects for future therapeutic interventions based on understanding the role of this newly identified pathway. Its products may possibly be effective as a topical treatment of ichthyosis and other skin disorders of cornification. The questions on the downstream signaling, such as whether the PPARα is the only target for the products from this novel pathway, and what other nuclear receptors or cell surface receptors are involved, also remain to be determined. Finally, the relationship between ichthyin and this novel eicosanoid formation pathway, and the roles of their mutations in ichthyosis are also interesting areas to be studied. Our work provides the basis from which such investigations can be undertaken.

REFERENCES

Aiello, R. J., Bourassa, P. A., Lindsey, S., Weng, W., Freeman, A. and Showell, H. J. (2002). Leukotriene B4 receptor antagonism reduces monocytic foam cells in mice. *Arterioscler Thromb Vasc Biol* **22**: 443-9.

Akiyama, M., Sawamura, D. and Shimizu, H. (2003). The clinical spectrum of nonbullous congenital ichthyosiform erythroderma and lamellar ichthyosis. *Clin Exp Dermatol* **28**: 235-40.

Anton, R., Abian, J. and Vila, L. (1995). Characterization of arachidonic acid metabolites through the 12-lipoxygenase pathway in human epidermis by high-performance liquid chromatography and gas chromatography/mass spectrometry. *Rapid Commun Mass Spectrom* **Spec No**: S169-82.

Anton, R., Puig, L., Esgleyes, T., de Moragas, J. M. and Vila, L. (1998). Occurrence of hepoxilins and trioxilins in psoriatic lesions. *J Invest Dermatol* **110**: 303-10.

Anton, R. and Vila, L. (2000). Stereoselective biosynthesis of hepoxilin B3 in human epidermis. *J Invest Dermatol* **114**: 554-9.

Arenberger, P., Kemeny, L. and Ruzicka, T. (1992). Defect of epidermal 12(S)-hydroxyeicosatetraenoic acid receptors in psoriasis. *Eur J Clin Invest* **22**: 235-43.

Armstrong, R. N. (1999). Kinetic and chemical mechanism of epoxide hydrolase. *Drug Metab Rev* **31**: 71-86.

Armstrong, R. N. and Cassidy, C. S. (2000). New structural and chemical insight into the catalytic mechanism of epoxide hydrolases. *Drug Metab Rev* **32**: 327-38.

Back, M., Norel, X., Walch, L., Gascard, J., de Montpreville, V., Dahlen, S. and Brink, C. (2000). Prostacyclin modulation of contractions of the human pulmonary artery by cysteinyl-leukotrienes. *Eur J Pharmacol* **401**: 389-95.

Basnayake, V. and Sinclair, H. M. (1954). Skin permeability in deficiency of essential fatty acids. *J Physiol* **126**: 55-6P.

Belkner, J., Chaitidis, P., Stender, H., Gerth, C., Kuban, R. J., Yoshimoto, T. and Kuhn, H. (2005). Expression of 12/15-lipoxygenase attenuates intracellular lipid deposition during in vitro foam cell formation. *Arterioscler Thromb Vasc Biol* **25**: 797-802.

Belkner, J., Wiesner, R., Rathman, J., Barnett, J., Sigal, E. and Kuhn, H. (1993). Oxygenation of lipoproteins by mammalian lipoxygenases. *Eur J Biochem* **213**: 251-61.

Beller, T. C., Maekawa, A., Friend, D. S., Austen, K. F. and Kanaoka, Y. (2004). Targeted gene disruption reveals the role of the cysteinyl leukotriene 2 receptor in

increased vascular permeability and in bleomycin-induced pulmonary fibrosis in mice. *J Biol Chem* **279**: 46129-34.

Bernart, M. W. and Gerwick, W. H. (1994). Eicosanoids from the tropical red alga *Murrayella periclados*. *Phytochemistry* **36**: 1233-1240.

Boeglin, W. E., Kim, R. B. and Brash, A. R. (1998). A 12*R*-lipoxygenase in human skin: Mechanistic evidence, molecular cloning and expression. *Proc. Natl. Acad. Sci. USA* **95**: 6744-6749.

Borngraber, S., Browner, M., Gillmor, S., Gerth, C., Anton, M., Fletterick, R. and Kuhn, H. (1999). Shape and specificity in mammalian 15-lipoxygenase active site. The functional interplay of sequence determinants for the reaction specificity. *J Biol Chem* **274**: 37345-50.

Bowers, R. C., Hevko, J., Henson, P. M. and Murphy, R. C. (2000). A novel glutathione containing eicosanoid (FOG7) chemotactic for human granulocytes. *J Biol Chem* **275**: 29931-4.

Bowser, P. A., Nugteren, D. H., White, R. J., Houtsmuller, U. M. and Prottey, C. (1985). Identification, isolation and characterization of epidermal lipids containing linoleic acid. *Biochim Biophys Acta* **834**: 419-28.

Boyington, J. C., Gaffney, B. J. and Amzel, L. M. (1993). The three-dimensional structure of an arachidonic acid 15-lipoxygenase. *Science* **260**: 1482-1486.

Brain, S., Camp, R. D. R., Dowd, P., Black, A. K. and Greaves, M. (1984). The release of leukotriene B_4-like material in biologically active amounts from the lesional skin of patients with psoriasis. *J. Invest. Dermatol.* **83**: 70-73.

Brash, A. R. (1999). Lipoxygenases: Occurrence, functions, catalysis, and acquisition of substrate. *J. Biol. Chem.* **274**: 23679-23682.

Brash, A. R., Boeglin, W. E. and Chang, M. S. (1997). Discovery of a second 15S-lipoxygenase in humans. *Proc. Natl. Acad. Sci. USA* **94**: 6148-6152.

Buckman, S. Y., Gresham, A., Hale, P., Hruza, G., Anast, J., Masferrer, J. and Pentland, A. P. (1998). COX-2 expression is induced by UVB exposure in human skin: implications for the development of skin cancer. *Carcinogenesis* **19**: 723-9.

Burr, G. O. and Burr, M. M. (1929). A new deficiency disease produced by the rigid exclusion of fat from the diet. *J. Biol. Chem.* **82**: 345-367.

Burr, G. O. and Burr, M. M. (1930). On the nature of the fatty acids essential in nutrition. *J. Biol. Chem.* **86**: 587-621.

Byrum, R. S., Goulet, J. L., Griffiths, R. J. and Koller, B. H. (1997). Role of the 5-lipoxygenase-activating protein (FLAP) in murine acute inflammatory responses. *J Exp Med* **185**: 1065-75.

Byrum, R. S., Goulet, J. L., Snouwaert, J. N., Griffiths, R. J. and Koller, B. H. (1999). Determination of the contribution of cysteinyl leukotrienes and leukotriene B4 in acute inflammatory responses using 5-lipoxygenase- and leukotriene A4 hydrolase-deficient mice. *J Immunol* **163**: 6810-9.

Camp, R., Jones, R. R., Brain, S., Woollard, P. and Greaves, M. (1984). Production of intraepidermal microabscesses by topical application of leukotriene B4. *J Invest Dermatol* **82**: 202-4.

Campbell, W. B., Spitzbarth, N., Gauthier, K. M. and Pfister, S. L. (2003). 11,12,15-Trihydroxyeicosatrienoic acid mediates ACh-induced relaxations in rabbit aorta. *Am J Physiol Heart Circ Physiol* **285**: H2648-56.

Carter, G. W., Young, P. R., Albert, D. H., Bouska, J., Dyer, R., Bell, R. L., Summers, J. B. and Brooks, D. W. (1991). 5-lipoxygenase inhibitory activity of zileuton. *J. Pharmacol. Exp. Ther.* **256**: 929-937.

Chang, M. S., Boeglin, W. E., Guengerich, F. P. and Brash, A. R. (1996). Cytochrome P450-dependent transformations of 15R- and 15S-hydroperoxyeicosatetraenoic acids: Stereoselective formation of epoxy alcohol products. *Biochemistry* **35**: 464-471.

Chapkin, R. S. and Ziboh, V. A. (1984). Inability of skin enzyme preparations to biosynthesize arachidonic acid from linoleic acid. *Biochem Biophys Res Commun* **124**: 784-92.

Corey, E. J. and Mehrotra, M. M. (1983). Stereochemistry of the lipoxygenase-catalyzed allylic hydroperoxide to oxiranylcarbinol rearrangement. *Tetrahedron. Lett.* **45**: 4921-4922.

Corey, E. J. and Su, W.-G. (1984). Total synthesis of biologically active metabolites of arachidonic acid. The two 8-hydroxy-11,12(S,S)-epoxyeicosa-5,14(Z),9(E)-trienoic acids. *Tetrahedron Lett.* **25**: 5119-5122.

Cowart, L. A., Wei, S., Hsu, M. H., Johnson, E. F., Krishna, M. U., Falck, J. R. and Capdevila, J. H. (2002). The CYP4A isoforms hydroxylate epoxyeicosatrienoic acids to form high affinity peroxisome proliferator-activated receptor ligands. *J Biol Chem* **277**: 35105-12.

Cyrus, T., Witztum, J. L., Rader, D. J., Tangirala, R., Fazio, S., Linton, M. F. and Funk, C. D. (1999). Disruption of the 12/15-lipoxygenase gene diminishes atherosclerosis in apo E-deficient mice. *J. Clin. Invest.* **103**: 1597-1604.

Dahlen, S. E., Hedqvist, P., Hammarstrom, S. and Samuelsson, B. (1980). Leukotrienes are potent constrictors of human bronchi. *Nature* **288**: 484-6.

De Carolis, E., Denis, D. and Riendeau, D. (1996). Oxidative inactivation of human 5-lipoxygenase in phosphatidylcholine vesicles. *Eur J Biochem* **235**: 416-23.

De Caterina, R., Mazzone, A., Giannessi, D., Sicari, R., Pelosi, W., Lazzerini, G., Azzara, A., Forder, R., Carey, F., Caruso, D. and et al. (1988). Leukotriene B4 production in human atherosclerotic plaques. *Biomed Biochim Acta* **47**: S182-5.

Devchand, P. R., Keller, H., Peters, J. M., Vazquez, M., Gonzalez, F. J. and Wahli, W. (1996). The PPARalpha-leukotriene B4 pathway to inflammation control. *Nature* **384**: 39-43.

Dix, T. A. and Marnett, L. J. (1985). Conversion of linoleic acid hydroperoxide to hydroxy, keto, epoxyhydroxy, and trihydroxy fatty acids by hematin. *J. Biol. Chem.* **260**: 5351-5357.

Dixon, R. A. F., Jones, R. E., Diehl, R. E., Bennet, C. D., Kargman, S. and Rouzer, C. A. (1988). Cloning of the cDNA for human 5-lipoxygenase. *Proc. Natl. Acad. Sci. USA* **85**: 416-420.

Drazen, J. M., Israel, E. and O'Byrne, P. M. (1999). Treatment of asthma with drugs modifying the leukotriene pathway. *New. Engl. J. Med.* **340**: 197-206.

Dwyer, J. H., Allayee, H., Dwyer, K. M., Fan, J., Wu, H., Mar, R., Lusis, A. J. and Mehrabian, M. (2004). Arachidonate 5-lipoxygenase promoter genotype, dietary arachidonic acid, and atherosclerosis. *N Engl J Med* **350**: 29-37.

Eckl, K. M., Krieg, P., Kuster, W., Traupe, H., Andre, F., Wittstruck, N., Furstenberger, G. and Hennies, H. C. (2005). Mutation spectrum and functional analysis of epidermis-type lipoxygenases in patients with autosomal recessive congenital ichthyosis. *Hum Mutat* **26**: 351-61.

Elias, P. M., Brown, B. E. and Ziboh, V. A. (1980). The permeability barrier in essential fatty acid deficiency: evidence for a direct role for linoleic acid in barrier function. *J Invest Dermatol* **74**: 230-3.

Elias, P. M., Schmuth, M., Uchida, Y., Rice, R. H., Behne, M., Crumrine, D., Feingold, K. R., Holleran, W. M. and Pharm, D. (2002). Basis for the permeability barrier abnormality in lamellar ichthyosis. *Exp Dermatol* **11**: 248-56.

Fartasch, M. (1997). Epidermal barrier in disorders of the skin. *Microsc Res Tech* **38**: 361-72.

Fauler, J., Neumann, C., Tsikas, D. and Frolich, J. (1992). Enhanced synthesis of cysteinyl leukotrienes in psoriasis. *J Invest Dermatol* **99**: 8-11.

Fiore, S., Maddox, J. F., Perez, H. D. and Serhan, C. N. (1994). Identification of a human cDNA encoding a functional high affinity lipoxin A4 receptor. *J Exp Med* **180**: 253-60.

Flower, R. J., Harvey, E. A. and Kingston, W. P. (1976). Inflammatory effects of prostaglandin D2 in rat and human skin. *Br J Pharmacol* **56**: 229-33.

Folcik, V. A., Nivar-Aristy, R. A., Krajewski, L. P. and Cathcart, M. K. (1995). Lipoxygenase contributes to the oxidation of lipids in human atherosclerotic plaques. *J Clin Invest.* **96**: 504-10.

Ford-Hutchinson, A. W. (1993). 5-Lipoxygenase activation in psoriasis: a dead issue? *Skin Pharmacol* **6**: 292-7.

Ford-Hutchinson, A. W., Bray, M. A., Doig, M. V., Shipley, M. E. and Smith, M. J. (1980). Leukotriene B, a potent chemokinetic and aggregating substance released from polymorphonuclear leukocytes. *Nature* **286**: 264-5.

Forman, B. M., Chen, J. and Evans, R. M. (1997). Hypolipidemic drugs, polyunsaturated fatty acids, and eicosanoids are ligands for peroxisome proliferator-activated receptors alpha and delta. *Proc Natl Acad Sci U S A* **94**: 4312-7.

Funk, C. D. (1996). The molecular biology of mammalian lipoxygenases and the quest for eicosanoid functions using lipoxygenase-deficient mice. *Biochim Biophys Acta* **1304**: 65-84.

Funk, C. D. (2001). Prostaglandins and leukotrienes: advances in eicosanoid biology. *Science* **294**: 1871-1875.

Funk, C. D., Keeney, D. S., Oliw, E. H., Boeglin, W. E. and Brash, A. R. (1996). Functional expression and cellular localization of a mouse epidermal lipoxygenase. *J Biol Chem* **271**: 23338-44.

Furstenberger, G., Hagedorn, H., Jacobi, T., Besemfelder, E., Stephan, M., Lehmann, W. D. and Marks, F. (1991). Characterization of an 8-lipoxygenase activity induced by the phorbol ester tumor promoter 12-O-tetradecanoylphorbol-13-acetate in mouse skin in vivo. *J Biol Chem* **266**: 15738-45.

Gao, X., Grignon, D. J., Chbihi, T., Zacharek, A., Chen, Y. Q., Sakr, W., Porter, A. T., Crissman, J. D., Pontes, J. E., Powell, I. J. and Honn, K. V. (1995). Elevated 12-lipoxygenase mRNA expression correlates with advanced stage and poor differentiation of human prostate cancer. *Urology* **46**: 227-237.

Gardner, H. W. (1989). Oxygen radical chemistry of polyunsaturated fatty acids. *Free Radical Biol. Med.* **7**: 65-86.

Garssen, G. J., Veldink, G. A., Vliegenthart, J. F. G. and Boldingh, J. (1976). The formation of *threo*-11-hydroxy-*trans*-12: 13-epoxy-9-*cis*-octadecenoic acid by enzymic isomerisation of 13-L-hydroperoxy-9-*cis*, 11-*trans*-octadecadienoic acid by soybean lipoxygenase-1. *Eur. J. Biochem.* **62**: 33-36.

Garssen, G. J., Vliegenthart, J. F. G. and Boldingh, J. (1971). An anaerobic reaction between lipoxygenase, linoleic acid and its hydroperoxides. *Biochem. J.* **122**: 327-332.

George, J., Afek, A., Shaish, A., Levkovitz, H., Bloom, N., Cyrus, T., Zhao, L., Funk, C. D., Sigal, E. and Harats, D. (2001). 12/15-Lipoxygenase gene disruption attenuates atherogenesis in LDL receptor-deficient mice. *Circulation* **104**: 1646-50.

Gillmor, S. A., Villasenor, A., Fletterick, R., Sigal, E. and Browner, M. F. (1997). The structure of mammalian 15-lipoxygenase reveals similarity to the lipases and the determinants of substrate specificity. *Nat Struct Biol* **4**: 1003-9.

Glasgow, W. C., Harris, T. M. and Brash, A. R. (1986). A short-chain aldehyde is a major lipoxygenase product in arachidonic acid-stimulated porcine leukocytes. *J. Biol. Chem.* **261**: 200-204.

Gonnella, N. C., Nakanishi, K., Martin, V. S. and Sharpless, B. K. (1982). General method for determining absolute configurations of acyclic allylic alcohols. *J. Am. Chem. Soc.* **104**: 3775-3776.

Goulet, J. L., Snouwaert, J. N., Latour, A. M., Coffman, T. M. and Koller, B. H. (1994). Altered inflammatory responses in leukotriene-deficient mice. *Proc Natl Acad Sci U S A* **91**: 12852-6.

Greeley, R. H. (1974). Rapid esterification for gas chromatography. *J. Chromatogr.* **88**: 229-233.

Gross, E., Ruzicka, T., Mauch, C. and Krieg, T. (1988). Evidence for LTB4/12-HETE binding sites in a human epidermal cell line. *Prostaglandins* **36**: 49-58.

Gupta, R. A., Tan, J., Krause, W. F., Geraci, M. W., Willson, T. M., Dey, S. K. and DuBois, R. N. (2000). Prostacyclin-mediated activation of peroxisome proliferator-activated receptor delta in colorectal cancer. *Proc Natl Acad Sci U S A* **97**: 13275-80.

Hamberg, M. (1991). Regiochemical and Stereochemical Analysis of Trihydroxyoctadecenoic Acids Derived from Linoleic-Acid 9-Hydroperoxide and 13-Hydroperoxide. *Lipids* **26**: 407-415.

Hamberg, M. and Samuelsson, B. (1967). Oxygenation of unsaturated fatty acids by the vesicular gland of sheep. *J. Biol. Chem.* **242**: 5344-5354.

Hamberg, M. and Samuelsson, B. (1974). Prostaglandin endoperoxides. Novel transformations of arachidonic acid in human platelets. *Proc. Natl. Acad. Sci. USA* **71**: 3400-3404.

Hammarstrom, S., Hamberg, M., Samuelsson, B., Duell, E. A., Stawiski, M. and Voorhees, J. J. (1975). Increased concentrations of nonesterified arachidonic acid, 12L-hydroxy-5,8,10,14-eicosatetraenoic acid, prostaglandin E2, and prostaglandin F2alpha in epidermis of psoriasis. *Proc Natl Acad Sci U S A* **72**: 5130-4.

Hammarstrom, S., Lindgren, J. A., Marcelo, C., Duell, E. A., Anderson, T. F. and Voorhees, J. J. (1979). Arachidonic acid transformations in normal and psoriatic skin. *J Invest Dermatol* **73**: 180-3.

Hampson, A. J. and Grimaldi, M. (2002). 12-hydroxyeicosatetrenoate (12-HETE) attenuates AMPA receptor-mediated neurotoxicity: evidence for a G-protein-coupled HETE receptor. *J Neurosci* **22**: 257-64.

Hanley, K., Jiang, Y., He, S. S., Friedman, M., Elias, P. M., Bikle, D. D., Williams, M. L. and Feingold, K. R. (1998). Keratinocyte differentiation is stimulated by activators of the nuclear hormone receptor PPARalpha. *J Invest Dermatol* **110**: 368-75.

Hansen, A. E., Haggard, M. E., Boelsche, A. N., Adam, D. J. and Wiese, H. F. (1958). Essential fatty acids in infant nutrition. III. Clinical manifestations of linoleic acid deficiency. *J Nutr* **66**: 565-76.

Hansen, H. S. and Jensen, B. (1985). Essential function of linoleic acid esterified in acylglucosylceramide and acylceramide in maintaining the epidermal water permeability barrier. Evidence from feeding studies with oleate, linoleate, arachidonate, columbinate and alpha-linolenate. *Biochim Biophys Acta* **834**: 357-63.

Harats, D., Shaish, A., George, J., Mulkins, M., Kurihara, H., Levkovitz, H. and Sigal, E. (2000). Overexpression of 15-lipoxygenase in vascular endothelium accelerates early atherosclerosis in LDL receptor-deficient mice. *Arterioscler Thromb Vasc Biol* **20**: 2100-5.

Hartel, B., Ludwig, P., Schewe, T. and Rapoport, S. M. (1982). Self-inactivation by 13-hydroperoxylinoleic acid and lipohydroperoxidase activity of the reticulocyte lipoxygenase. *Eur J Biochem* **126**: 353-7.

Heidt, M., Furstenberger, G., Vogel, S., Marks, F. and Krieg, P. (2000). Diversity of mouse lipoxygenases: identification of a subfamily of epidermal isozymes exhibiting a differentiation-dependent mRNA expression pattern. *Lipids* **35**: 701-7.

Heise, C. E., O'Dowd, B. F., Figueroa, D. J., Sawyer, N., Nguyen, T., Im, D. S., Stocco, R., Bellefeuille, J. N., Abramovitz, M., Cheng, R., Williams, D. L., Jr., Zeng, Z., Liu, Q., Ma, L., Clements, M. K., Coulombe, N., Liu, Y., Austin, C. P., George, S. R., O'Neill, G. P., Metters, K. M., Lynch, K. R. and Evans, J. F. (2000). Characterization of the human cysteinyl leukotriene 2 receptor. *J. Biol. Chem.* **275**: 30531-30536.

Heller, E. A., Liu, E., Tager, A. M., Sinha, S., Roberts, J. D., Koehn, S. L., Libby, P., Aikawa, E. R., Chen, J. Q., Huang, P., Freeman, M. W., Moore, K. J., Luster, A. D. and Gerszten, R. E. (2005). Inhibition of atherogenesis in BLT1-deficient mice reveals a role for LTB4 and BLT1 in smooth muscle cell recruitment. *Circulation* **112**: 578-86.

Henneicke-von Zepelin, H. H., Schroder, J. M., Smid, P., Reusch, M. K. and Christophers, E. (1991). Metabolism of arachidonic acid by human epidermal cells depends upon maturational stage. *J Invest Dermatol* **97**: 291-7.

Hennig, R., Ding, X. Z., Tong, W. G., Schneider, M. B., Standop, J., Friess, H., Buchler, M. W., Pour, P. M. and Adrian, T. E. (2002). 5-Lipoxygenase and leukotriene B(4) receptor are expressed in human pancreatic cancers but not in pancreatic ducts in normal tissue. *Am J Pathol* **161**: 421-8.

Hennig, R., Grippo, P., Ding, X. Z., Rao, S. M., Buchler, M. W., Friess, H., Talamonti, M. S., Bell, R. H. and Adrian, T. E. (2005). 5-Lipoxygenase, a marker for early pancreatic intraepithelial neoplastic lesions. *Cancer Res* **65**: 6011-6.

Herbertsson, H. and Hammarstrom, S. (1997). Cytosolic 12(S)-hydroxy-5,8,10,14-eicosatetraenoic acid binding sites in carcinoma cells. *Adv Exp Med Biol* **400A**: 287-93.

Holtzman, M. J., Turk, J. and Pentland, A. (1989). A regiospecific monooxygenase with novel stereopreference is the major pathway for arachidonic acid oxygenation in isolated epidermal cells. *J. Clin. Invest.* **84**: 1446-1453.

Holvoet, P. and Collen, D. (1994). Oxidized lipoproteins in atherosclerosis and thrombosis. *Faseb J* **8**: 1279-84.

Huber, M., Rettler, I., Bernasconi, K., Frenk, E., Lavrijsen, S. P., Ponec, M., Bon, A., Lautenschlager, S., Schorderet, D. F. and Hohl, D. (1995). Mutations of keratinocyte transglutaminase in lamellar ichthyosis. *Science* **267**: 525-8.

Hugou, I., Blin, P., Henri, J., Daret, D. and Larrue, J. (1995). 15-Lipoxygenase expression in smooth muscle cells from atherosclerotic rabbit aortas. *Atherosclerosis* **113**: 189-95.

Humpf, H.-U., Berova, N., Nakanishi, K., Jarstfer, M. B. and Poulter, C. D. (1995). Allylic and homoallylic exciton coupled CD: A sensitive method for determining the absolute stereochemistry of natural products. *J. Org. Chem.* **60**: 3539-3542.

Hussain, H., Shornick, L. P., Shannon, V. R., Wilson, J. D., Funk, C. D., Pentland, A. P. and Holtzman, M. J. (1994). Epidermis contains platelet-type 12-lipoxygenase that is overexpressed in germinal layer keratinocytes in psoriasis. *Am. J. Physiol.* **266**: C243-C253.

Jisaka, M., Kim, R. B., Boeglin, W. E., Nanney, L. B. and Brash, A. R. (1997). Molecular cloning and functional expression of a phorbol ester-inducible 8*S*-lipoxygenase from mouse skin. *J. Biol. Chem.* **272**: 24410-24416.

Jobard, F., Lefevre, C., Karaduman, A., Blanchet-Bardon, C., Emre, S., Weissenbach, J., Ozguc, M., Lathrop, M., Prud'homme, J. F. and Fischer, J. (2002). Lipoxygenase-3 (ALOXE3) and 12(R)-lipoxygenase (ALOX12B) are mutated in non-bullous congenital ichthyosiform erythroderma (NCIE) linked to chromosome 17p13.1. *Hum Mol Genet* **11**: 107-13.

Johnson, E. N., Brass, L. F. and Funk, C. D. (1998). Increased platelet sensitivity to ADP in mice lacking platelet-type 12-lipoxygenase. *Proc. Natl. Acad. Sci. USA* **95**: 3100-3105.

Johnson, E. N., Nanney, L. B., Virmani, J., Lawson, J. A. and Funk, C. D. (1999). Basal transepidermal water loss is increased in platelet-type 12-lipoxygenase deficient mice. *J Invest Dermatol* **112**: 861-5.

Jones, R. L., Kerry, P. J., Poyser, N. L., Walker, I. C. and Wilson, N. H. (1978). The identification of trihydroxyeicosatrienoic acids as products from the incubation of arachidonic acid with washed blood platelets. *Prostaglandins* **16**: 583-589.

Kalinin, A. E., Kajava, A. V. and Steinert, P. M. (2002). Epithelial barrier function: assembly and structural features of the cornified cell envelope. *Bioessays* **24**: 789-800.

Kamohara, M., Takasaki, J., Matsumoto, M., Saito, T., Ohishi, T., Ishii, H. and Furuichi, K. (2000). Molecular cloning and characterization of another leukotriene B4 receptor. *J Biol Chem* **275**: 27000-4.

Kanaoka, Y., Maekawa, A., Penrose, J. F., Austen, K. F. and Lam, B. K. (2001). Attenuated zymosan-induced peritoneal vascular permeability and IgE-dependent passive cutaneous anaphylaxis in mice lacking leukotriene C4 synthase. *J Biol Chem* **276**: 22608-13.

Kelavkar, U., Cohen, C., Eling, T. and Badr, K. (2002). 15-lipoxygenase-1 overexpression in prostate adenocarcinoma. *Adv Exp Med Biol* **507**: 133-45.

Kemal, C., Louis-Flamberg, P., Krupinski-Olsen, R. and Shorter, A. L. (1987). Reductive inactivation of soybean lipoxygenase 1 by catechols: a possible mechanism for regulation of lipoxygenase activity. *Biochemistry* **26**: 7064-7072.

Kilty, I., Logan, A. and Vickers, P. J. (1999). Differential characteristics of human 15-lipoxygenase isozymes and a novel splice variant of 15S-lipoxygenase. *Eur. J. Biochem.* **266**: 83-93.

Kim, E., Rundhaug, J. E., Benavides, F., Yang, P., Newman, R. A. and Fischer, S. M. (2005). An antitumorigenic role for murine 8S-lipoxygenase in skin carcinogenesis. *Oncogene* **24**: 1174-87.

Kinzig, A., Heidt, M., Furstenberger, G., Marks, F. and Krieg, P. (1999). cDNA cloning, genomic structure, and chromosomal localization of a novel murine epidermis-type lipoxygenase. *Genomics* **58**: 158-164.

Kliewer, S. A., Sundseth, S. S., Jones, S. A., Brown, P. J., Wisely, G. B., Koble, C. S., Devchand, P., Wahli, W., Willson, T. M., Lenhard, J. M. and Lehmann, J. M. (1997). Fatty acids and eicosanoids regulate gene expression through direct interactions with peroxisome proliferator-activated receptors alpha and gamma. *Proc. Natl. Acad. Sci. USA* **94**: 4318-4323.

Komuves, L. G., Hanley, K., Lefebvre, A. M., Man, M. Q., Ng, D. C., Bikle, D. D., Williams, M. L., Elias, P. M., Auwerx, J. and Feingold, K. R. (2000). Stimulation of

PPARalpha promotes epidermal keratinocyte differentiation in vivo. *J Invest Dermatol* **115**: 353-60.

Krieg, P., Marks, F. and Furstenberger, G. (2001). A gene cluster encoding human epidermis-type lipoxygenases at chromosome 17p13.1: cloning, physical mapping, and expression. *Genomics* **73**: 323-300.

Krieg, P., Siebert, M., Kinzig, A., Bettenhausen, R., Marks, F. and Furstenberger, G. (1999). Murine 12(R)-lipoxygenase: functional expression, genomic structure and chromosomal localization. *FEBS Lett* **446**: 142-8.

Kuenzli, S. and Saurat, J. H. (2003). Peroxisome proliferator-activated receptors in cutaneous biology. *Br J Dermatol* **149**: 229-36.

Kuhn, H., Belkner, J., Suzuki, H. and Yamamoto, S. (1994a). Oxidative modification of human lipoproteins by lipoxygenases of different positional specificities. *J Lipid Res* **35**: 1749-59.

Kuhn, H., Belkner, J., Zaiss, S., Fahrenklemper, T. and Wohlfeil, S. (1994b). Involvement of 15-lipoxygenase in early stages of atherogenesis. *J Exp Med* **179**: 1903-11.

Kuhn, H. and Thiele, B. J. (1999). The diversity of the lipoxygenase family. Many sequence data but little information on biological significance. *FEBS Lett* **449**: 7-11.

Lee, T. H., Austen, K. F., Corey, E. J. and Drazen, J. M. (1984). Leukotriene E4-induced airway hyperresponsiveness of guinea pig tracheal smooth muscle to histamine and evidence for three separate sulfidopeptide leukotriene receptors. *Proc Natl Acad Sci U S A* **81**: 4922-5.

Lefevre, C., Bouadjar, B., Karaduman, A., Jobard, F., Saker, S., Ozguc, M., Lathrop, M., Prud'homme, J. F. and Fischer, J. (2004). Mutations in ichthyin a new gene on chromosome 5q33 in a new form of autosomal recessive congenital ichthyosis. *Hum Mol Genet* **13**: 2473-82.

Lehmann, W. D., Stephan, M. and Furstenberger, G. (1992). Profiling assay for lipoxygenase products of linoleic and arachidonic acid by gas chromatography-mass spectrometry. *Anal. Biochem.* **204**: 158-170.

Leong, J., Hughes-Fulford, M., Rakhlin, N., Habib, A., Maclouf, J. and Goldyne, M. E. (1996). Cyclooxygenases in human and mouse skin and cultured human keratinocytes: association of COX-2 expression with human keratinocyte differentiation. *Exp Cell Res* **224**: 79-87.

Lowe, N. J. and DeQuoy, P. R. (1978). Linoleic acid effects on epidermal DNA synthesis and cutaneous prostaglandin levels in essential fatty acid deficiency. *J Invest Dermatol* **70**: 200-3.

Lumin, S., Falck, J. R., Capdevila, J. H. and Karara, A. (1992). Palladium mediated allylic Mitsunobu displacement: Stereocontrolled synthesis of hepoxilin A_3 and trioxilin A_3 methyl esters. *Tetrahedron Lett.* **33**: 2091-2094.

Lusis, A. J. (2000). Atherosclerosis. *Nature* **407**: 233-41.

Lynch, K. R., O'Neill, G. P., Liu, Q., Im, D. S., Sawyer, N., Metters, K. M., Coulombe, N., Abramovitz, M., Figueroa, D. J., Zeng, Z., Connolly, B. M., Bai, C., Austin, C. P., Chateauneuf, A., Stocco, R., Greig, G. M., Kargman, S., Hooks, S. B., Hosfield, E., Williams, D. L., Jr., Ford-Hutchinson, A. W., Caskey, C. T. and Evans, J. F. (1999). Characterization of the human cysteinyl leukotriene CysLT1 receptor. *Nature* **399**: 789-793.

Madison, K. C. (2003). Barrier function of the skin: "la raison d'etre" of the epidermis. *J Invest Dermatol* **121**: 231-41.

Madsen, L., Petersen, R. K., Sorensen, M. B., Jorgensen, C., Hallenborg, P., Pridal, L., Fleckner, J., Amri, E. Z., Krieg, P., Furstenberger, G., Berge, R. K. and Kristiansen, K. (2003). Adipocyte differentiation of 3T3-L1 preadipocytes is dependent on lipoxygenase activity during the initial stages of the differentiation process. *Biochem J* **375**: 539-49.

Maekawa, A., Austen, K. F. and Kanaoka, Y. (2002). Targeted gene disruption reveals the role of cysteinyl leukotriene 1 receptor in the enhanced vascular permeability of mice undergoing acute inflammatory responses. *J Biol Chem* **277**: 20820-4.

Matsumoto, T., Funk, C. D., Radmark, O., Hoog, J. O., Jornvall, H. and Samuelsson, B. (1988). Molecular cloning and amino acid sequence of human 5-lipoxygenase. *Proc Natl Acad Sci U S A* **85**: 26-30.

Matthew, J. A., Chan, H. W.-S. and Galliard, T. (1977). A simple method for the preparation of pure 9-D-hydroperoxide of linoleic acid and methyl linoleate based on the positional specificity of lipoxygenase in tomato fruit. *Lipids* **12**: 324-326.

McCowen, K. C. and Bistrian, B. R. (2005). Essential fatty acids and their derivatives. *Curr Opin Gastroenterol* **21**: 207-15.

McDonnell, M., Davis, W., Jr., Li, H. and Funk, C. D. (2001). Characterization of the murine epidermal 12/15-lipoxygenase. *Prostaglandins Other Lipid Mediat* **63**: 93-107.

Mehrabian, M., Allayee, H., Wong, J., Shi, W., Wang, X. P., Shaposhnik, Z., Funk, C. D. and Lusis, A. J. (2002). Identification of 5-lipoxygenase as a major gene contributing to atherosclerosis susceptibility in mice. *Circ Res* **91**: 120-6.

Meijer, L., Brash, A. R., Bryant, R. W., Ng, K., Maclouf, J. and Sprecher, H. (1986). Stereospecific induction of starfish oocyte maturation by (8R)-hydroxyeicosatetraenoic acid. *J. Biol. Chem.* **261**: 17040-17047.

Melton, J. L., Wertz, P. W., Swartzendruber, D. C. and Downing, D. T. (1987). Effects of essential fatty acid deficiency on epidermal O-acylsphingolipids and transepidermal water loss in young pigs. *Biochim Biophys Acta* **921**: 191-7.

Mitchell, J. A., Akarasereenont, P., Thiemermann, C., Flower, R. J. and Vane, J. R. (1993). Selectivitity of nonsteroidal antiinflammatory drugs as inhibitors of constitutive and inducible cyclooxygenase. *Proc. Natl. Acad. Sci. USA* **90**: 11693-11697.

Morris, L. J. (1963). Separation Of Isomeric Long-Chain Polyhydroxy Acids By Thin-Layer Chromatography. *J Chromatogr* **12**: 321-8.

Muga, S. J., Thuillier, P., Pavone, A., Rundhaug, J. E., Boeglin, W. E., Jisaka, M., Brash, A. R. and Fischer, S. M. (2000). 8S-lipoxygenase products activate peroxisome proliferator-activated receptor alpha and induce differentiation in murine keratinocytes. *Cell Growth Differ.* **11**: 447-454.

Muller, K., Siebert, M., Heidt, M., Marks, F., Krieg, P. and Furstenberger, G. (2002). Modulation of epidermal tumor development caused by targeted overexpression of epidermis-type 12S-lipoxygenase. *Cancer Res* **62**: 4610-6.

Murphy, R. C. and Zarini, S. (2002). Glutathione adducts of oxyeicosanoids. *Prostaglandins Other Lipid Mediat* **68-69**: 471-82.

Nakao, J., Ooyama, T., Ito, H., Chang, W. C. and Murota, S. (1982). Comparative effect of lipoxygenase products of arachidonic acid on rat aortic smooth muscle cell migration. *Atherosclerosis* **44**: 339-42.

Narumiya, S., Salmon, J. A., Cottee, F. H., Weatherley, B. C. and Flower, R. J. (1981). Arachidonic acid 15-lipoxygenase from rabbit peritoneal polymorphonuclear leukocytes. Partial purification and properties. *J. Biol. Chem.* **256**: 9583-9592.

Nie, D. and Honn, K. V. (2004). Eicosanoid regulation of angiogenesis in tumors. *Semin Thromb Hemost* **30**: 119-25.

Nugteren, D. H., Christ-Hazelhof, E., van der Beek, A. and Houtsmuller, U. M. (1985). Metabolism of linoleic acid and other essential fatty acids in the epidermis of the rat. *Biochim Biophys Acta* **834**: 429-36.

Ota, K. and Hammock, B. D. (1980). Cytosolic and microsomal epoxide hydrolases: differential properties in mammalian liver. *Science* **207**: 1479-81.

Pace-Asciak, C. R. and Asotra, S. (1989). Biosynthesis, catabolism, and biological properties of HPETEs, hydroperoxide derivatives of arachidonic acid. *Free Radic Biol Med* **7**: 409-433.

Pace-Asciak, C. R., Granstrom, E. and Samuelsson, B. (1983). Arachidonic acid epoxides. Isolation and structure of two hydroxy epoxide intermediates in the formation of 8,11,12- and 10,11,12- trihydroxyeicosatrienoic acids. *J. Biol. Chem.* **258**: 6835-6840.

Pace-Asciak, C. R. and Lee, W. S. (1989). Purification of hepoxilin epoxide hydrolase from rat liver. *J Biol Chem* **264**: 9310-3.

Pace-Asciak, C. R., Reynaud, D. and Demin, P. M. (1995). Hepoxilins: a review on their enzymatic formation, metabolism and chemical synthesis. *Lipids* **30**: 107-114.

Patricia, M. K., Kim, J. A., Harper, C. M., Shih, P. T., Berliner, J. A., Natarajan, R., Nadler, J. L. and Hedrick, C. C. (1999). Lipoxygenase products increase monocyte adhesion to human aortic endothelial cells. *Arterioscler Thromb Vasc Biol* **19**: 2615-22.

Peers, K. F. and Coxon, D. T. (1983). Controlled synthesis of monohydroperoxides by α-tocopherol inhibited autoxidation of polyunsaturated lipids. *Chem. Phys. Lipids* **32**: 49-56.

Pfister, S. L., Spitzbarth, N., Nithipatikom, K., Edgemond, W. S., Falck, J. R. and Campbell, W. B. (1998). Identification of the 11,14,15- and 11,12, 15-trihydroxyeicosatrienoic acids as endothelium-derived relaxing factors of rabbit aorta. *J. Biol. Chem.* **273**: 30879-30887.

Pfister, S. L., Spitzbarth, N., Nithipatikom, K., Falck, J. R. and Campbell, W. B. (2003). Metabolism of 12-hydroperoxyeicosatetraenoic acid to vasodilatory trioxilin C3 by rabbit aorta. *Biochim Biophys Acta* **1622**: 6-13.

Pidgeon, G. P., Tang, K., Rice, R. L., Zacharek, A., Li, L., Taylor, J. D. and Honn, K. V. (2003). Overexpression of leukocyte-type 12-lipoxygenase promotes W256 tumor cell survival by enhancing alphavbeta5 expression. *Int J Cancer* **105**: 459-71.

Porta, H. and Rocha-Sosa, M. (2001). Lipoxygenase in bacteria: a horizontal transfer event? *Microbiology* **147**: 3199-200.

Powell, W. S. (1982). Rapid extraction of arachidonic acid metabolites from biological samples using octadecylsilyl silica. *Methods Enzymol.* **86**: 467-477.

Reilly, K. B., Srinivasan, S., Hatley, M. E., Patricia, M. K., Lannigan, J., Bolick, D. T., Vandenhoff, G., Pei, H., Natarajan, R., Nadler, J. L. and Hedrick, C. C. (2004). 12/15-Lipoxygenase activity mediates inflammatory monocyte/endothelial interactions and atherosclerosis in vivo. *J Biol Chem* **279**: 9440-50.

Reynaud, D., Demin, P. M., Sutherland, M., Nigam, S. and Pace-Asciak, C. R. (1999). Hepoxilin signaling in intact human neutrophils: biphasic elevation of intracellular calcium by unesterified hepoxilin A_3. *FEBS Lett.* **446**: 236-238.

Riccioni, G., Di Ilio, C., Conti, P., Theoharides, T. C. and D'Orazio, N. (2004). Advances in therapy with antileukotriene drugs. *Ann Clin Lab Sci* **34**: 379-87.

Riendeau, D., Falgueyret, J. P., Guay, J., Ueda, N. and Yamamoto, S. (1991). Pseudoperoxidase activity of 5-lipoxygenase stimulated by potent benzofuranol and N-hydroxyurea inhibitors of the lipoxygenase reaction. *Biochem J* **274 (Pt 1)**: 287-92.

Rippke, F., Schreiner, V. and Schwanitz, H. J. (2002). The acidic milieu of the horny layer: new findings on the physiology and pathophysiology of skin pH. *Am. J. Clin. Dermatol.* **3**: 261-272.

Robillard, P. Y. and Christon, R. (1993). Lipid intake during pregnancy in developing countries: possible effect of essential fatty acid deficiency on fetal growth. *Prostaglandins Leukot Essent Fatty Acids* **48**: 139-42.

Samuelsson, B., Dahlen, S. E., Lindgren, J. A., Rouzer, C. A. and Serhan, C. N. (1987a). Leukotrienes and lipoxins: structures, biosynthesis, and biological effects. *Science* **237**: 1171-1176.

Samuelsson, B., Rouzer, C. A. and Matsumoto, T. (1987b). Human leukocyte 5-lipoxygenase: an enzyme possessing dual enzymatic activities and a multicomponent regulatory system. *Adv Prostaglandin Thromboxane Leukot Res* **17A**: 1-11.

Schneider, C., Keeney, D. S., Boeglin, W. E. and Brash, A. R. (2001a). Detection and cellular localization of 12*R*-lipoxygenase in human tonsils. *Arch. Biochem. Biophys.* **386**: 268-274.

Schneider, C., Schreier, P. and Humpf, H.-U. (1997). Exciton-coupled circular dichroism (ECCD) in acyclic hydroxylated dienes: a sensitive method for the direct stereochemical assignment of lipoxygenase products. *Chirality* **9**: 563-567.

Schneider, C., Strayhorn, W. D., Brantley, D. M., Nanney, L. B., Yull, F. E. and Brash, A. R. (2004). Upregulation of 8-lipoxygenase in the dermatitis of IκB-α-deficient mice. *J. Invest. Dermatol.* **122**: in press.

Schneider, C., Tallman, K. A., Porter, N. A. and Brash, A. R. (2001b). Two distinct pathways of formation of 4-hydroxynonenal. Mechanisms of nonenzymatic transformation of the 9- and 13-hydroperoxides of linoleic acid to 4-hydroxyalkenals. *J. Biol. Chem.* **276**: 20831-20838.

Schweiger, D., Furstenberger, G. and Krieg, P. (2005). Inducible expression of human 15-lipoxygenase-2 (15-LOX-2) and its mouse orthologue 8-lipoxygenase (8-LOX) inhibits growth of premalignant mouse keratinocytes: evidence for activation of similar signaling pathways. *9th International Conference in Eicosanoids and other Bioactive Lipids in Cancer, Inflammation and Related Diseases* **Abstract 134**: San Francisco, CA.

Sendobry, S. M., Cornicelli, J. A., Welch, K., Bocan, T., Tait, B., Trivedi, B. K., Colbry, N., Dyer, R. D., Feinmark, S. J. and Daugherty, A. (1997). Attenuation of diet-induced atherosclerosis in rabbits with a highly selective 15-lipoxygenase inhibitor lacking significant antioxidant properties. *Br J Pharmacol* **120**: 1199-206.

Serhan, C. N., Hamberg, M. and Samuelsson, B. (1984). Lipoxins: novel series of biologically active compounds formed from arachidonic acid in human leukocytes. *Proc Natl Acad Sci U S A* **81**: 5335-9.

Shappell, S. B., Boeglin, W. E., Olson, S. J., Kasper, S. and Brash, A. R. (1999). 15-Lipoxygenase-2 (15-LOX-2) is expressed in benign prostatic epithelium and reduced in prostate adenocarcinoma. *Amer. J. Path.* **155**: 235-245.

Shappell, S. B., Gupta, R. A., Manning, S., Whitehead, R., Boeglin, W. E., Schneider, C., Case, T., Price, J., Jack, G. S., Wheeler, T. M., Matusik, R. J., Brash, A. R. and DuBois, R. N. (2001a). 15-Hydroxyeicosatetraenoic acid (15-HETE) activates peroxisome proliferator activated receptor gamma (PPARγ) and inhibits proliferation in PC3 prostate carcinoma cells. *Cancer Res.* **61**: 497-503.

Shappell, S. B., Keeney, D. S., Zhang, J., Page, R., Olson, S. J. and Brash, A. R. (2001b). 15-Lipoxygenase-2 (15-LOX-2) expression in benign and neoplastic sebaceous glands and other cutaneous adnexa. *J. Invest. Dermatol.* **117**: 36-43.

Shappell, S. B., Manning, S., Boeglin, W. E., Guan, Y. F., Roberts, R. L., Davis, L., Olson, S. J., Jack, G. S., Coffey, C. S., Wheeler, T. M., Breyer, M. D. and Brash, A. R. (2001c). Alterations in lipoxygenase and cyclooxygenase-2 catalytic activity and mRNA expression in prostate carcinoma. *Neoplasia* **3**: 287-303.

Shappell, S. B., Olson, S. J., Hannah, S. E., Manning, S., Roberts, R. L., Masumori, N., Jisaka, M., Boeglin, W. E., Vader, V., Dave, D. S., Shook, M. F., Thomas, T. Z., Funk, C. D., Brash, A. R. and Matusik, R. J. (2003). Elevated expression of 12/15-lipoxygenase and cyclooxygenase-2 in a transgenic mouse model of prostate carcinoma. *Cancer Res* **63**: 2256-67.

Shen, J., Herderick, E., Cornhill, J. F., Zsigmond, E., Kim, H. S., Kuhn, H., Guevara, N. V. and Chan, L. (1996). Macrophage-mediated 15-lipoxygenase expression protects against atherosclerosis development. *J Clin Invest* **98**: 2201-8.

Siebert, M., Krieg, P., Lehmann, W. D., Marks, F. and Furstenberger, G. (2001). Enzymic characterization of epidermis-derived 12-lipoxygenase isoenzymes. *Biochem J* **355**: 97-104.

Simon, T. C., Makheja, A. N. and Bailey, J. M. (1989). Formation of 15-hydroxyeicosatetraenoic acid (15-HETE) as the predominant eicosanoid in aortas from Watanabe Heritable Hyperlipidemic and cholesterol-fed rabbits. *Atherosclerosis* **75**: 31-8.

Skrzypczak-Jankun, E., Amzel, L. M., Kroa, B. A. and Funk, M. O., Jr. (1997). Structure of soybean lipoxygenase L3 and a comparison with its L1 isozyme. *Proteins: Struct. Funct. Genet.* **29**: 15-31.

Sloane, D. L., Leung, R., Barnett, J., Craik, C. S. and Sigal, E. (1995). Conversion of human 15-lipoxygenase to an efficient 12-lipoxygenase: the side-chain geometry of amino acids 417 and 418 determine positional specificity. *Protein Eng* **8**: 275-82.

Smit, E. N., Muskiet, F. A. and Boersma, E. R. (2004). The possible role of essential fatty acids in the pathophysiology of malnutrition: a review. *Prostaglandins Leukot Essent Fatty Acids* **71**: 241-50.

Spanbroek, R., Grabner, R., Lotzer, K., Hildner, M., Urbach, A., Ruhling, K., Moos, M. P., Kaiser, B., Cohnert, T. U., Wahlers, T., Zieske, A., Plenz, G., Robenek, H., Salbach, P., Kuhn, H., Radmark, O., Samuelsson, B. and Habenicht, A. J. (2003). Expanding expression of the 5-lipoxygenase pathway within the arterial wall during human atherogenesis. *Proc Natl Acad Sci U S A* **100**: 1238-43.

Stone, S. J., Myers, H. M., Watkins, S. M., Brown, B. E., Feingold, K. R., Elias, P. M. and Farese, R. V., Jr. (2004). Lipopenia and skin barrier abnormalities in DGAT2-deficient mice. *J Biol Chem* **279**: 11767-76.

Suzuki, H., Kishimoto, K., Yoshimoto, T., Yamamoto, S., Kanai, F., Ebina, Y., Miyatake, A. and Tanabe, T. (1994). Site-directed mutagenesis studies on the iron-binding domain and the determinant for the substrate oxygenation site of porcine leukocyte arachidonate 12-lipoxygenase. *Biochim Biophys Acta* **1210**: 308-16.

Tan, N. S., Michalik, L., Desvergne, B. and Wahli, W. (2003). Peroxisome proliferator-activated receptor (PPAR)-beta as a target for wound healing drugs: what is possible? *Am J Clin Dermatol* **4**: 523-30.

Tan, N. S., Michalik, L., Noy, N., Yasmin, R., Pacot, C., Heim, M., Fluhmann, B., Desvergne, B. and Wahli, W. (2001). Critical roles of PPAR beta/delta in keratinocyte response to inflammation. *Genes Dev* **15**: 3263-77.

Tang, D. G., Chen, Y. Q. and Honn, K. V. (1996). Arachidonate lipoxygenases as essential regulators of cell survival and apoptosis. *Proc. Natl. Acad. Sci. USA* **93**: 5241-5246.

Tang, S., Bhatia, B., Maldonado, C. J., Yang, P., Newman, R. A., Liu, J., Chandra, D., Traag, J., Klein, R. D., Fischer, S. M., Chopra, D., Shen, J., Zhau, H. E., Chung, L. W. and Tang, D. G. (2002). Evidence that arachidonate 15-lipoxygenase 2 is a negative cell cycle regulator in normal prostate epithelial cells. *J. Biol. Chem.* **277**: 16189-16201.

Vane, J. R., Bakhle, Y. S. and Botting, R. M. (1998). Cyclooxygenases 1 and 2. *Annu. Rev. Pharmacol. Toxicol.* **38**: 97-120.

Vasiljeva, L. L., Manukina, T. A., Demin, P. M., Lapitskaja, M. A. and Pivnitsky, K. K. (1993). Synthetic study of hepoxilins. 3. Synthesis, properties, and identification of epimeric hepoxilins (-)-(10R)-B_3 and (+)-(10S)-B_3. *Tetrahedron* **49**: 4099-4106.

Vonakis, B. M. and Vanderhoek, J. Y. (1992). 15-Hydroxyeicosatetraenoic acid (15-HETE) receptors. Involvement in the 15-HETE-induced stimulation of the cryptic 5-lipoxygenase in PT-18 mast/basophil cells. *J Biol Chem* **267**: 23625-31.

Webster, D., France, J. T., Shapiro, L. J. and Weiss, R. (1978). X-linked ichthyosis due to steroid-sulphatase deficiency. *Lancet* **1**: 70-2.

Wertz, P. W. and Downing, D. T. (1983). Ceramides of pig epidermis: structure determination. *J Lipid Res* **24**: 759-65.

Wertz, P. W. and Downing, D. T. (1990). Metabolism of linoleic acid in porcine epidermis. *J Lipid Res* **31**: 1839-44.

Woollard, P. M. (1986). Stereochemical difference between 12-hydroxy-5,8,10,14-eicosatetraenoic acid in platelets and psoriatic lesions. *Biochem Biophys Res Commun* **136**: 169-76.

Yamamoto, S. (1992). Mammalian lipoxygenases: molecular structures and functions. *Biochim. Biophys. Acta* **1128**: 117-31.

Yla-Herttuala, S., Luoma, J., Viita, H., Hiltunen, T., Sisto, T. and Nikkari, T. (1995). Transfer of 15-lipoxygenase gene into rabbit iliac arteries results in the appearance of oxidation-specific lipid-protein adducts characteristic of oxidized low density lipoprotein. *J Clin Invest* **95**: 2692-8.

Yla-Herttuala, S., Rosenfeld, M. E., Parthasarathy, S., Glass, C. K., Sigal, E., Witztum, J. L. and Steinberg, D. (1990). Colocalization of 15-lipoxygenase mRNA and protein with epitopes of oxidized low density lipoprotein in macrophage-rich areas of atherosclerotic lesions. *Proc Natl Acad Sci U S A* **87**: 6959-63.

Yokomizo, T., Izumi, T., Chang, K., Takuwa, Y. and Shimizu, T. (1997). A G-protein-coupled receptor for leukotriene B4 that mediates chemotaxis. *Nature* **387**: 620-624.

Yokomizo, T., Kato, K., Terawaki, K., Izumi, T. and Shimizu, T. (2000). A second leukotriene B(4) receptor, BLT2. A new therapeutic target in inflammation and immunological disorders. *J. Exp. Med.* **192**: 421-432.

Yu, K., Bayona, W., Kallen, C. B., Harding, H. P., Ravera, C. P., McMahon, G., Brown, M. and Lazar, M. A. (1995). Differential activation of peroxisome proliferator-activated receptors by eicosanoids. *J. Biol. Chem.* **270**: 23975-23983.

Yu, Z., Schneider, C., Boeglin, W. E. and Brash, A. R. (2005). Mutations associated with a congenital form of ichthyosis (NCIE) inactivate the epidermal lipoxygenases 12R-LOX and eLOX3. *Biochim Biophys Acta* **1686 3**: 238-47.

Yu, Z., Schneider, C., Boeglin, W. E., Marnett, L. J. and Brash, A. R. (2003). The lipoxygenase gene *ALOXE3* implicated in skin differentiation encodes a hydroperoxide isomerase. *Proc Natl Acad Sci U S A* **100**: 9162-7.

Zeldin, D. C., Wei, S., Falck, J. R., Hammock, B. D., Snapper, J. R. and Capdevila, J. H. (1995). Metabolism of epoxyeicosatrienoic acids by cytosolic epoxide hydrolase: substrate structural determinants of asymmetric catalysis. *Arch Biochem Biophys* **316**: 443-51.

Zhao, L. and Funk, C. D. (2004). Lipoxygenase pathways in atherogenesis. *Trends Cardiovasc Med* **14**: 191-5.

Ziboh, V. A. and Chapkin, R. S. (1987). Biologic significance of polyunsaturated fatty acids in the skin. *Arch Dermatol* **123**: 1686a-1690.

Ziboh, V. A., Cho, Y., Mani, I. and Xi, S. (2002). Biological significance of essential fatty acids/prostanoids/lipoxygenase-derived monohydroxy fatty acids in the skin. *Arch Pharm Res* **25**: 747-58.